AEDC-TR-90-32
Volume I

C.3

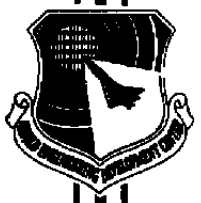

Application of System Identification Techniques to Turbine Engine Post-Stall Test and Evaluation

Robert P. Anex
Systems Control Technology, Inc.
Advanced Technology Division
Palo Alto, California 94303

December 1990

Final Report for Period March 1988 through November 1989

ARNOLD ENGINEERING DEVELOPMENT CENTER
ARNOLD AIR FORCE BASE, TENNESSEE
AIR FORCE SYSTEMS COMMAND
UNITED STATES AIR FORCE

NOTICES

When U. S. Government drawings, specifications, or other data are used for any purpose other than a definitely related Government procurement operation, the Government thereby incurs no responsibility nor any obligation whatsoever, and the fact that the Government may have formulated, furnished, or in any way supplied the said drawings, specifications, or other data, is not to be regarded by implication or otherwise, or in any manner licensing the holder or any other person or corporation, or conveying any rights or permission to manufacture, use, or sell any patented invention that may in any way be related thereto.

Qualified users may obtain copies of this report from the Defense Technical Information Center.

References to named commercial products in this report are not to be considered in any sense as an endorsement of the product by the United States Air Force or the Government.

This report has been reviewed by the Office of Public Affairs (PA) and is releasable to the National Technical Information Service (NTIS). At NTIS, it will be available to the general public, including foreign nations.

APPROVAL STATEMENT

This report has been reviewed and approved.

Marjorie S. Collier

MARJORIE S. COLLIER
Directorate of Technology
Deputy for Operations

Approved for publication:

FOR THE COMMANDER

Keith L. Kushman

KEITH L. KUSHMAN
Technical Director
Directorate of Technology
Deputy for Operations

REPORT DOCUMENTATION PAGE

Form Approved
OMB No. 0704-0188

1. AGENCY USE ONLY (Leave blank)	2. REPORT DATE	3. REPORT TYPE AND DATES COVERED
	December 1990	Final, March 1988 -- November 1989

4. TITLE AND SUBTITLE
Application of System Identification Techniques to Turbine Engine Post-Stall Test and Evaluation, Volume I

5. FUNDING NUMBERS
F40600-85-C-0011

6. AUTHOR(S)
Anex, Robert P., Systems Control Technology, Inc.

7. PERFORMING ORGANIZATION NAME(S) AND ADDRESS(ES)
Systems Control Technology, Inc.
Advanced Technology Division
Palo Alto, CA 94303

8. PERFORMING ORGANIZATION REPORT NUMBER
AEDC-TR-90-32, Volume I

9. SPONSORING/MONITORING AGENCY NAMES(S) AND ADDRESS(ES)
Arnold Engineering Development Center/DO
Air Force Systems Command
Arnold AFB, TN 37389-5000

10. SPONSORING/MONITORING AGENCY REPORT NUMBER

11. SUPPLEMENTARY NOTES
Available in Defense Technical Information Center (DTIC).

12a. DISTRIBUTION/AVAILABILITY STATEMENT
Approved for public release; distribution is unlimited.

12b. DISTRIBUTION CODE

13. ABSTRACT (Maximum 200 words)

"Application of System Identification Techniques to Turbine Engine Post-Stall Test and Evaluation" was an Air Force funded study to investigate and apply system identification techniques to post-stall engine models in a manner which allowed AEDC personnel to become proficient in the use of these techniques. The final technical report for the second phase of this study is divided into two volumes. This, the first volume, describes the estimation of post-stall characteristics of a 10-stage compressor rig model, using rig test data. Volume II describes the application of parameter estimation theory to gas turbine engines and the use of the SCIDNT estimation code used in this effort.

14. SUBJECT TERMS			15. NUMBER OF PAGES
turbine engines	stability	gas turbine engines	109
stall	surge		16. PRICE CODE
system identification	post-stall		

17. SECURITY CLASSIFICATION OF REPORT	18. SECURITY CLASSIFICATION OF THIS PAGE	19. SECURITY CLASSIFICATION OF ABSTRACT	20. LIMITATION OF ABSTRACT
UNCLASSIFIED	UNCLASSIFIED	UNCLASSIFIED	SAME AS REPORT

PREFACE

The work reported herein was performed by Systems Control Technology, Inc. (SCT), Palo Alto, California, under contract F40600-85-C-0011 for the Arnold Engineering Development Center (AEDC), Arnold Air Force Base, Tennessee. The Technical Monitors of this program were Dr. Milton Davis, Sverdrup Technology, Inc., and Marjorie S. Collier, AEDC/DOTR. The SCT Program Manager was Mr. Robert P. Anex. SCT would like to acknowledge the following personnel for their invaluable support and contributions to this program: 1st Lt. Keith M. Boyer and Dr. Bill Copenhaver, Wright Research and Development Center, Aero Propulsion and Power Laboratory, and Dr. Walter O'Brien, Virginia Polytechnic Institute. The reproducibles used in this report was supplied by the authors.

TABLE OF CONTENTS

LIST OF FIGURES

LIST OF TABLES

1.0 Introduction

'Application of System Identification Techniques to Turbine Engine Post-Stall Test and Evaluation' was an Air Force funded study to investigate and apply system identification techniques to post-stall engine models in a manner which allowed AEDC personnel to become proficient in the use of these techniques. This document is the final technical report for the second phase of this study which was aimed at estimating post-stall characteristics of a 10 stage compressor rig model.

In addition to developing system identification capability at Arnold Engineering Development Center, the motivation for this study was the difficult task of producing post-stall compressor characteristics for a complex stage compressor model. When a model form is proposed it is always difficult to identify the correct model parameter values and to test the model's validity. This is particularly true for post-stall compressor characteristics. A series of recent programs [1-3] have demonstrated that system identification techniques can help solve this problem by providing the model designers with the ability to estimate compressor model parameters in an efficient manner using transient data. Moreover, these tools also allow qualitative model performance evaluation and provide insight into the sensitivity of model performance to selected model parameters.

1.1 Program Goals

There were two principal goals of this program: the first was to investigate the application of system identification techniques to a stage-by-stage compression system model and the second was to transfer this technology to AEDC personnel, so that they could become proficient in its use.

The goals associated with the identification of the stage compression system model were to evaluate the capabilities of both the estimation procedure as well as those of a newly proposed model structure. The goal of technology transfer was to enable AEDC personnel to execute all steps of an engine identification. Toward this end, each task in the estimation procedure was carried out in parallel by both AEDC personnel and in more detail at SCT, with several working sessions and coordination meetings supplementing these parallel efforts. This proved to be a very valuable program structure which facilitated both technology transfer and progress toward the technical goals. It was particularly valuable to have the original model designer and test engineers involved in the estimation process.

1.2 Summary of the Method of Approach

The approach taken to achieve the goals of this program is summarized in the following tasks:

1. Install the stage-by-stage compression system model in the system identification software (SCIDNT), and extend the model to include required facility inlet and exit nozzle models.

2. Analyze and pre-process test data. Combine digitally recorded data and digitized analog recorded data for estimation.

3. Apply system identification techniques to the 10-stage model and test data to estimate post-stall compressor characteristics.

4. Support AEDC personnel in performing the above tasks in parallel with the SCT effort and transfer system identification technology to the AEDC personnel through a series of tutorials and working sessions.

The merger of the compressor stage model into the SCIDNT code involves the follow steps: (1) modification of the compressor model to operate as a subroutine which can be called by SCIDNT, (2) description of the compressor characteristics and governing variables as identifiable parameters, (3) merging the code with SCIDNT, and (4) verification of the operation of the model in SCIDNT.

The data analysis and pre-processing involves: (1) the selection of the data which are to be used in identification, (2) determination of the signal composition of the data, (3) preparation of the data for use in identification, which includes signal averaging, filtering of unmodelled components such as rotating stall, and combination of digitally and analog recorded data, and (4) determination of signal noise characteristics and stage stall times.

Post-stall model parameters were estimated to minimize the output prediction error between the model and test data. A modified Gauss-Newton optimization strategy was employed to perform the minimization. The estimation techniques embodied in the SCIDNT estimation code and a description of the general application of SCIDNT are contained in Part II of this report.

1.3 Summary of Results

The program goals were accomplished. The application of parameter estimation to a stage-by-stage compressor model using high quality test cell

data has been evaluated, and the technology employed has been successfully transferred to AEDC personnel.

It has been determined that individual compressor stage characteristics can be estimated. The stage characteristics estimated during this program improved model fidelity, but not to the extent that had been anticipated. However, the estimation results have pointed out a likely reason for this shortcoming, which is that important physical effects are not included in the model, and thus the model is unable to achieve the desired fidelity in its current form. It has also been determined that interstage data are required at all stages in order to estimate post-stall characteristics for individual compressor stages. Without interstage measurements only the combined dynamic characteristic for the indivisible stages can be determined, and thus interstage dynamic effects are lost or are inaccurate.

1.4 Report Outline

This is the final report for the program entitled "Application of System Identification Techniques to Turbine Engine Post-Stall Test and Evaluation", sponsored by the United States Air Force. This report documents the program approach, the results obtained during this effort, general conclusions and recommendations, as well as a description of how to apply the SCIDNT system identification code to a new engine or compression system model. This report is organized as follows.

Volume I of this report describes the procedures and results of the application of system identification techniques to a stage compression system model. Volume I is composed of the following Sections: Section 2 describes the stage-by-stage 10-stage compression system model used in this effort. Section 3 briefly describes the parameter estimation procedures employed in this program. Section 4 details the source and nature of the data used, and the data reduction and analysis techniques employed. Section 5 describes the pre-stall model matching which was performed, and Section 6 describes the parameter estimation results achieved. In Section 7 the conclusion and recommendations generated during this effort are presented.

Volume II of this report contains a description of the parameter estimation theory embodied in the SCIDNT code and describes how to install an new model into the SCIDNT code.

2.0 Dynamic Compression System Model

This program applies nonlinear parameter estimation techniques to a dynamic model of a 10-stage compression system. The model simulates steady-state and transient prestall axial compression system operation as well as surge and rotating stall. The model uses a stage by stage control volume approach to solve the one-dimensional continuity, momentum and energy equations. Blade forces and shaft work are derived from quasi-steady stage characteristics and adjusted by a first order lag to approximate dynamic stage characteristics. It is the goal of this effort to estimate the post-stall characteristics and associated lag time constants in the model to improve post-stall model performance and to gain insight into the characterization of post-stall compressor dynamics.

This report section provides a brief description of the physics and mathematical formulation of the compression system model. The model was provided to SCT by the AEDC at the start of the program. The simulation was subsequently modified to include control volumes representing the facility inlet of the Compressor Research Facility (CRF) at Wright Research and Development Center, and to incorporate quasi-steady characteristics developed from CRF test data. The updated model was provided to SCT in November 1988, and was incorporated into the parameter estimation code that same month. Further modifications to the characteristics were made by CRF personnel during the course of the program, and another update of these characteristics was transmitted to SCT in June of 1989. For ease of communication, the modified models are herein referred to as the CRF ten-stage model.

2.1 Dynamic Model Description

The dynamic compression system model represents one-dimensional flow field physics. It predicts average annular conditions throughout the compressor in both stalled and unstalled conditions. In this way the model represents the global effect of three dimensional phenomena such as rotating stall on the overall compression system.

The model includes both the compression and ducting systems in an overall control volume. Acting on this control volume are an overall axial force distribution due to the effects of the compressor blading and compressor wall, the heat and shaft work distributions, and a distribution representing mass transfer across boundaries other than the inlet or exit (bleeds). In forward flow the inlet boundary conditions are the total pressure and total temperature at

the inlet. The exit boundary condition is supplied by the use of an imaginary isentropic sonic nozzle which specifies unity Mach number downstream of the last control volume. In reverse flow, the inlet also acts as the exit boundary, with ambient static pressure being specified.

The overall CRF control volume is divided into 38 elemental control volumes. The first sixteen control volumes model the CRF inlet ducting and bellmouth. Numbers 17 through 26 represent the actual compressor stages, and 27 through 38 the diffuser and discharge volume. In the compression section, each elemental control volume represents a stator followed by a rotor. Figure 2.1.1 defines the elemental control volumes of the CRF. Figure 2.1.2 defines the elemental control volumes in the compression section.The choice of defining the control volume to be stator-rotor rather than rotor-stator was made to be consistent with the way the steady-state pressures and temperatures were measured during testing. Pressure and temperature probes were located on the leading edge of the stator blades following each rotor.

2.2 Compressor Stage Characteristics

The dynamic compression system model used in this program represents a ten-stage compression system by virtue of the particular system geometry and the stage characteristics incorporated into the model. All other model terms represent fundamental physical relationships which are common to all compression systems. It is assumed that the system geometry is well known, therefore this effort has concentrated on identifying the stage characteristics and the parameters which modify them (such as the characteristic lag time constants). In this section the implementation of the stage characteristics in the nominal ten-stage model is described.

Each compressor stage is represented by two characteristics: one which models the pressure change across the stage, and one which models the temperature change. The pressure characteristic is represented in terms of the nondimensional flow and pressure coefficients, ϕ and ψ^P. The temperature characteristic is similarly defined in terms of the flow and temperature coefficients, ϕ and Ψ^T. Here the stage flow coefficient is defined as,

$$\phi = \left\{\left[\frac{W\sqrt{TT}}{PT\ A}\right]\left[\frac{(N/\sqrt{\theta})_{design}}{(N/\sqrt{\theta})_{actual}}\right]\right\} \Big/ \left\{\frac{W^*\sqrt{TT^*}}{PT^*\ A^*}\right\}$$

where,

$$\frac{W^*\sqrt{TT^*}}{PT^*\ A^*} = \text{Constant} = 0.5318.$$

The stage temperature coefficient, ψ^T, is defined as,

$$\Psi^T = \left[TR - 1\right]\left[\frac{(N/\sqrt{\theta})_{design}}{(N/\sqrt{\theta})_{actual}}\right]^2$$

where TR is the stagnation or total temperature ratio. Similarly, the stage pressure coefficient, Ψ^P, is defined as,

$$\Psi^P = \left[PR^{\frac{\gamma-1}{\gamma}} - 1\right]\left[\frac{(N/\sqrt{\theta})_{design}}{(N/\sqrt{\theta})_{actual}}\right]^2$$

where PR is the stagnation or total pressure ratio.

A typical set of quasi-steady-state stage characteristics are presented in Figure 2.2.1. The stage characteristics are divided into three flow regions: prestall, rotating stall and reverse flow. The prestall characteristics model the performance of the blade row with fully attached flow. In the rotating stall region the characteristics are based upon the flow-weighted average of the stalled and unstalled portions of the stage. The reverse flow regions represent the pressure loss and temperature rise associated with full annulus reverse flow.

The compressor stage characteristics are implemented in the model by a sequence of third order polynomials whose independent variable is flow coefficient. Each characteristic is stored as a sequence of polynomial coefficients scheduled against flow coefficient and speed. Thus for a given stage flow coefficient and speed the model determines which polynomial coefficients apply in that region, and then the stage pressure or temperature coefficient for that flow is computed from the polynomial.

3.0 Parameter Estimation Methods

The integrated system identification process is a multi-step iterative procedure which includes test planning, testing, model structure selection, parameter estimation, and model validation steps. Test planning and testing are included in the system identification process because often the instrumentation and test inputs required for parameter estimation are different from those chosen for general testing or testing for some other specific purpose. In this effort the test planning and test operations have been performed at the CRF and no iteration on the testing process is possible. Thus, only the model structure selection, parameter estimation and model validation steps are possible in this effort.

This Section describes the tools used for parameter estimation and model structure selection, and the model structure used in this program. Because there was only one set of test data available at each test point, model validation to verify the model predictive capability could not be performed.

3.1 Parameter Estimation Computer Code - SCIDNT

The goal of parameter estimation is to tune a model to match the observed outputs of a physical system. Mathematically this can be stated as minimizing a cost function such as the weighted sum square errors between model outputs and sensed test article outputs. During this effort, an SCT developed parameter estimation package, SCIDNT, was used to perform this function. SCIDNT is a nonlinear parameter estimation code which has been used to estimate aircraft, surface ship and submarine dynamic models.

SCIDNT minimizes the weighted sum square model/data error through a gradient search technique. First, the Jacobian of the cost function is computed through off-set derivative calculations. Then an approximation of the second derivative of the cost function with respect to the parameters to be estimated is formed from the Jacobian. Conceptually, this is accomplished by running the model several times, perturbing one parameter at a time. The cost function is computed for each run using the difference between the model outputs and measured data. From the variations in cost function and model parameters an approximation to the Jacobian, gradient and second derivative are formed. Using these approximations a search is performed to minimize the cost function.

The actual minimization process is somewhat complicated and so is only summarized here. For the interested reader, details of parameter estimation theory and its implementation are presented in Volume II of this report.

The minimization process is begun by generating approximations to the gradient and second derivative of the cost function with respect to the model parameters to be estimated. Then a gradient search is performed to minimize the cost function. The first step of this search is the second order "Newton" step, based on the gradient and second derivative. The model is then propagated using the parameter values determined by this step. If the cost function is reduced this step is accepted, the model is updated and a new iteration is begun.

A new iteration means that the model is once again propagated repeatedly to form new gradient and second derivative estimates for the new model parameter values. If the step is not an improvement a smaller step in the Newton direction is taken. This process of shrinking the step size is repeated, searching for an improvement in the cost function. When the step length is reduced below a user-defined amount, the direction of the step is moved from the Newton direction to the negative gradient direction. The search continues using continually smaller steps until a lowered cost function is achieved or the step size is reduced below some minimum value. The minimization process repeatedly computes the derivatives of the cost function and then performs a gradient search to reduce the cost function. Minimization continues until some convergence criterion, such as minimum reduction of cost function or step size, or the user specified limit on number of iterations is reached.

3.2 Identifiability/Sensitivity Analysis Tool - SENSIT

Identifiability/Sensitivity (I/S) analysis allows the user to predict, prior to estimation, how factors such as measurement availability, measurement noise, and estimation parameter choice will affect the estimation process. This allows an "optimal" set of measurements and parameters to be selected for estimation, and also provides a means of specifying requirements for future testing.

The computer program used for I/S analysis, SENSIT, uses partial derivative information generated by SCIDNT and a user specified description of the estimation case to be evaluated. The output of the code is a detailed prediction of the estimation outcome including predicted parameter covariance, estimation bias caused by inaccurate values of non-estimated model parameters, estimation set correlation, and a variety of other useful analysis results.

This prediction of estimation success is based on parameter estimation theory that is described in more detail in Volume II of this report. In summary, the theory states that in the absence of process noise, the error in the estimated parameters of a linear system will be less than the Cramer Rao bound. The Cramer Rao bound can be computed from the partial derivative information produced by SCIDNT (in response to a particular user request) and user specified inputs.

The assumptions under which the Cramer Rao bound is valid are not actually met in this case; however, the general trends which are indicated and the information which allows selection of the best set of parameters to be estimated are valid and very useful. One of the most important uses of the I/S analysis is in performing model structure selection. This process is described in the following Section.

3.3 Model Structure Selection

The model structure determination phase consists of processing the input/output data to determine the significant linear and nonlinear equations and associated parameters that are necessary to represent the observed system response. Choices of model structure include the determination of model order and the mathematical form to represent any nonlinear characteristics in the dynamic equations.

For this effort much of the model structure has been defined by the designers of the ten-stage model. The task which remains is to describe the portions of the model which are to be estimated in terms of the best set of identifiable parameters.

For example, the compressor stage characteristics are implemented in the 10-stage model by a sequence of third order polynomials whose independent variable is flow coefficient. Each characteristic is stored as a sequence of polynomial coefficients scheduled against flow coefficient and speed. This amounts to several dozen coefficients for each compressor stage characteristic. This is many more parameters than could be identified through parameter estimation, thus a different way to describe the characteristics must be developed if their shapes are to be estimated.

One option is to use simple parameters which modify whole regions of the existing characteristic descriptions, such as a bias on the entire rotating stall region. This would produce only 10 parameters, one for each stage. This reduction in the number of parameters is accompanied by a loss in the flexibility of the estimation process to do more than simply shift the existing characteristics up and down. There is a fundamental trade-off between the flexibility of the parametric description and the identifiability of the

parameters. Many parameters allows greater flexibility, but depending on the number and quality of the measurements available, only a limited number of parameters can be estimated. Thus the goal in the model structure selection process is to minimize estimation error while maximizing the flexibility of the model. The structure which is most flexible, and which is predicted by SENSIT to produce acceptable estimation accuracy is chosen.

The model structure selection process is thus performed by iterating between model structure choice and I/S evaluation using the SENSIT code to find an acceptable model structure. The estimation parameters set chosen in this program is described below.

For this effort much of the model structure has been defined by the designers of the 10-stage model. The task which remains is to describe the portions of the model which are to be estimated in terms of the best set of identifiable parameters.

3.3.1 Model "Parameterization" - The Model Structure

This Section describes the model variables which were estimated during this program. For a model term to be estimated it must be a constant and be placed in an array which is modifiable by the parameter estimation code. This is described in Part II of this report where installing a new model in the SCIDNT code is discussed.

The model variables which were made available to the SCIDNT estimation code are as follow:

TAU - This is the time constant of a first order lag on the force produced by the compressor. This lag models the effects of the stall cell dynamics on the compressor's ability to pump. Because the lag models stall cell dynamics, it is only applied when the compressor is stalled. Initially a single time constant was used for the entire compressor, later estimation efforts allowed different time constants for each stage.

TAUFAC - Modifies the lagging time constant (tau) during the reacceleration phase of a surge cycle. This allows a different time constant during blow-down and reacceleration. TAUFAC = 2.0 cuts the lagging constant in half on reacceleration.

HYSCOF - Hysteresis coefficient; provides a mechanism to introduce hysteresis into the dynamic stage characteristic. The hysteresis was implemented as a percentage of the flow coefficient at the stall point. When recovering from stall the pressure rise coefficient is taken from a straight-line continuation of the rotating stall characteristic above the critical flow point

until this hysteresis flow is reached, at which point the nominal quasi-steady characteristic is used. Thus if HYSCOF = 1.3 the pressure rise on recovery is computed from a straight line continuation of the rotating stall portion of the characteristic until the flow coefficient exceeds 130 percent of the critical flow. Individual HYSCOF values were implemented for each stage; these were termed HYSTP(x), where x is the stage number.

RSLOPE - Coefficient for changing the slope of the backflow characteristic. This is implemented by multiplying the flow coefficient (which is the independent variable on the characteristic curves) by the RSLOPE coefficient for all flow values less than zero. Thus, for RSLOPE greater than 1 (one) an effectively steeper sloping backflow characteristic results.

PRSLOP - Coefficient for causing a discontinuity in the quasi-steady pressure characteristics at zero flow. This is implemented as a multiplication factor on the pressure coefficients computed from the backflow portions of the characteristics. Thus, if the pressure coefficient is nonzero, PRSLOP =.98 results in a 2 percent discontinuity at zero flow as well as a warping of the backflow characteristic.

BIAS4 - This coefficient defines a triangular shaped bias added to the rotating stall portion of the stage four characteristic. This bias is of zero magnitude at stall flow and of size BIAS4 at zero flow. Bias values lie on a straight line between these end values.

This was implemented because at 78.5 percent speed the zero flow pressure coefficient for the fourth stage characteristic happens to be zero and would thus be unaffected by the PRSLOP term described above unless some mechanism to alter its value from zero were created.

ATERM - Defines the location of the peak of a triangular bias added to the rotating stall portion of the characteristic. As shown in Figure 3.3.1.1 for stage 8, Aterm8 is the distance between zero flow and the stall point flow at which the peak of the bias occurs. If Aterm=0.0 then the bias will be a right triangle with magnitude Bterm at Phi=0.0 and magnitude zero at the stall flow. Aterm is constrained to always be greater than or equal to zero and less than or equal to the stall flow.

BTERM - The height of a triangular bias added to the rotating stall portion of the characteristic. As shown in Figure 3.3.1.1 for stage 8, Bterm8 is the largest magnitude of the bias. The remainder of the bias is formed by straight lines which pass through zero at zero flow and at the stall flow. If Bterm=0.0 no bias results. If Bterm is negative, a negative bias occurs.
BIASES - A bias value is added to each model output which is compared to measured data during the estimation process. These biases allow for the elimination of any pre-stall mismatch between the model and the test data.

The need to remove the pre-stall model error is discussed in Section 6.1 of this report.

4.0 Test Data Analyses and Reduction

This section presents a discussion of the analyses and pre-processing which were performed on the 10-stage test data to prepare them for use in parameter estimation. Data analysis and reduction are very important steps in the identification of compression systems. Data analysis is required to insure that the channels are valid and consistent, as well as to determine the measurement noise levels which are used to set the relative weightings placed on the outputs during the estimation process. In addition, because the model to be identified is one dimensional, the presence of any two dimensional flow phenomena such as rotating stall must be identified and removed in the data reduction process. Data reduction also consists of filtering, re-sampling data, and averaging channels to yield average annular measurements.

4.1 Test Data Description

The data used in this study were gathered from tests of a high speed ten stage axial compressor conducted in the Compressor Research Facility (CRF) at Wright Research and Development Center (WRDC). The data used are from two tests, a stagnation stall event at 78.5% design corrected speed and a surge event at 82% speed. Digitally recorded data from test at 75% speed were also received; however because the model contains no characteristic data below 77% speed, these data were not processed.

The measurements of the two events processed were each of two types: real time digitally recorded, and frequency modulated (FM) analog recorded data. The data which were recorded digitally were received early in the program (August 25, 1988) and were used as the only measurements for many of the identifiability/sensitivity (I/S) and estimation runs. The analog data were digitized at AEDC and were received by SCT in May of 1989. The analog data were subsequently added to the measurement sets and used for the remaining I/S and estimation efforts.

The analysis and reduction of the analog and digitally recorded data for each event are described in the following sections.

4.2 Digitally Recorded Data at 82% Speed

The digitally recorded data sets contain 90 channels which have a nominal frequency response of 70Hz. Details of the data collection process can be found in Reference [4-1 Copenhaver]. There were 45 channels which corresponded to model outputs and were ultimately combined to form the estimation measurement set. These measurements are compressor inlet and exit total pressures and temperatures, and total and static pressures at stages 3, 5, 7, and 9. (The stages are defined as stator-rotor pairs, and the stage measurements are physically made on the leading edge of the stator. Thus the measurement station is technically the exit of the preceding stage and the inlet of the nominal stage.) The digital data sets had no measurement of the exit valve area which was the input used to drive the test.

Data Analysis

The data analysis process performed in preparation for parameter estimation consists of 1) checking consistency of the data channels, 2) determining the signal composition in terms of both the dynamic phenomena and the measurement noise and bias levels, and 3) determination of the characteristics of the stall event. The stall characteristics of interest include the time of stall in each stage, the extent of the pressure disturbance both across the annulus and along the axis of the compressor, and the number, size, location and propagation speed of any rotating stall cells which developed.

The methods used in the data analysis included plotting and cross-plotting of the measurements to check for data consistency and to determine the time and characteristics of the stall event, and detrending and power spectral density analyses to determine bias and signal composition. All signal analysis and preprocessing was performed using the CTRL-C commercial software package. CTRL-C is an interactive tool for digital signal processing and control design which is particularly well suited for manipulating, analyzing, processing, and plotting large amounts of data in vector or matrix form.

Figure 4.2.1 shows typical interstage total pressure measurements from the digitally recorded data at 82% speed. The transient exhibits four complete surges. The five graphs in Figure 4.2.1 show close coupled total pressures at 5 different radial locations at the 5th stage (measurement station 7). The 6th graph is the overplot of the first five plots. Immersion A is near the inside of the span, while immersion E is near the outside. Note that the pressure spike at the onset of surge is much more pronounced at the outer radii. In addition, it can be seen that the pressure disturbance of the stall is over the complete span of the stage.

Figure 4.2.2 shows the overplot of 10 close coupled total pressures at 5 radial immersions on two different circumferential octants. The steady-state values of the 10 channels agree very well. Also visible is data drop-out from approximately 1.8 to 2.07 seconds. Since this occurs after the stall transient, it is of no importance to the current effort.

Figure 4.2.3 shows typical total temperature measurements at two radial immersions. Note that the temperature probes exhibit a large time constant which necessitates the inclusion of a sensor model in the compressor simulation if the temperature measurements are to be of use in estimation. (The delay in the pressure probes is small and relatively uniform on all pressure channels, and so is neglected.)

Figure 4.2.4 shows static pressures at stage 9, inside and outside diameter locations and total pressures from stage 9 at 5 different radial immersions. The pressure disturbance is still over the entire span of the stage and since the ID static pressure remains higher than the OD static pressure, no radial flow direction reversal is indicated.

Figure 4.2.5 is a detailed view of total pressure measured in two nearly opposite circumferential octants at the compressor inlet. From this plot it can be clearly seen that the pressure disturbance is present around the entire annulus of the compressor inlet.

The data at 82% speed were all found to have very low noise levels and to be free of significant rotating stall or other two dimensional flow phenomenon. This observation was supported by power spectral density (PSD) analysis of the the various measurements. Figure 4.2.6 shows a typical PSD plot from this analysis. The PSD shows that the overwhelming majority of the power in the total pressure measurement at stage 5 is at the surge frequency of 4.8 Hz. The lack of unmodelled dynamic effects or significant noise in the data makes it possible to utilize this data without any additional filtering.

The final analysis task was to determine the time of stall in each stage of the compressor. Figure 4.2.7 shows the total pressure at stages 3, 5, 7 and 9 of the compressor plotted against data point number. With the available data coverage it is impossible to determine which stage stalled first. At best, it can be said that as expected, one of the latter stages stalls first and that the surrounding stages quickly follow.

Data Processing

The data at 82% speed were free of any significant noise and unmodelled dynamics and so required very little processing to prepare them for use in estimation. The processing which was required was to average the measurements at each station to produce an average annular measurement and then "resample" the data to achieve a regular sampling interval.

The "resampling" was required because the sample time used in the digital recording process was not a rational fraction and thus not an even multiple of any integration time step which might be used in the simulation. (The data were originally recorded with a sampling period of approximately 0.00144 seconds.) Since the simulation must be able to produce the model outputs at each measured data point, using the original data set would require constant interpolation of the data. It was decided to resample the data at 1000 Hz. to save computation time and to make it possible to combine these data with the analog data which were anticipated later in the program, and would be digitized at 1000 Hz.

A number of methods to resample the data were investigated. Among these were fitting the data with polynomials of various orders, high order digital filtering of the data and fitting a spline through the data. After evaluation, a cubic spline fit was chosen. This method insures that the resampled measurements will pass through the original data points while removing some of the obvious "chopping" associated with linear fits. Figure 4.2.8 (Cubic Spline) shows a comparison of cubic spline and linear fits of a portion of the data versus data point number.

After averaging and resampling the measurements were saved in a binary file for utilization by the SCIDNT parameter estimation code. Figure 4.2.9 (PS30....TT07) shows a sample of the measurement channels saved for use in estimation.

4.3 Digitized Analog Data at 82% Speed

The data which were collected through FM analog recording were from high response probes and had a nominal bandwidth of 200 Hz. The data sets received by SCT following digitization at AEDC contained 58 channels. Of these channels many were redundant measurements also included in the digital data sets previously processed. There were 19 channels of use in the estimation process. The channels utilized represented static pressures at stages 2, 4, 6, 8, 10, and the exit of stage 10 and total pressure at stage 8. In addition, a voltage measured across a potentiometer at the exit valve was available, providing a signal from which an approximate test input could be derived.

As with the digital data at 82% speed the analog data were very clean. Figure 4.3.1 (PS04LH30 PSOFLH20) presents a sample of two of the interstage static pressure measurements directly from the data set. Unfortunately the data were not digitized at 1000 Hz. as expected, but rather the sampling interval varied from 0.0010418 to 0.0010421 seconds. Thus the analog data also had to be resampled to match the digital data (which had been previously resampled to yield measurements with a 0.001 second sampling period).

The time channel on the analog data, in addition to having an inconsistent sampling period, did not match the time recorded on the digital data sets. Figure 4.3.2 (ANALOG VS. DIGITAL) is a comparison of the static pressure at station 11 from the digital data set (PS11L10) and from the analog data set (PS11LH20). Although these measurements were made at different circumferential locations, previous analysis had shown that the pressure disturbance was present across the entire annulus. Therefore there is evidently a discrepancy between the time channels from the two data sets. The time lag is too large to be due to differences in the probe bandwidths, pressure tube lengths, transducer volumes, or a combination of these. In addition, the digital data does not show the signal attenuation which would be expected with such a large delay due to sensor dynamics. Thus it was decided to shift the analog data to match the digital data. This was done by matching the transients shown in Figure 4.3.2, and shifting all of the other analog data channels the same amount, assuming that the data were consistent within the data set, but tagged with the incorrect time.

Following the resampling and time shifting process the data were averaged as shown in Table 4.3.1 to yield average annular measurements. Digital and analog data were never averaged together to form any of the channels. If an output channel was available from the digital data set, measurements at the same station in the analog data set were not used. The measurements from the analog data were assembled with the digital data channels and saved in a binary file for use by the parameter estimation code. Table 4.3.2 contains a list of the measurements produced by the full data reduction process and their data set of origin.

4.4 Digitally Recorded Data at 78.5% Speed

The data obtained at 78.5% design corrected speed represent a rotating stall event. The data channels available in the data set are the same as those described for the 82% speed case. The data analysis and processing performed on the 78.5% data was substantially the same as that for the 82% data; however the 78.5% data were filtered to reduce the rotating stall component.

Data Analysis

Figure 4.4.1 (PT09L1A-E PS09L1ID+OD) shows typical interstage total and static pressure measurements from the digitally recorded data at 78.5% speed. The static pressures are from stage 7, inside and outside diameter locations and the total pressures are stage 7 at 5 different radial immersions. Immersion A is near the inside of the span, while immersion E is near the outside. Note that the pressure disturbance from the rotating stall cell is quite pronounced over the complete span of the stage.

Compressor inlet total pressure measured at two circumferential locations is plotted in Figure 4.4.2 (PT2507A PT2504A). The two pressure measurements were made in octants 4 and 7 which are separated by 135 degrees. The period of the stall cell pressure fluctuations varies from approximately 16 ms when the stall cell first develops, to approximately 18 ms when fully developed. The time lag between the two measurements is approximately 7.3 ms. If a single stall cell is assumed, the frequency of the stall cell as determined from the measurement spacing and time lag would vary from 65 to 55 Hz. This is 38.5% to 45.2% of the rotor speed of 143.9 Hz. The bandwidth of the pressure transducers is not sufficient to determine the size of the stall cell.

Spectral analysis was applied to determine the frequency content of the measured data. Figure 4.4.3 (PT07L1A PSIA) shows the time history of total pressure at stage 5. Figure 4.4.4 contains plots of the power spectral density (PSD) of this signal computed from a 512 point fast Fourier transform. The upper plot is of the entire PSD, the lower plot is scaled to show the lower frequencies. The rotating stall frequency is the most powerful spectral component of this signal. This component around 60 Hz. and its higher harmonics dominate the PSD's. The rotating stall phenomenon which created this signal component is not modelled in the 10-stage simulation, however the estimation process will try to tune the model dynamics to match this signal as best possible. Thus it is desirable to remove or reduce the rotating stall signal in the 78.5% speed measurements to facilitate the estimation process.

Table 4.3.1 Test Measurement Processing

TEST MEASUREMENT PROCESSING		CORRESPONDING TEN-STAGE MODEL OUTPUT
ΣPT25XY/10	X = 04, 07 Y = A-E	PTIPC
ΣTT25FXC/3	X = 3, 6, 8	TTIPC
PS05L10		PS05
ΣPT05LX/4	X = A, B, D, E	PT05
ΣPS07L1X/2	X = I, O	PS07
ΣPT07L1X/5	X = A-E	PT07
ΣPS09L4X/2	X = I,O	PS09
ΣPT09L1X/5	X = A - E	PT09
ΣPS11L1X/2	X=I,O	PS011
ΣPT11L1X/5	X = A-E	PT011
ΣPT30XY/10	X = 01,06 Y = A-E	PTEXIT

Table 4.3.2 Full Estimation Measurement Set

MEASUREMENT	DATA SET OF ORIGIN
PS04	ANALOG
PS05	DIGITAL
PT05	DIGITAL
PS06	ANALOG
PS07	DIGITAL
PT07	DIGITAL
PS08	ANALOG
PS09	DIGITAL
PT09	DIGITAL
PS10	ANALOG
PT10	ANALOG
PS11	DIGITAL
PT11	DIGITAL
PS12	ANALOG
PS13	ANALOG
TT07	ANALOG
PT30	DIGITAL

Data Processing

The data processing procedures for the 78.5% speed signals were the same as those described for the 82% case, except that the raw signals were first filtered to reduce the rotating stall component of the signal. The data were filtered using an FFT filtering process, then averaged to yield average annular measurements, and finally resampled to yield 1000 Hz. data.

The filtering technique used was to transform the time series (raw data) into the frequency domain using the Fast Fourier Transform (FFT) and remove the undesired portion of the frequency spectrum. The filtered signal in the time domain is obtained by applying the inverse FFT to the filtered frequency domain signal. To remove the rotating stall components from the frequency domain signal, the principal signal component (55 - 65 Hz.) and its first three harmonics were selectively notched out by convolving the spectrum with a series of cosine waves. The cosine waves form a notch with zero amplitude at the frequencies to be removed. A cosine is used (rather than outright removal using an inverted box car function) to reduce the rippling effects caused by the Gibbs phenomenon. This technique introduces some rippling in the time domain signal, but is superior to standard time domain filtering because it does not introduce any phase shift and little signal attenuation both of which can disrupt the estimation process.

The FFT filtering techniques was applied to the 78.5% speed digital data. Figure 4.4.5 shows the FFT of the total pressure at stage 5 before and after the spectral notching. Figure 4.4.6 shows the time domain signals before and after the filtering process. Note that as the stall cell developed its frequency was above the filtered region and so is not attenuated significantly, but once fully developed the signal is greatly reduced. Note also the ringing introduced prior to the start of the stall transient. This artifact of the filtering process will not affect the estimation process since it occurs prior to the stall, and can be eliminated by utilizing the prestall portion of the unfiltered raw data and the filtered poststall data.

The goal of the filtering process was to reduce the rotating stall signal while altering the measurements as little as possible. A small remaining unmodelled signal will not have a large adverse effect on the estimation, while significant alteration of the desired component will. Thus removal of the rotating stall was not pursued in an aggressive manner, but rather the minimal amount of filtering was performed.

4.5 Digitized Analog Data at 78.5% Speed

The data channels available in the data set are the same as those described for the 82% speed case. The data analysis and processing performed on the 78.5% data was substantially the same as that for the 82% data, however the 78.5% data were filtered to reduce the rotating stall component.

Samples of static pressures at stages 8 and 10 from the raw data set are presented in Figure 4.5.1. The raw data were resampled to yield 1000 Hz. data using the cubic spline technique. The data were then filtered using the FFT method described above (as applied to the digitally recorded data). The measurement at each station were then averaged together, the analog data were then shifted in time to match the digitally recorded data and the two processed data sets were combined into one file for use in estimation. The resampled, filtered and averaged static pressures at stages 8 and 10 are shown in Figure 4.5.2

5.0 Pre-Stall Model Matching

One of the principal goals of this effort is to estimate the post-stall 10-stage model. However, prior to post-stall estimation it is necessary to match the pre-stall model to the test data as well as possible. This is because mismatch between the model and data prior to stall will persist in post-stall operation and tend to bias estimation results. In this effort, matching of the pre-stall model and data involved several steps including generation of a model input, selection of measurement biases, and estimation of the pre-stall characteristics.

5.1 Input Generation

The tests of the 10-stage compressor which generated the data used in this effort were driven by closing an exit valve to throttle back the compressor flow until stall. During testing the valve angle was lowered approximately one half percent per second until stall was detected, and then opened until recovery. The throttle valve position was not recorded in the digitally recorded data and so no definite input was available to drive the model to match the test data. In the absence of a measured input an approximate input was created which best matched the measured outputs and produced stall in a reasonable amount of time.

The starting point for the model was produced by running the steady-state stacking model repeatedly to find the lowest mass flow rate which did not produce stall in the model (given the measured compressor inlet total pressure and temperature). From steady-state measurements the valve closure could be approximated, but closure rate was unknown. A closure rate on the order of one half a percent per second would require very large amounts of computer time just to propagate the model to the point of stall, and would produce an almost random time of stall which would be very difficult to match with the test data. For these reasons an exaggerated closure rate of 14 percent throttle function reduction in 0.1 sec. was used.

Studies using the dynamic compression system model were performed at both SCT and the CRF to determine the effect of throttle closure and closure rate on the stall dynamics. The conclusion of these analyses was that both closure and closure rate could affect the surge/rotating stall boundary. However, the SCT analysis found that if this boundary were not crossed the throttle closure rate had little effect on the stall transient itself. Thus our selection of an unrealistically fast closure rate should not bias estimation results.

Figure 5.1.1 shows the three throttling function ramps imposed on the model to evaluate the effect of throttle closure rate. When different closure rates are used, the stall point is reached at different times (a slower closure rate takes ' longer to reach the stall point). Figure 5.1.2 shows selected model outputs for the transients which correspond to the inputs in Figure 5.1.1. To determine the true effect of the closure rate on stall dynamics, these transients were aligned in time. Perfect alignment cannot be achieved due the discrete nature of the data. The aligned model outputs are shown in Figure 5.1.3. It can be seen that the closure rate has very little effect on the shape of the transient if the stall/surge boundary is not crossed.

5.2 Model Modifications

As mentioned in the previous Section, in order to achieve successful post-stall parameter estimation, the compressor model must enter the stall event at the correct operating point. That is, the pre-stall model outputs must match the measured outputs. In order to achieve this match, several modifications were made to the 10-stage model including inclusion of a simple facility model and the addition of sensor bias models in the simulation.

The need for pre-stall model/data agreement can be explained with a simple example. The heavy solid line in Figure 5.2.1 is some imaginary measured output representative of a total pressure. The light solid line represents the identical output from a model but subject to a slight bias. The goal of the estimation process is to eliminate the error represented by the shaded region. If the estimation process has access only to parameters which affect the post-stall model performance, the best it can do is to drive the model to perform in some very different manner such as represented by the dashed line in Figure 5.2.1. Obviously, the model which would produce the dashed output would be very different from that which would produce either solid transient. To avoid this type of estimation bias, the pre-stall model must be matched to the measured outputs as well as possible prior to estimation of the post-stall model.

To improve the pre-stall match the simulation was modified to include control volumes representing the facility inlet of the Compressor Research Facility (CRF), and to incorporate quasi-steady characteristics developed from CRF test data. Further modifications to the characteristics were made by CRF personnel during the course of the program, and updates of these characteristics were transmitted to SCT. The goal of these modifications was to match the model to the specific test facility and test article which produced the data used in this program. These modifications greatly increased the fidelity of the model, particularly in the pre-stall regime.

In order to remove the remaining error at the stall point, constant biases were added to the model outputs. The model outputs were seen to exhibit pre-stall errors that were generally consistent with reduced mass flow, however the model could not match this flow rate. This may well indicate that some blockage had developed in the compressor but since no explicit blockage model exists in the simulation (other than that inherent in the compressor in-stall characteristics) the best solution to this mismatch was to simply bias the model outputs. This is equivalent to modelling a sensor bias on the outputs which were measured during test.

The bias levels used at 78.5% and 82% corrected speed are shown in Table 5.1 and 5.2 respectively. The biases were input as parameters which could be estimated by SCIDNT if desired, thus the bias values appear in parameter lists of the SCIDNT input files.

Table 5.1 Sensor Bias Values for 78.5% Corrected Speed

PS04 = -1.65	PS10 = -3.0
PS05 = -1.65	PT10 = 0.0
PT05 = -0.13	PS11 = -3.0
PS06 = -1.05	PT11 = 0.88
PS07 = -1.05	PS12 = -4.0
PT07 = 1.02	PS13 = -3.0
PS08 = -1.98	TT07 = 7.0
PS09 = -1.95	PT30 = 0.6
PT09 = 0.85	

Table 5.2 Sensor Bias Values for 82% Corrected Speed

PS04 = -2.3	PS10 = -3.6
PS05 = -1.2	PT10 = 0.8
PT05 = -0.42	PS11 = -3.0
PS06 = -2.0	PT11 = 1.88
PS07 = -1.55	PS12 = -20.0
PT07 = 1.42	PS13 = -16.7
PS08 = -3.0	TT07 = -9.0
PS09 = -2.45	PT30 = 2.2
PT09 = 0.9	

6.0 System Identification Results

The primary objective of this study was to develop and demonstrate techniques to identify post-stall compressor characteristics for a stage-by-stage compressor model. The estimation was performed in two stages: the first estimated the stall point in each stage so that the compressor would enter stalled operation at the correct conditions, the second estimated the post-stall characteristics themselves.

This study included a very large number of parameter estimation runs. The runs made early in the program made use only of digitally recorded data since the analog data were not yet available. As modifications were made to upgrade the model capabilities many more estimation runs were made. Estimation efforts near the end of the program made use of both digitally and analog recorded data. Many of these runs provided intermediate results or helped point out problems in the model or estimation process which were subsequently remedied. Thus the estimation runs will not be reported on individually, but rather results of summary runs and general conslusions about groups of runs will be presented.

6.1 Estimation Using Digitally Recorded Data

The first propagation and estimation runs used only the digitally recorded test data. These data are described in some detail in Section 4 of this report. The most important characteristic of these data is that they only include measurements at four interstage locations. Therefore these runs serve as a test of how well estimation can be performed with limited interstage measurements. The digitally recorded data were used in two types of estimations. In the first the stall points of the quasi-steady stage characteristics were estimated using the steady state stacking model. Based on the success of the stall point estimation, the digitally recorded data were also used to estimate the dynamic post-stall characteristics. This effort was not successful and demonstrated that measurements are required at each interstage location in order to estimate the dynamic post-stall stage characteristics.

Initial propagations of the model using the digitally recorded data uncovered a number of modelling problems such as lack of necessary facility inlet modelling in the model and limitations in the simulation equation solver which constrained the range of certain parameter values.

It was known from the start of the program that the original model did not include volumes which represented the CRF inlet. This volume is important

to match the frequency of surge behavior as well as to set the inlet boundary conditions accurately from test data. It was discovered as additional control volumes were added to the model that the model volumes could not decrease in size as quickly as the physical rig because the Mac Cormack equation solver would not converge. Thus the simulation used a more gradually decreasing inlet geometry than actually existed in the rig.

The MacCormack solver also limited the estimation process in these early runs. If the estimation routine attempted to modify parameters beyond a certain range, the conditions through the compressor model would change too quickly and the simulation would fail to converge.

6.2 Stall Point Estimation

In order to achieve successful post-stall parameter estimation, the compressor model must enter the stall event at the correct operating point. That is, the pre-stall model steady state values must be accurate. The preliminary pre-stall characteristics included in the stacked stage model were approximated from tests of a differently configured machine than the one which produced the test data used in this study, and so were somewhat different. Rather than generate more accurate characteristics from the steady state test data (this was already being done at the CRF) it was decided to try to estimate the characteristics. At this time only the digitally recorded test data were available, and thus estimation was performed with measurements at only four interstage locations.

The stall points (the flow and pressure coefficient values at which the pressure rise characteristics become positively sloped for lower flow coefficient values) were estimated using the compressor stacking model installed in the SCIDNT parameter estimation code. This exercise produced confidence in the estimation procedure developed in this study and in addition, allowed us to avoid duplicating the effort of the Compressor Research Facility (CRF) which was in the process of building a set of characteristics from the steady-state test data.

The available pre-stall transient digitally recorded test data were very sparse in the sense that measurements were available only at alternating stages and the testing was performed in a quasi-steady state condition. This dearth of data makes estimation more difficult. Since the testing was quasi-steady, with the compressor stages operating approximately at a single point near stall, only the stall point was estimated. This was implemented by forcing each stage of the model to operate at the critical, or stall, flow coefficient and to estimate a bias on the pressure rise at this point. It is important to recognize that this is a much simpler estimation problem than estimating the dynamic post-stall stage characteristics. This is because the pressure rise at the stall

points are desired rather than entire characteristics, and because the stacking model balances the steady state equations, no compressor dynamics complicate the problem.

The identified stall points are plotted versus the nominal characteristics from the model and the characteristics computed from CRF steady state test data in Figure 6.2.1. These estimates are the result of five iterations of the SCIDNT estimation code. Using only the digitally recorded data the estimation process was able to significantly improve the model fidelity and in general moved a good way toward the "true" answer as defined by the stall points measured during CRF testing.

In order to remove the remaining error at the stall point, constant biases were added to the model outputs. The model outputs were seen to exhibit pre-stall errors that were generally consistent with reduced mass flow, however the model could not match this flow rate. This may well indicate that some blockage had developed in the compressor but since no explicit blockage model exists in the simulation (other than that inherent in the compressor in-stall characteristics) the best solution to this mismatch was to simply bias the model outputs. This is equivalent to modelling a sensor bias on the outputs which were measured during test.

6.3 Characteristic Estimation

Estimation of the dynamic post-stall stage characteristics was attempted using only the digitally recorded data. The estimation code was unable to estimate the individual characteristics using these measurements which were made at every other interstage location. When the two adjacent stages, around which measurements were available, were coupled together by estimating one bias which was applied to both stage characteristics, estimation was possible, but only limited improvement in model fidelity was achieved.

The estimation of the pairs of stage characteristics was never able to improve the model performance more than a small amount. It is unclear whether this is because the few measurements were incorrectly matched with model outputs or if interstage dynamics are important enough that stages could not be coupled in this manner. In any case, because the estimation process was trying to make the model match erroneous data, the results of this brief study are inconclusive at best.

6.4 Estimation Using Combined Data Sets

The post-stall characteristics were estimated using both the digital and analog data. These data sets provided measurements at all interstage locations as previously described. In addition, improved nominal post-stall characteristics were used for the estimation process.. These characteristics were the result of steady-state testing performed at the CRF using the same machine and test facilities as were used to generate the transient test data. The use of the updated characteristics and model calibration by CRF personnel [4,5,6], resulted in relatively good agreement prior to estimation.

6.5 Post-Stall Characteristic Estimation

The post-stall estimation was an iterative process. In the SCIDNT code the user has control over a variety of parameters which influence the gradient search process, and which for highly nonlinear estimation problems often require some tuning. Thus, many estimation runs served as intermediate steps towards final results. These intermediate runs will not be described here, rather final results will be presented.

In Table 6.1 the nominal and estimated parameter values are presented for estimation at 78.5% corrected speed. The resulting changes in the post-stall stage characteristics are shown in Figure 6.5.1. The stage 9 and 10 characteristics and stage 5 and 8 time constants exhibit the largest and most interesting changes due to estimation. The first three stage characteristics were not modified by the estimation process. These stages are unusual in that they stall at very low flow coefficients and during normal operation actually take energy out of the gas stream. The estimation process, by not modifying these characteristics, verifies this unusual behavior and poor component matching.

From the large changes in the estimated characteristics for stages 9 and 10, it appears that some physical phenomenon exists during a stall transient which is not included in the current model structure. It is speculated that this estimated dynamic characteristic represents some type of dynamic blockage or choking which is occurring in stages 9 and 10 and is not modelled.

In Figure 6.5.2 the test data, pre-estimation model outputs and estimated model outputs are compared. These outputs represent an average reduction in rms output error of 39.04%, with rms error reduced in all outputs, ranging from 16.7% to 61.6%. The total average percentage output error was reduced to 5.9% of the mean measured output values.

Table 6.1 Estimated Parameter Values At 78.5% Speed

PARAMETER NUMBER	PARAMETER LABEL	NOMINAL VALUE	ESTIMATED VALUE
15	BETERM4	0.0	-0.001
17	BETERM5	0.0	-0.001
19	BETERM6	0.0	-0.002
21	BETERM7	0.0	-0.003
23	BETERM8	0.0	0.001
24	ATERM9	0.25	0.0
25	BETERM9	0.0	-0.01
26	ATERM10	0.24	0.0
27	BETERM10	0.0	-0.08
30	TAU3	0.03	0.027
31	TAU4	0.03	0.027
32	TAU5	0.03	0.023
35	TAU8	0.03	0.064

7.0 SUMMARY AND CONCLUSIONS

There were two principal goals of this program: the first was to investigate the application of system identification techniques to a stage-by-stage compression system model and the second was to transfer this technology to AEDC personnel, so that they could become proficient in its use.

The goals associated with the identification of the stage compression system model were to evaluate the capabilities of both the estimation procedure as well as those of a newly proposed model structure. The goal of technology transfer was to enable AEDC personnel to execute all steps of an engine identification. Toward this end, each task in the estimation procedure was carried out in parallel by both AEDC personnel and in more detail at SCT, with several working sessions and coordination meetings supplementing these parallel efforts. This proved to be a very valuable program structure which facilitated both technology transfer and progress toward the technical goals. It was particularly valuable to have the original model designer and CRF test engineers involved in the estimation process. The program goals were accomplished.

This study has shown that individual compressor stage characteristics can be estimated. Stage characteristic stall points have been estimated using measurements at only four interstage locations. Dynamic stage characteristics have been estimated using measurements at each stage.

The stage characteristics estimated during this program improved model fidelity significantly; however considerable model output error still exits. The estimation results have pointed out a likely reason for this shortcoming, which is that important physical effects are not included in the model, and thus the model is unable to achieve the desired fidelity in its current form. It has also been determined that interstage data are required at all stages in order to estimate post-stall dynamic characteristics for individual compressor stages. Without interstage measurements only the combined dynamic characteristic for the indivisible stages can be determined, and thus interstage dynamic effects are lost or are inaccurate.

REFERENCES

1. Anex, R. P., Rock, S. M., "Identification of Quasi-Steady In-Stall Compressor Maps From Transient Data." Presented at the AIAA/SAE/ASME/ASEE 21st Joint Propulsion Conference, AIAA-85-1351,1985.

2. Anex, R. P., Jellison, T.G., Rock, S. M., "Evaluation Of Compressor Stall Characteristics Using System Identification Techniques." Presented at the AIAA/SAE/ASME/ASEE 22nd Joint Propulsion Conference, AIAA-86-1851,1986.

3. Copenhaver, W. W., Worland, C. J., "Acquistion of Unsteady Pressure Measurements from a High Speed Multi-Stage Compressor." Presented at the Gas Turbine and Aeroengine Congress, Amsterdam, The Netherlands, June 6-9, 1988.

4. Boyer, K. M. and O'Brien, W. F. , "Model Prediction for Improved Recoverability of a Multistage Axial-Flow Compressor." Presented at the AIAA/SAE/ASME/ASEE 25th Joint Propulsion Conference, AIAA-89-2687, 1989.

5. Davis, M. W. and O'Brien, W. F., "A Stage-by-Stage Post-Stall Compression System Modeling Technique." Presented at the AIAA/SAE/ASME/ASEE 23rd Joint Propulsion Conference, AIAA-87-2088, 1987.

6. Copenhaver, W. W., T. H. Okiishi, "Rotating Stall Performance and Recoverability of a High-Speed 10-Stage Axial-Flow Compressor." Presented at the AIAA/SAE/ASME/ASEE 25th Joint Propulsion Conference, AIAA-89-2684, 1989.

7. Moore, F.K., "A Theory of Rotating Stall of Multistage Axial Compressors: Part I - Small Disturbances", ASME Journal of Engineering for Gas Turbines and Power, Vol. 106, April 1984, pp 313-320.

8. Greitzer, E.M., "Surge and Rotating Stall in Axial Flow Compressors, Part I: Theoretical Compression System Model", ASME Journal of Engineering for Power, April 1976, pp 190-198.

9. Lorenzo, C.F., Chiaramonte, F.P., "Determination of Compressor In-Stall Characteristics from Engine Surge Transients", prepared for the

Twentieth Joint Propulsion Conference, Cincinnati, Ohio, June 11-13, 1984.

10. Trankle, T.L., Vincent, J.H., Franklin, S.N., "System Identification of Nonlinear Aerodynamic Models",prepared for NATO AGARDOGRAPH "The Techniques and Technology of Nonlinear Filtering and Kalman Filtering," February 1982.

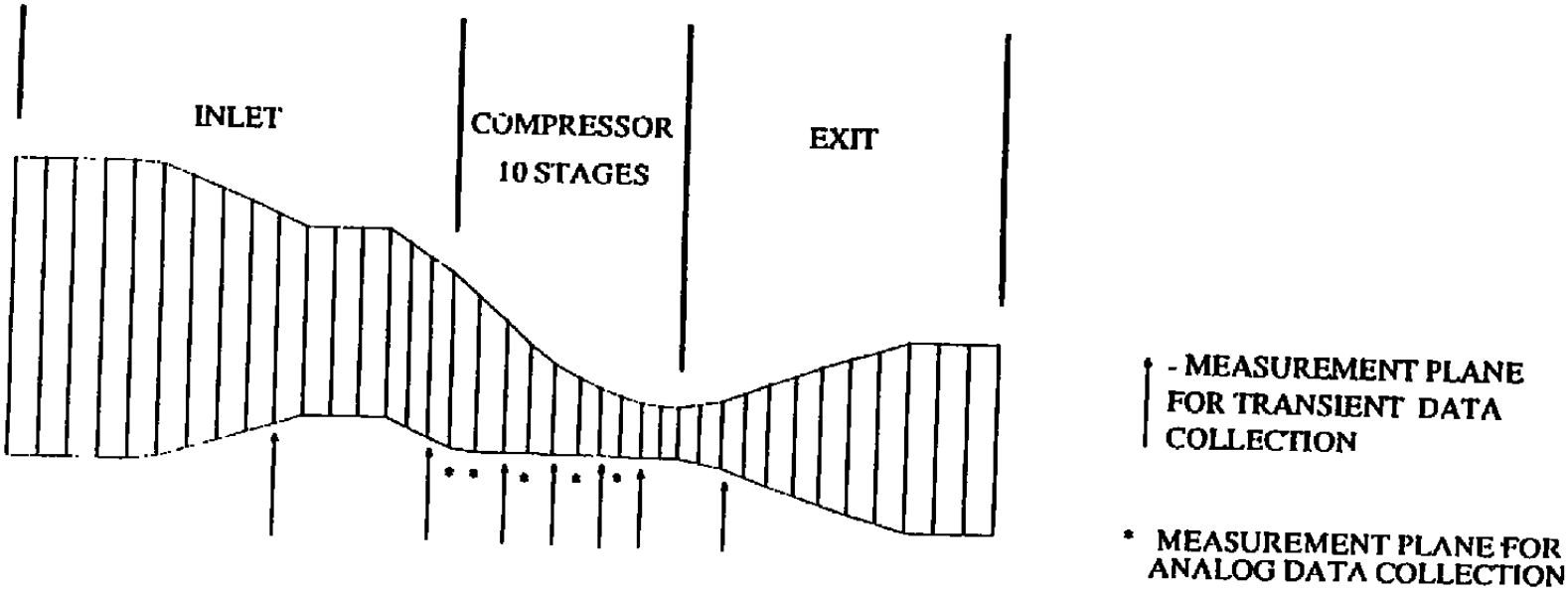

Figure 2.1.1 Schematic of Modeled Ten Stage Compressor

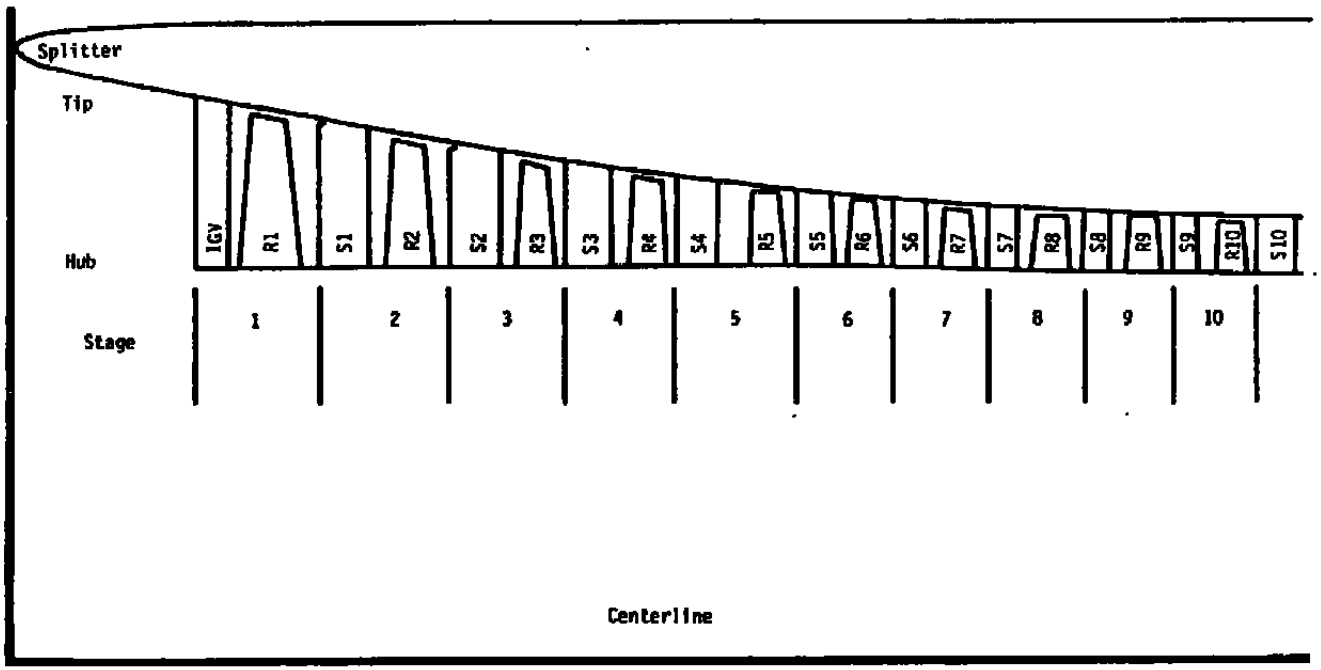

Figure 2.1.2 Compression System Control Volume Definition

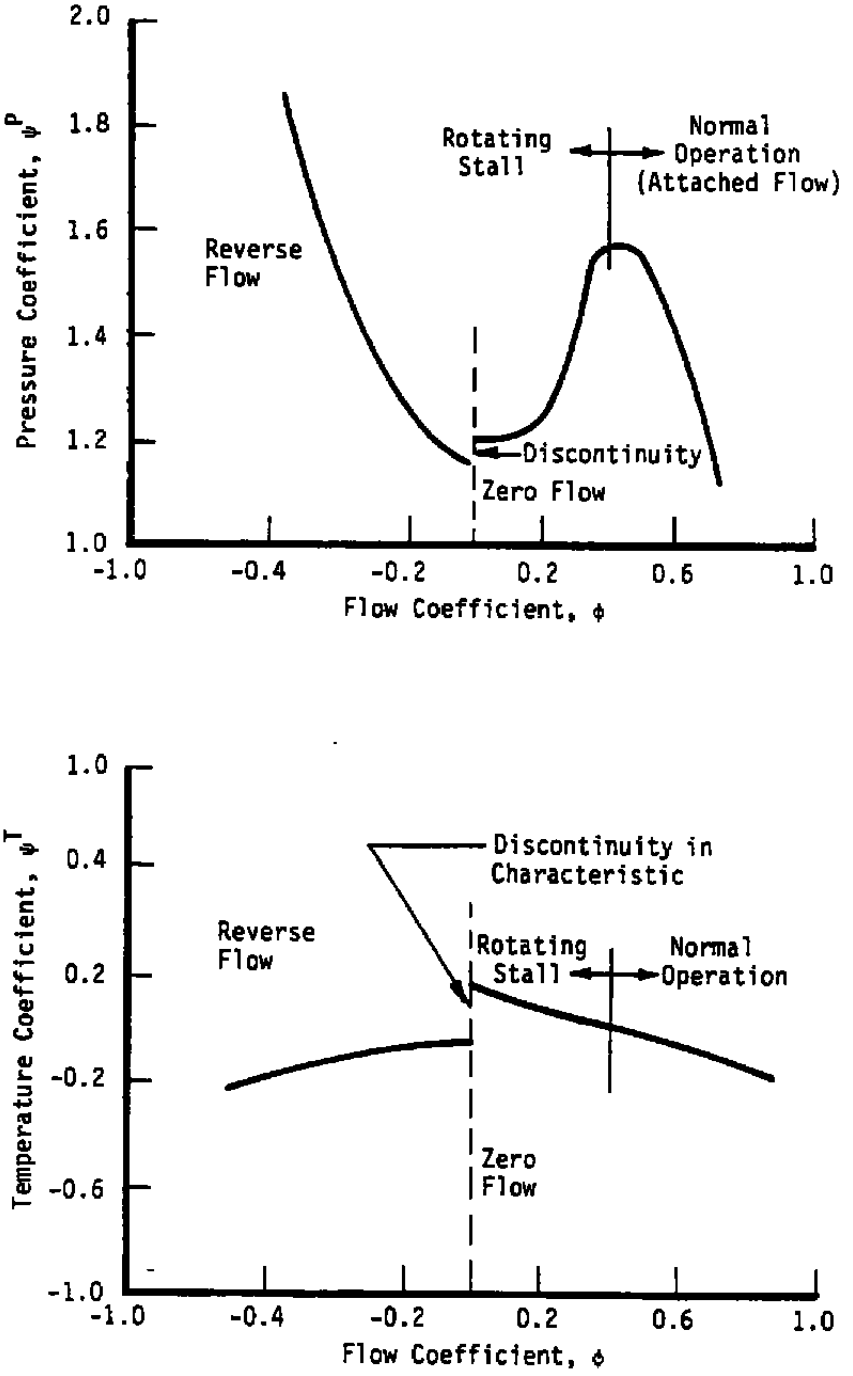

Figure 2.2.1 Typical Steady Stage Characteristics

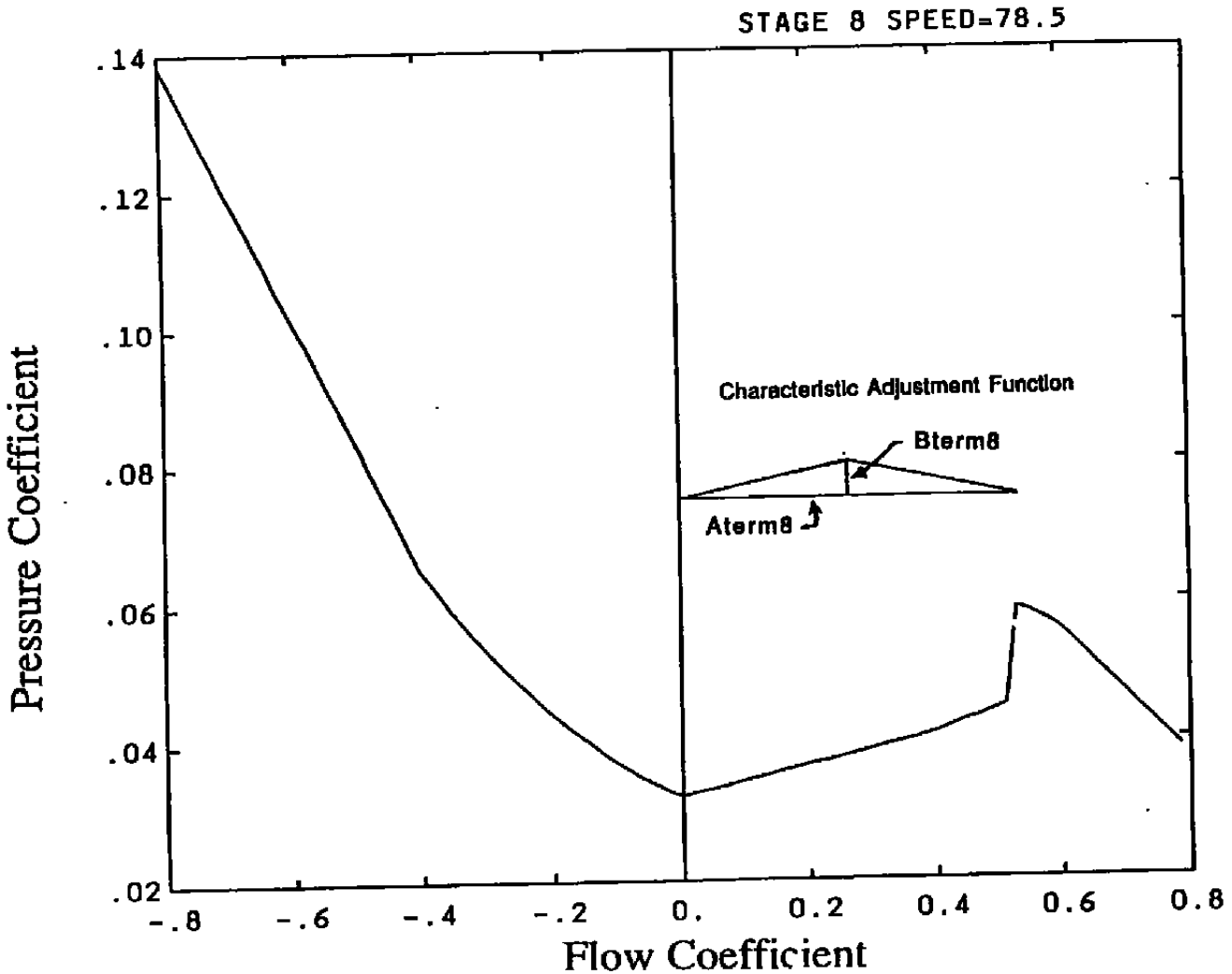

Figure 3.3.1.1 AtermN and BtermN Define the Adjustment Function Added to Stage Characteristic

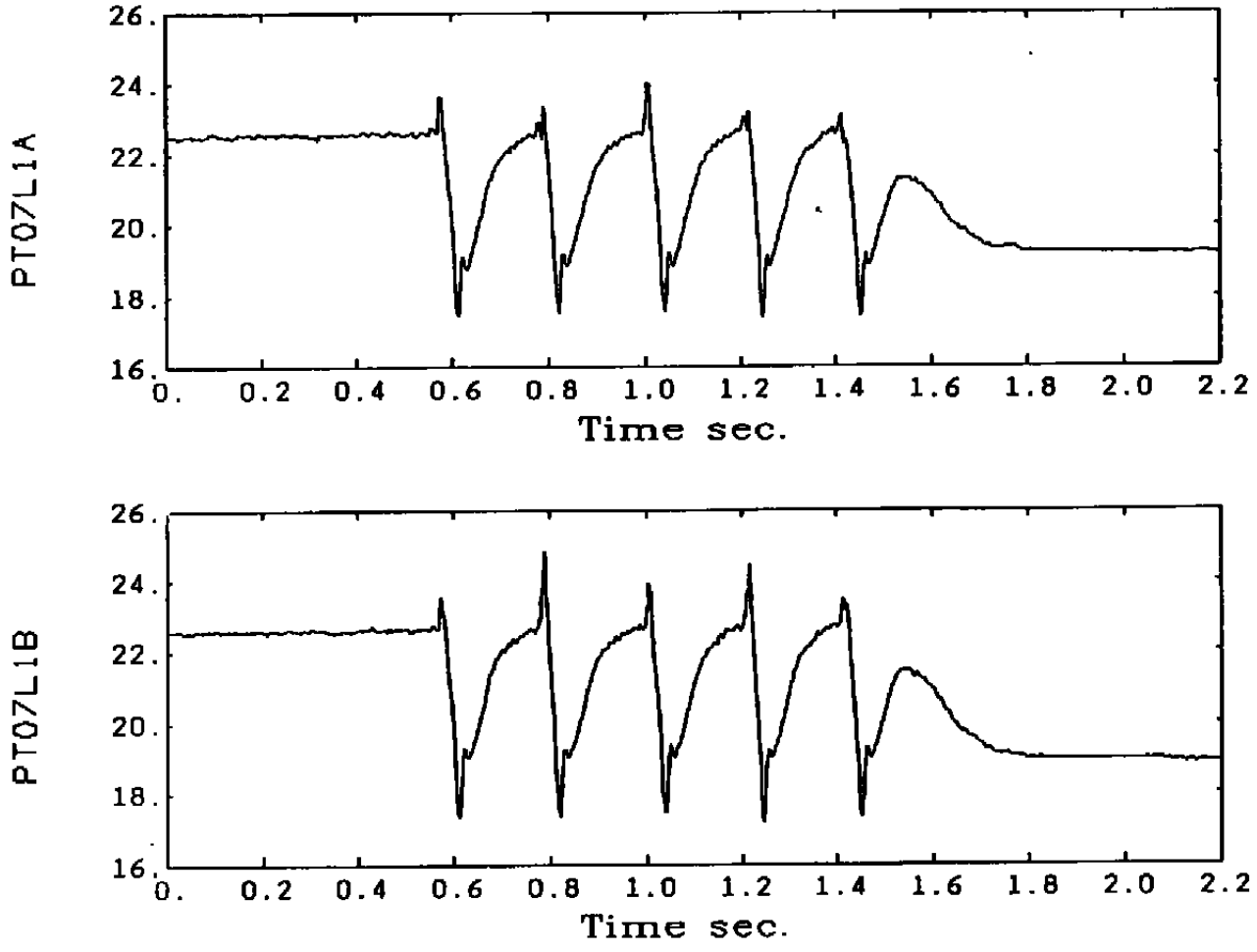

Figure 4.2.1 Typical Interstage Measurements at the 5th Stage

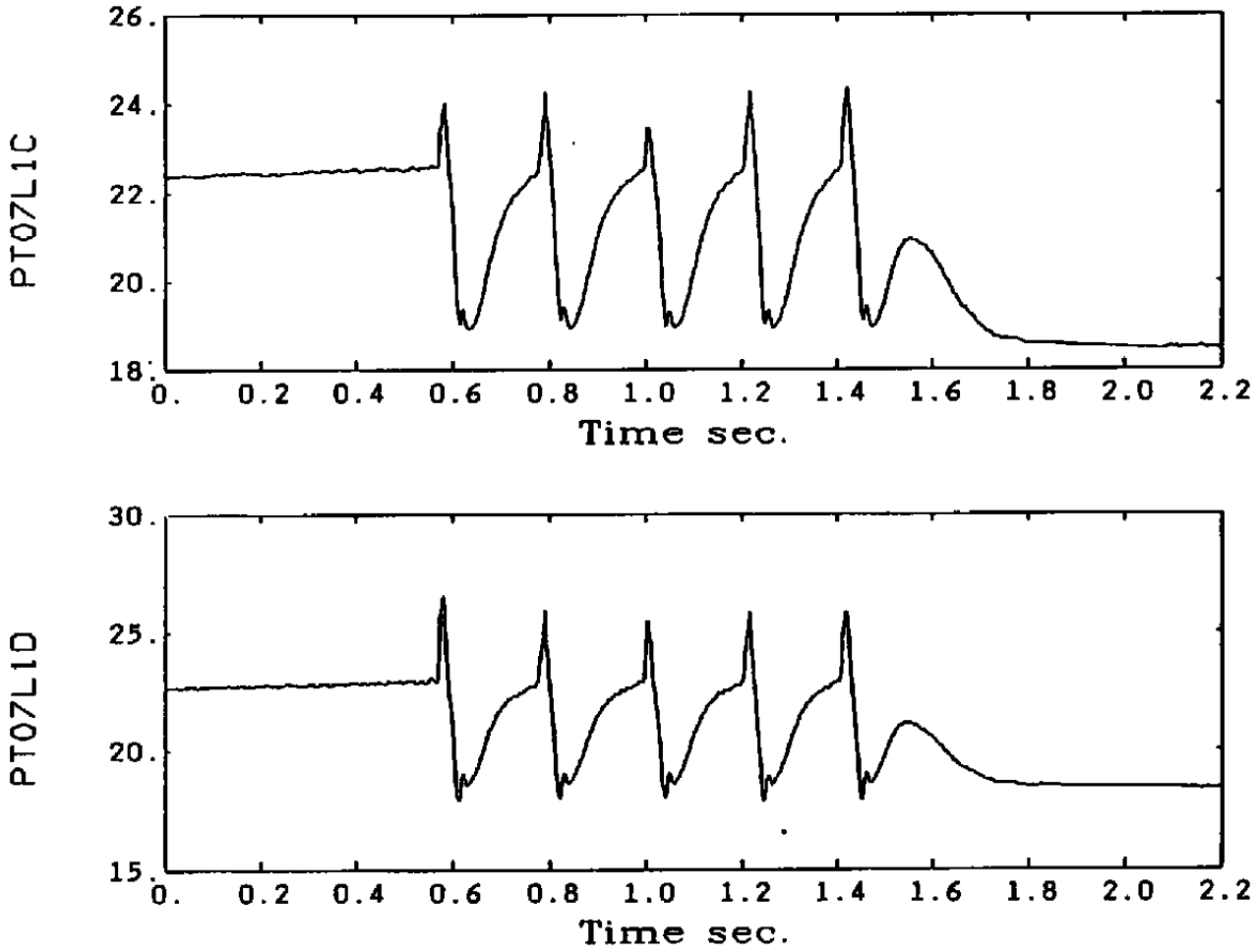

Figure 4.2.1 Typical Interstage Measurements at the 5th Stage (Cont'd)

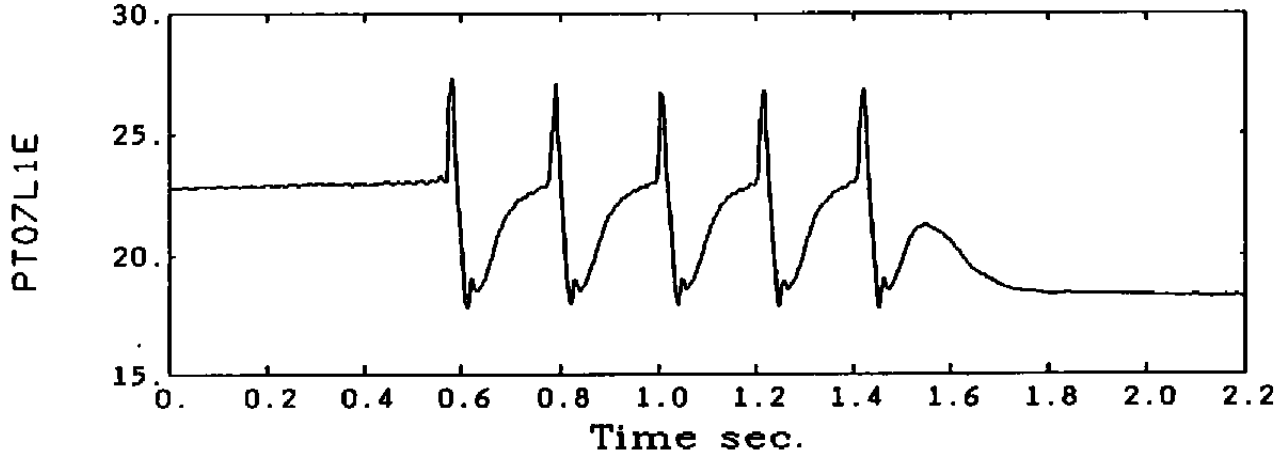

Figure 4.2.1 Typical Interstage Measurements at the 5th Stage (Cont'd)

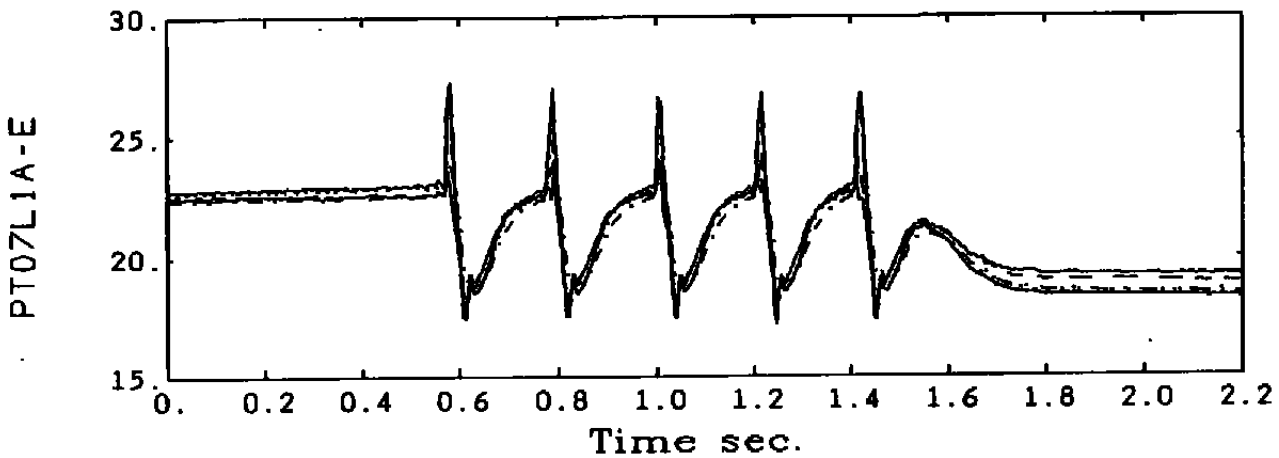

Figure 4.2.1 Typical Interstage Measurements at the 5th Stage (Cont'd)

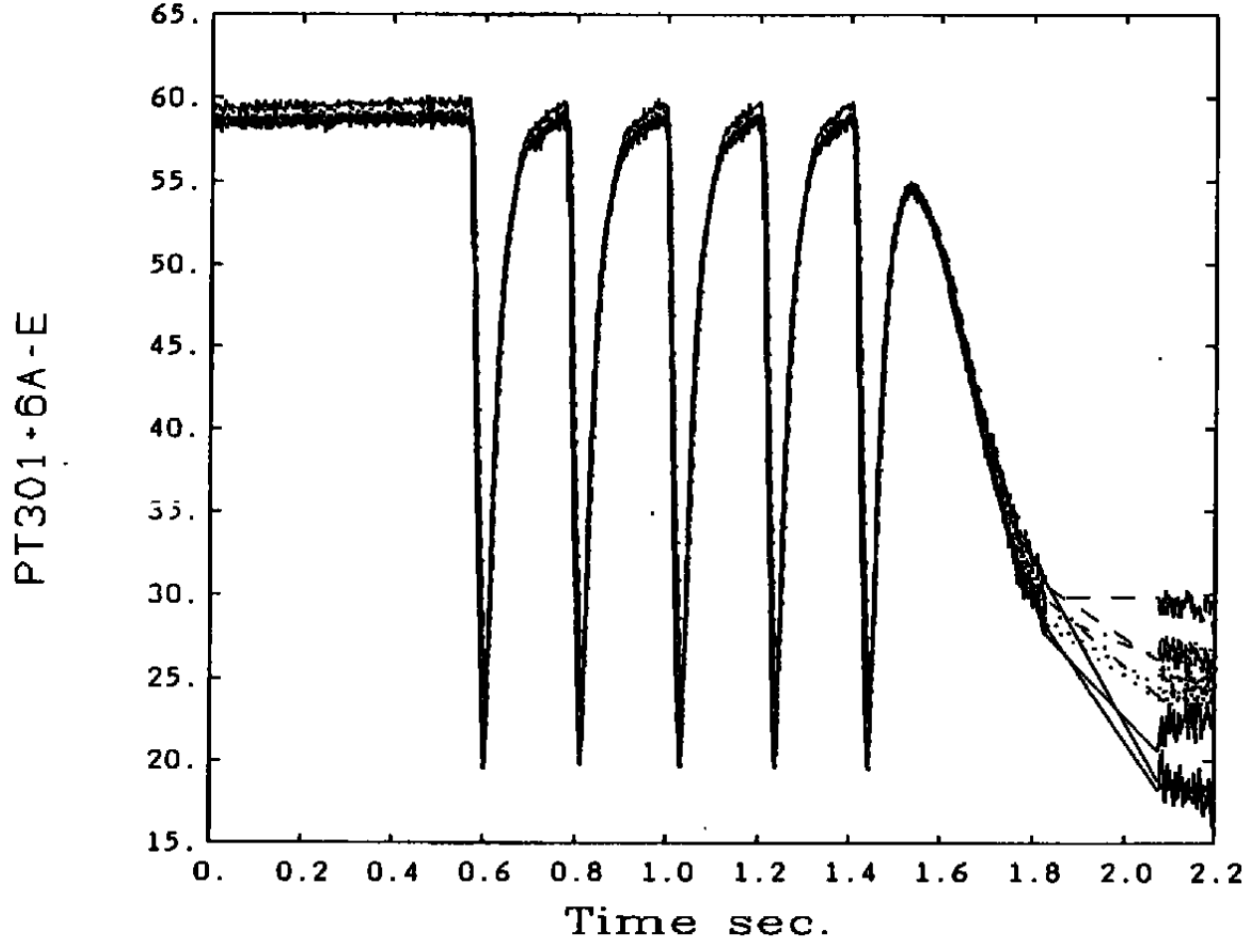

Figure 4.2.2 Total Pressure at Exit from 10 Close Coupled Probes

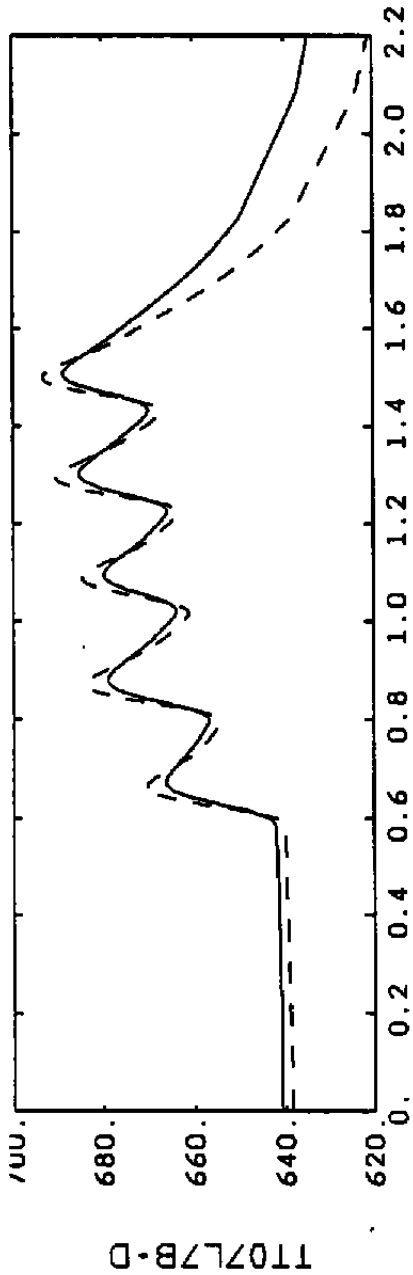

Figure 4.2.3 Typical Total Temperature Measurements

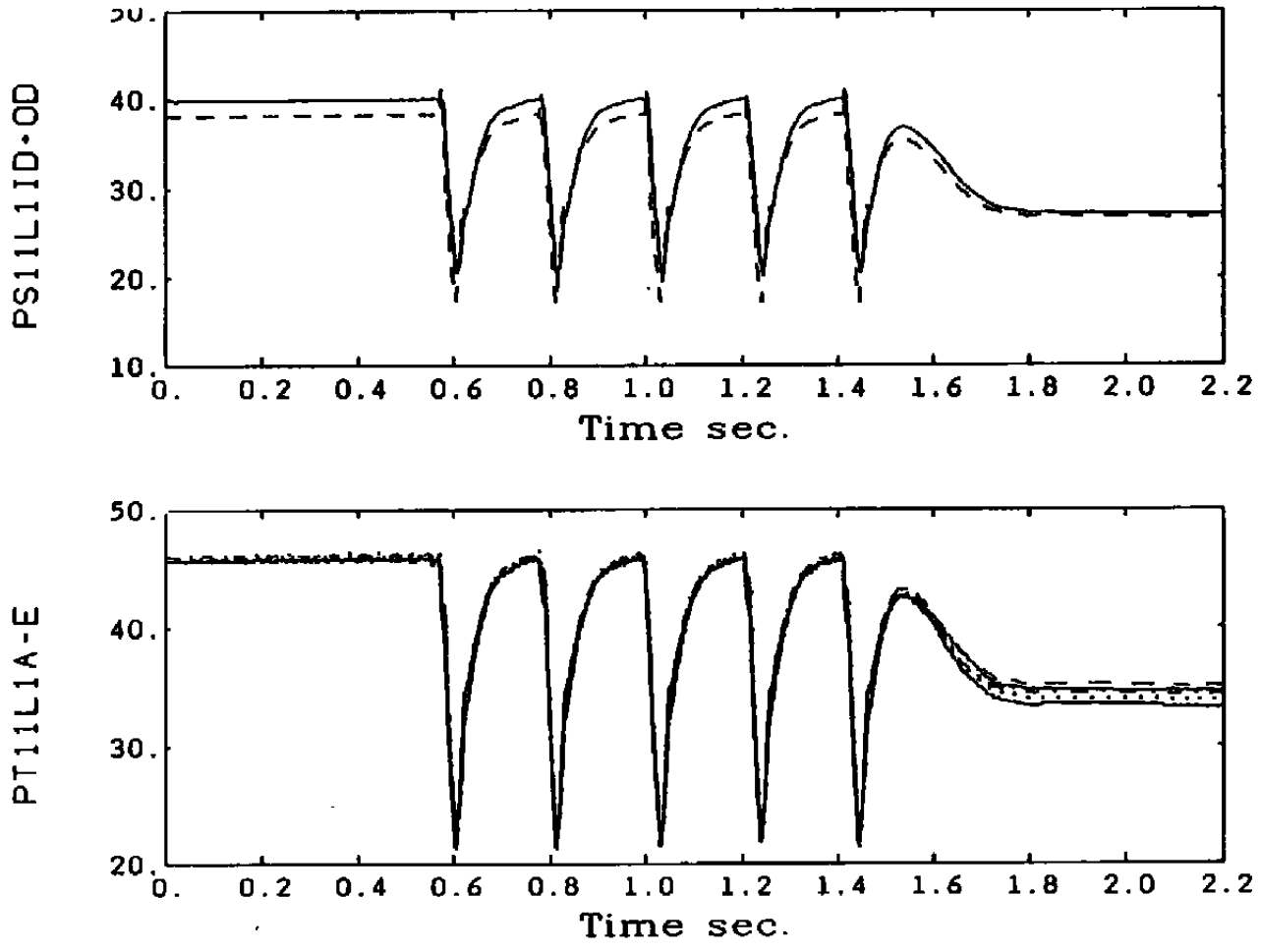

Figure 4.2.4 Static Pressure Measurements at Stage 9 Show Disturbance Over Entire Span

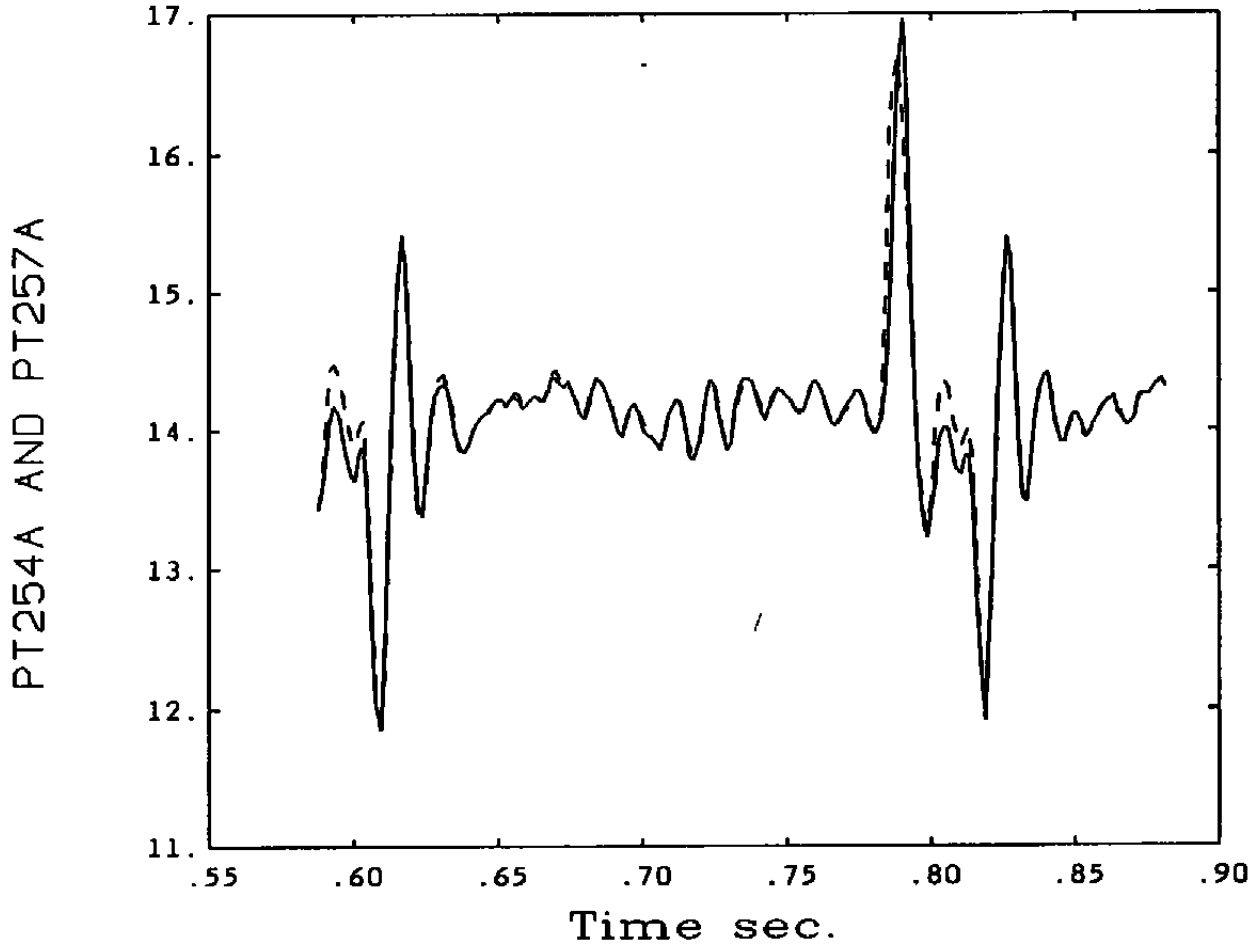

Figure 4.2.5 Circumferentially Opposite Total Pressure Probes At Inlet Show that Disturbance Is Over Entire Annulus

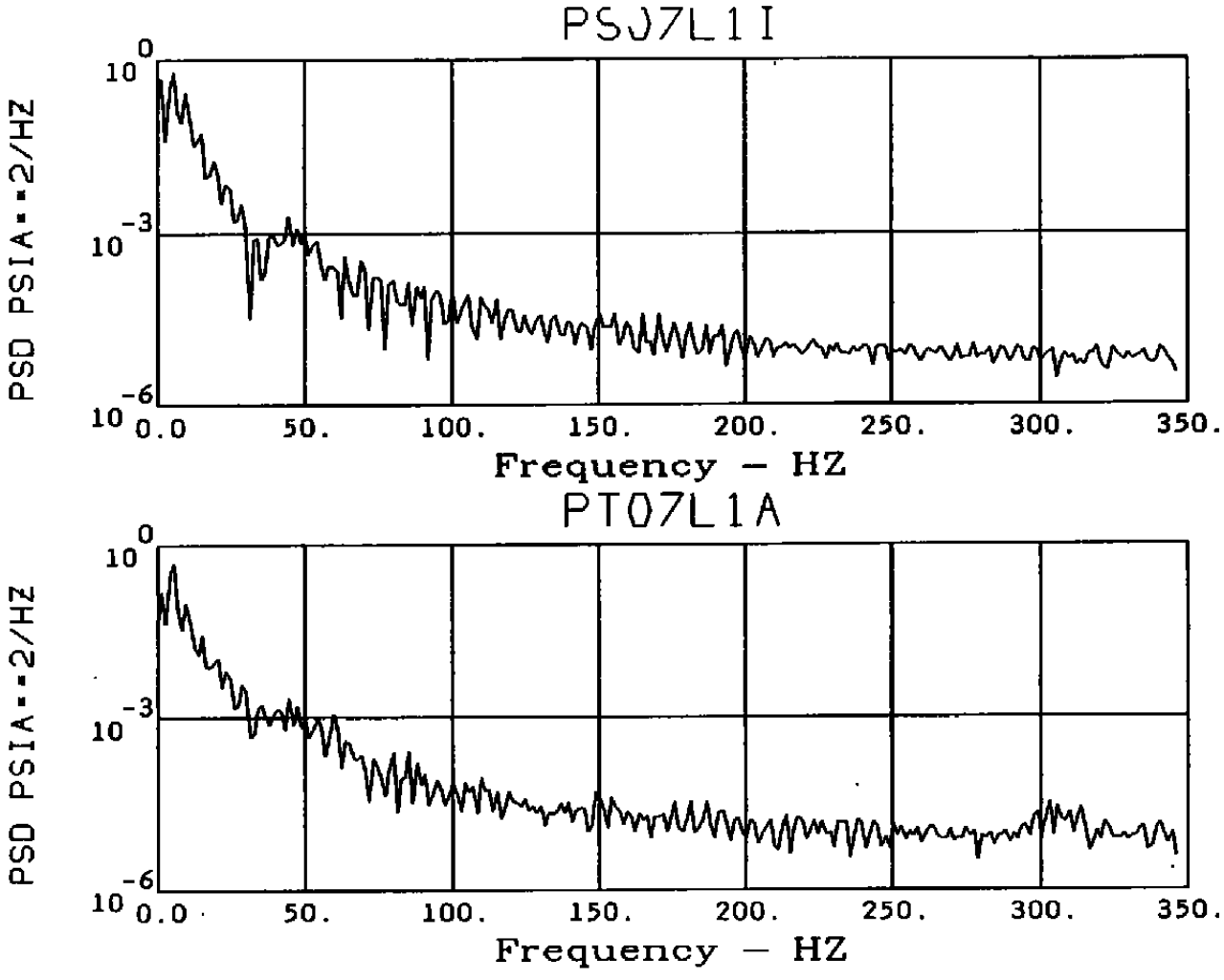

Figure 4.2.6 Power Spectral Density of Total Pressure at Stage 5

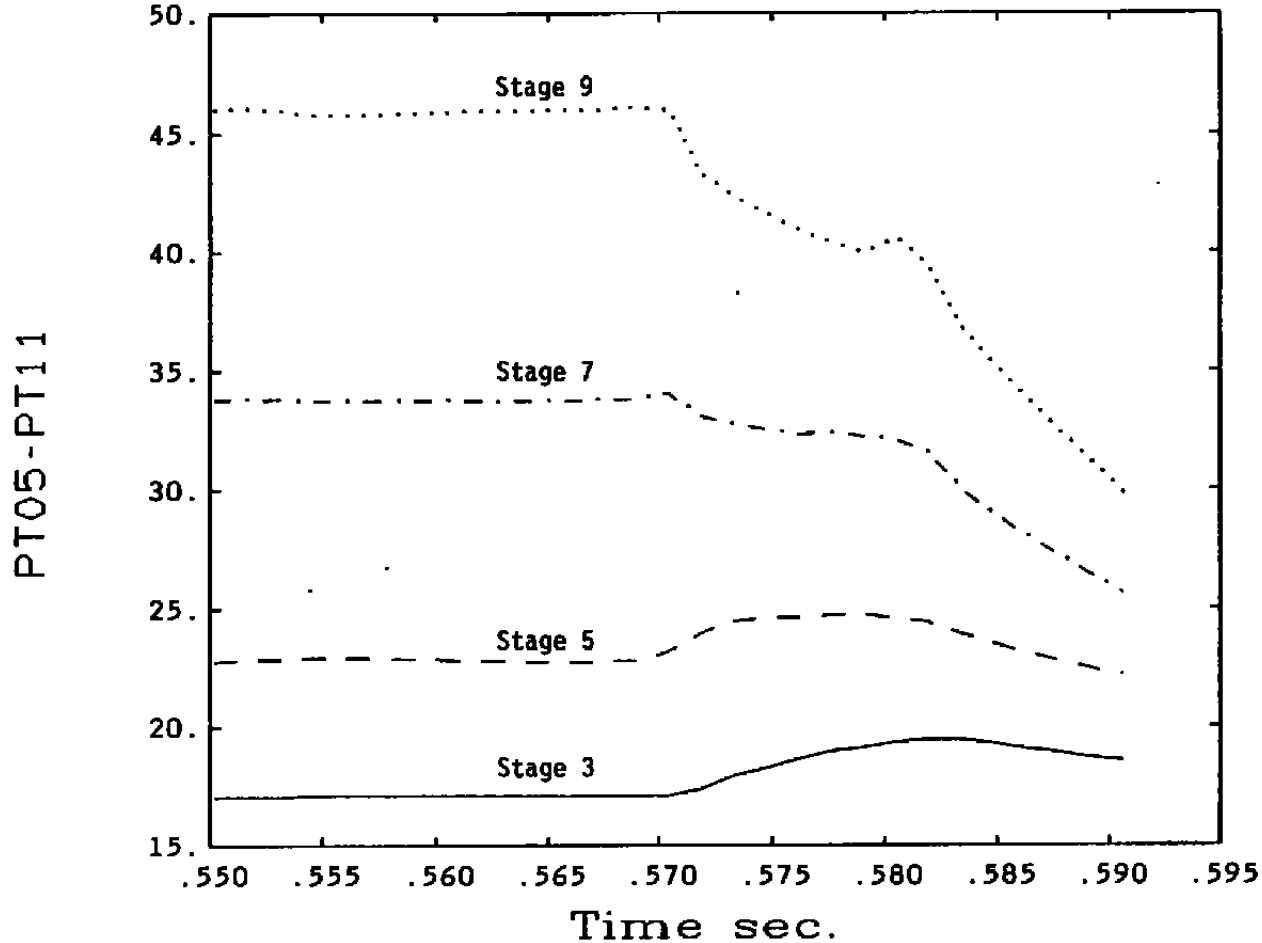

Figure 4.2.7 Total Pressures at Stages 3, 5, 7 and 9 Versus Data Point Number

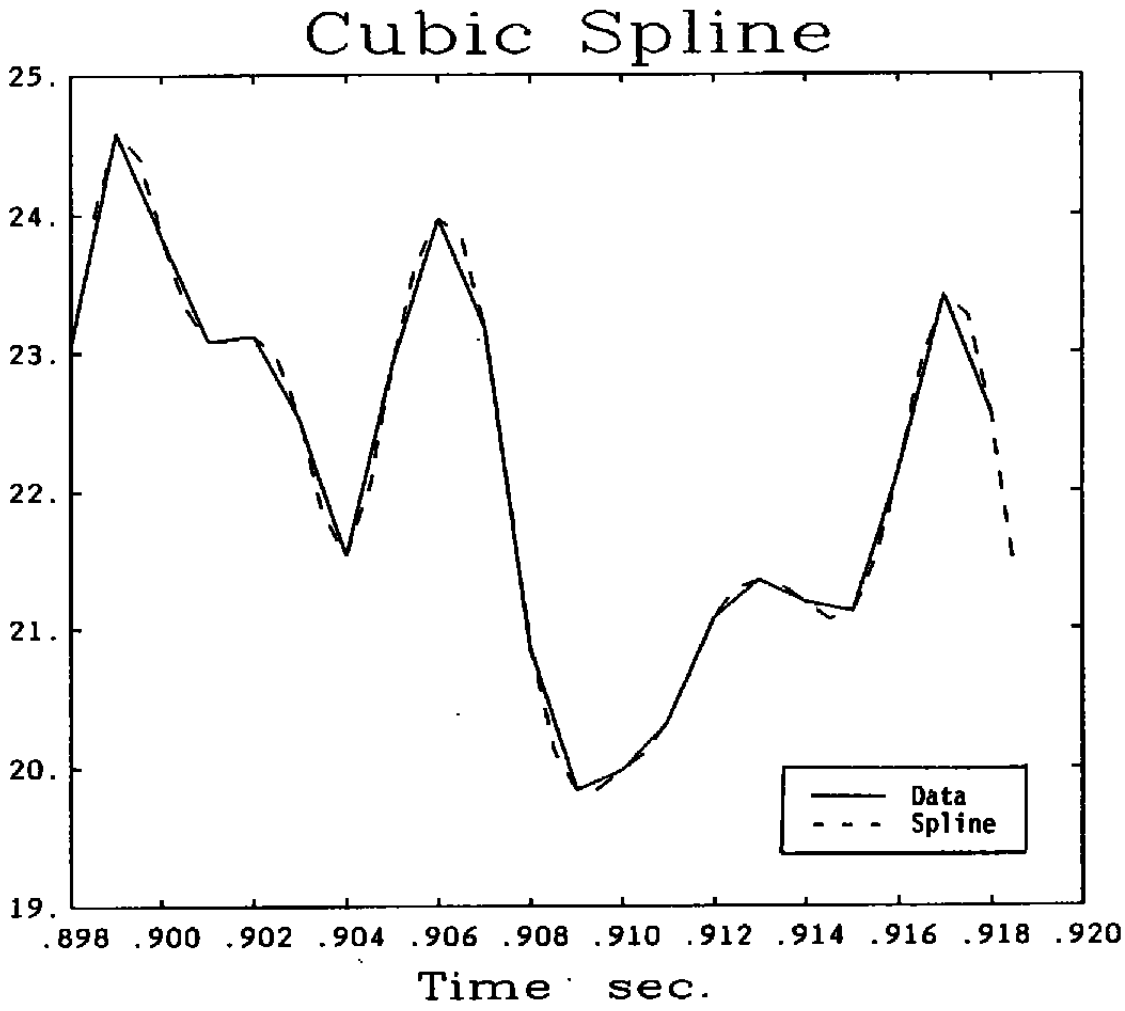

Figure 4.2.8 Comparison of Cubic Spine and Linear Fits to Stall Test Data

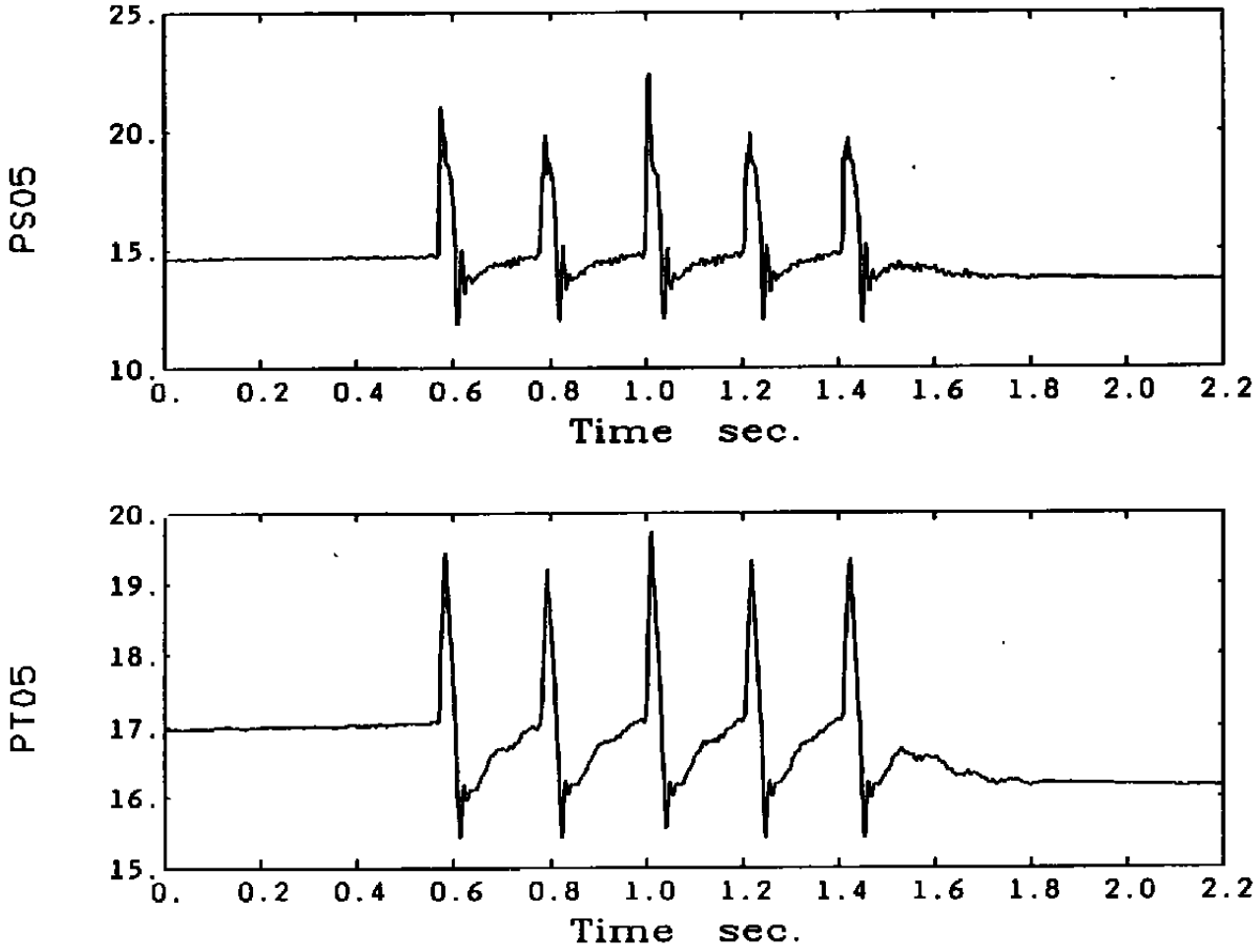

Figure 4.2.9 Sample Plots of Data Saved for Use in Estimation

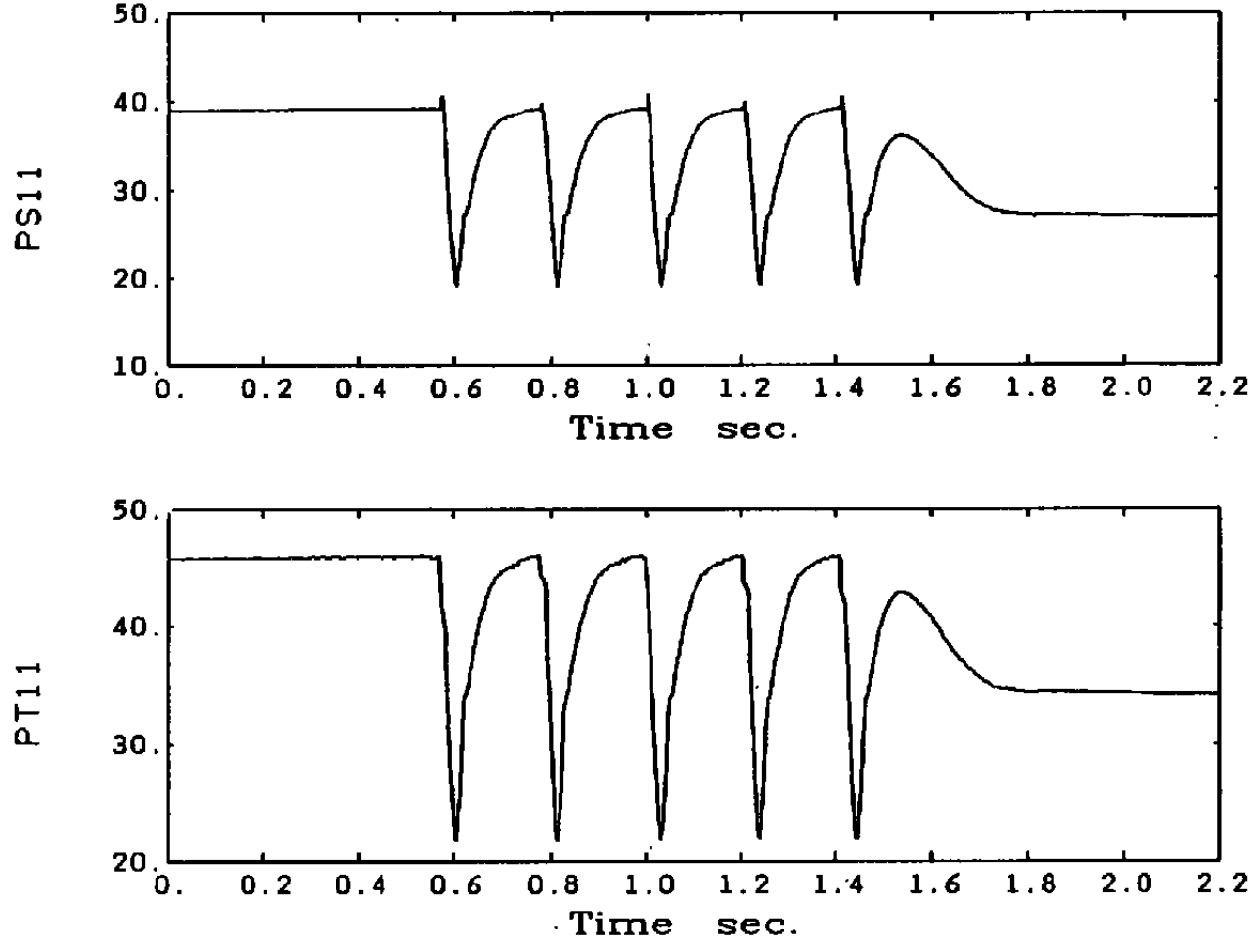

Figure 4.2.9 Sample Plots of Data Saved for Use in Estimation (Cont'd)

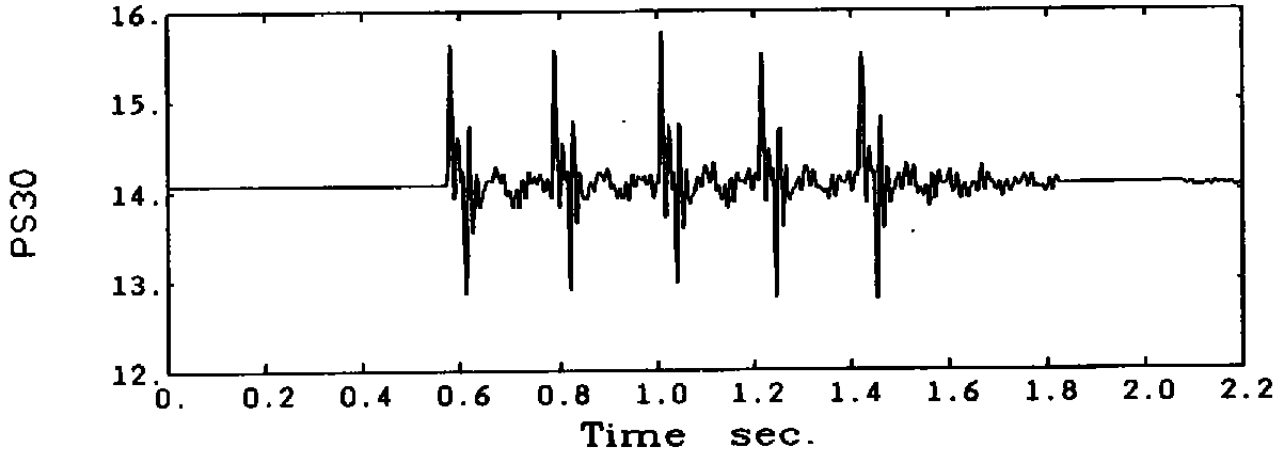

Figure 4.2.9 Sample Plots of Data Saved for Use in Estimation (Cont'd)

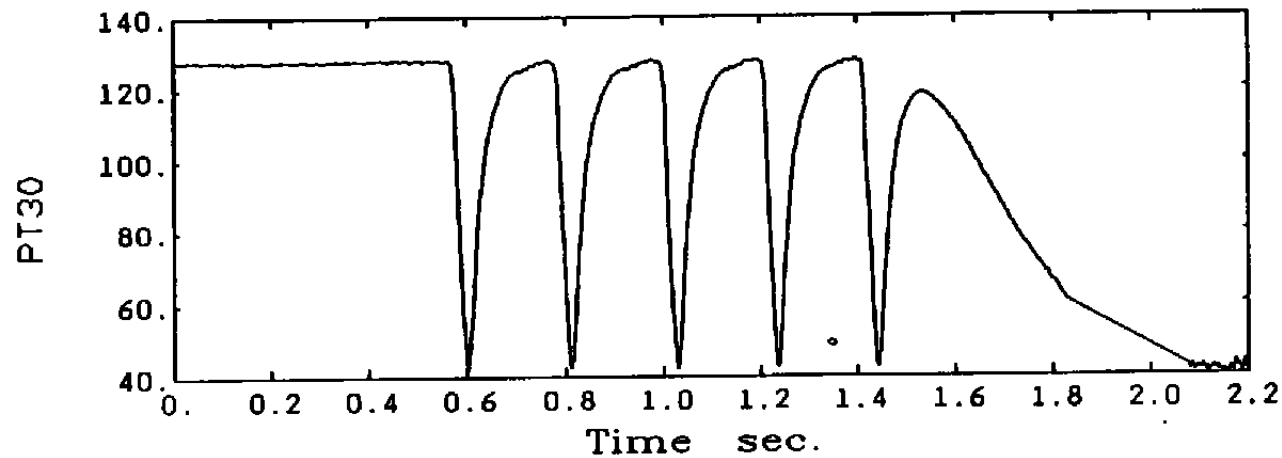

Figure 4.2.9 Sample Plots of Data Saved for Use in Estimation (Cont'd)

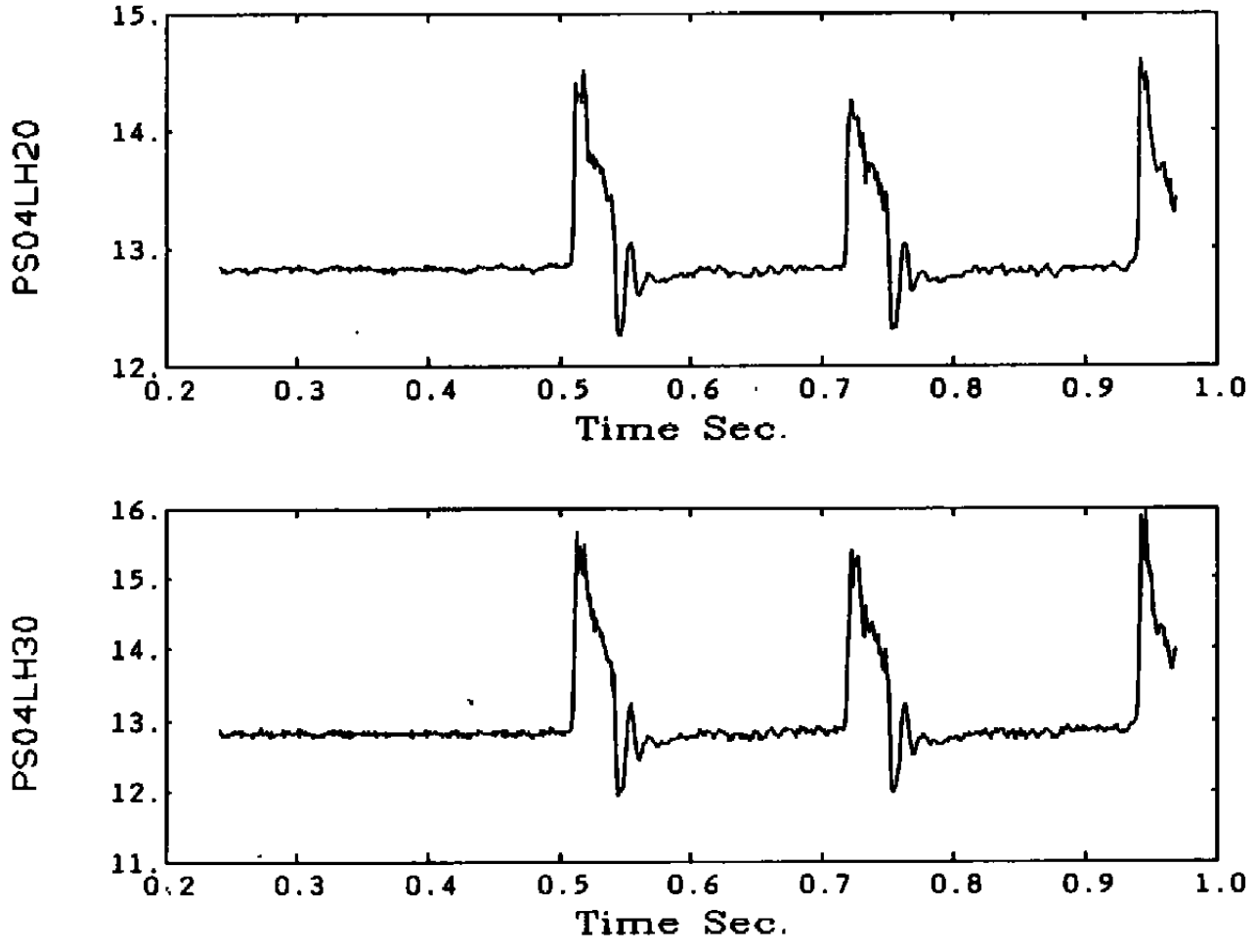

Figure 4.3.1 Interstage Static Pressures from Analog Recorded Data at 82% Speed

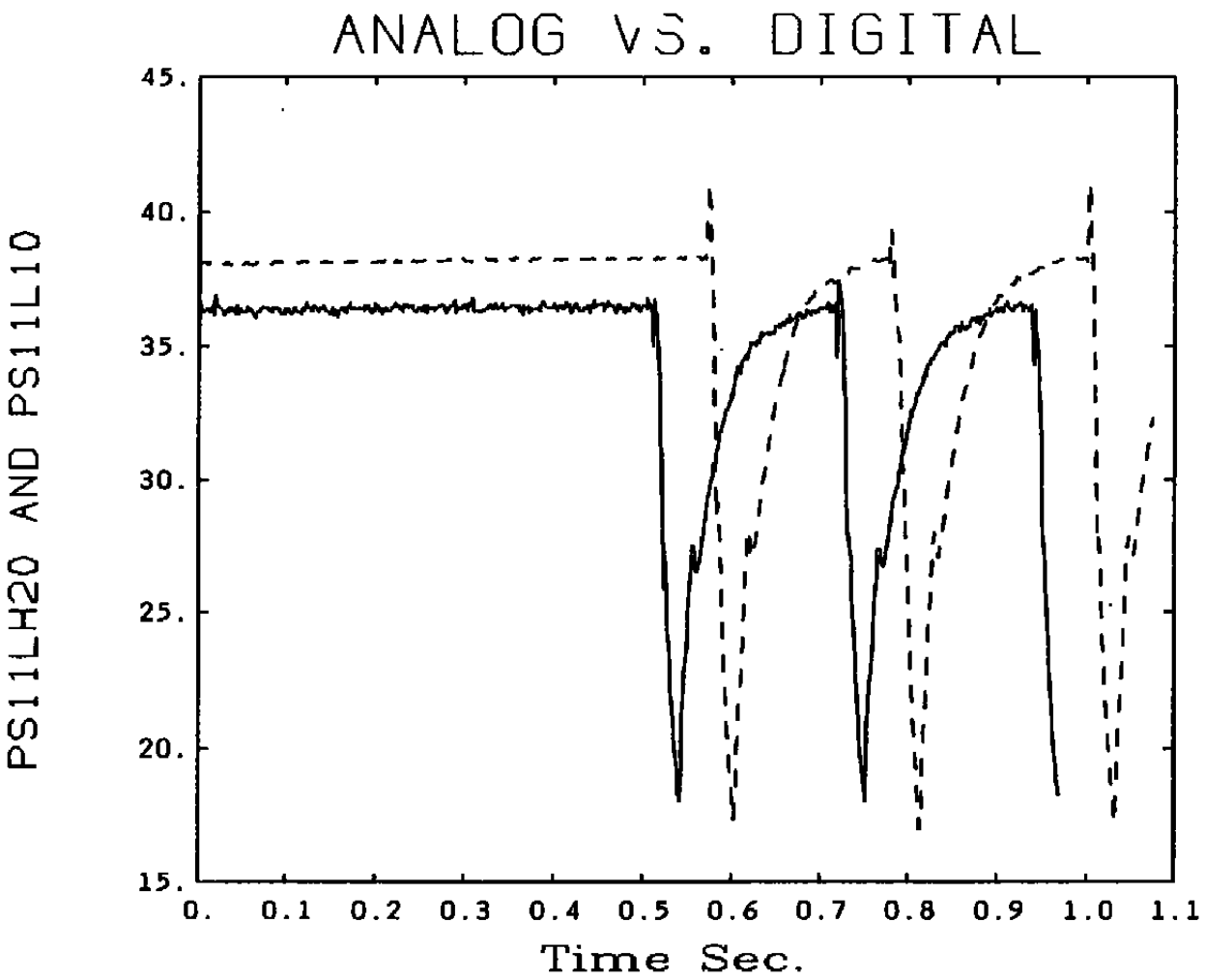

Figure 4.3.2 Comparison of Static Pressure at Station 11 from Digital and Analog Recorded Data Sets

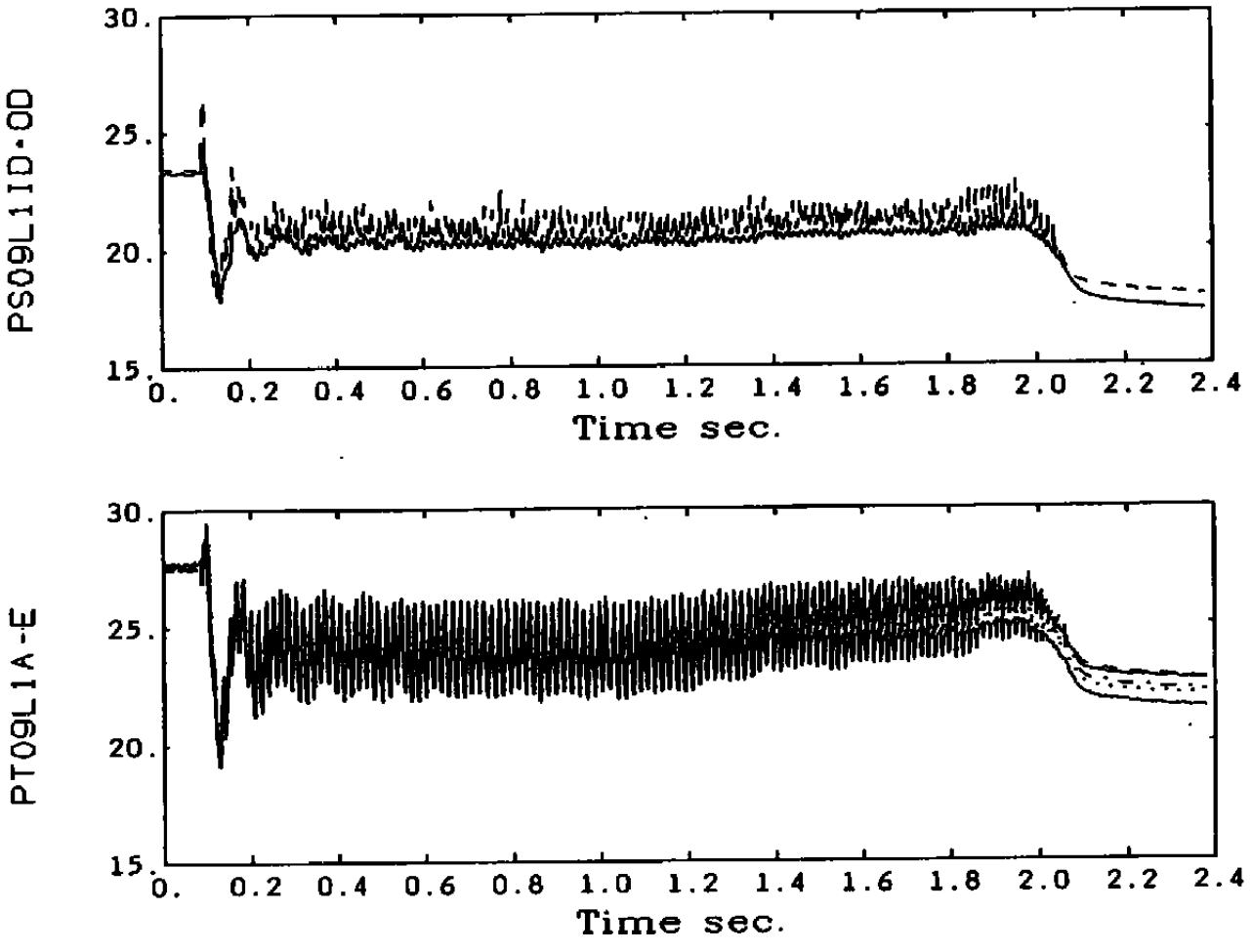

Figure 4.4.1 Interstage Pressure Measurements from Digitally Recorded Data at 78.5% Speed

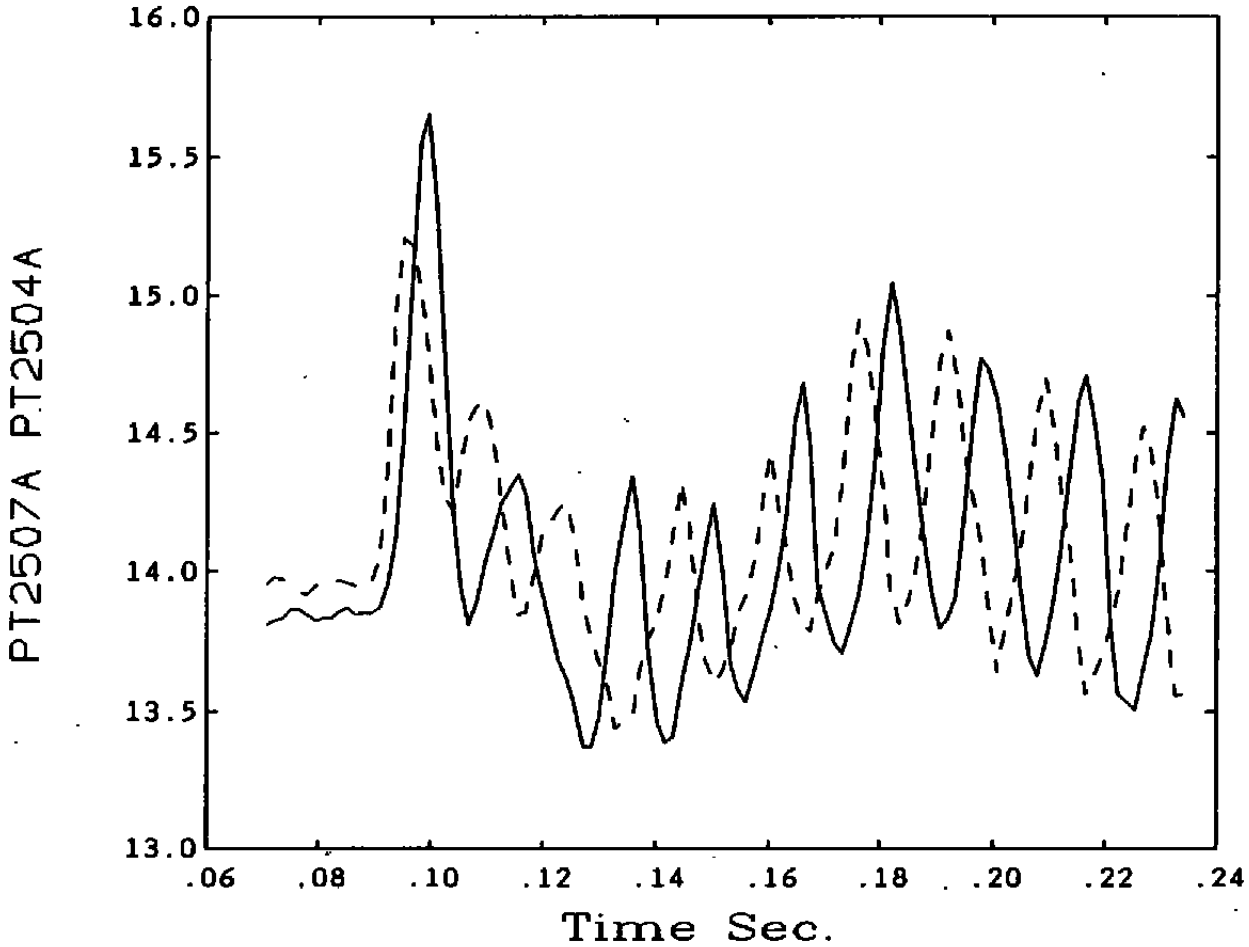

Figure 4.4.2 Circumferentially Separated Total Pressure Measurements at Inlet Show Movement of Single Stall Call Around Annulus

Figure 4.4.3 Total Pressure at Stage 5

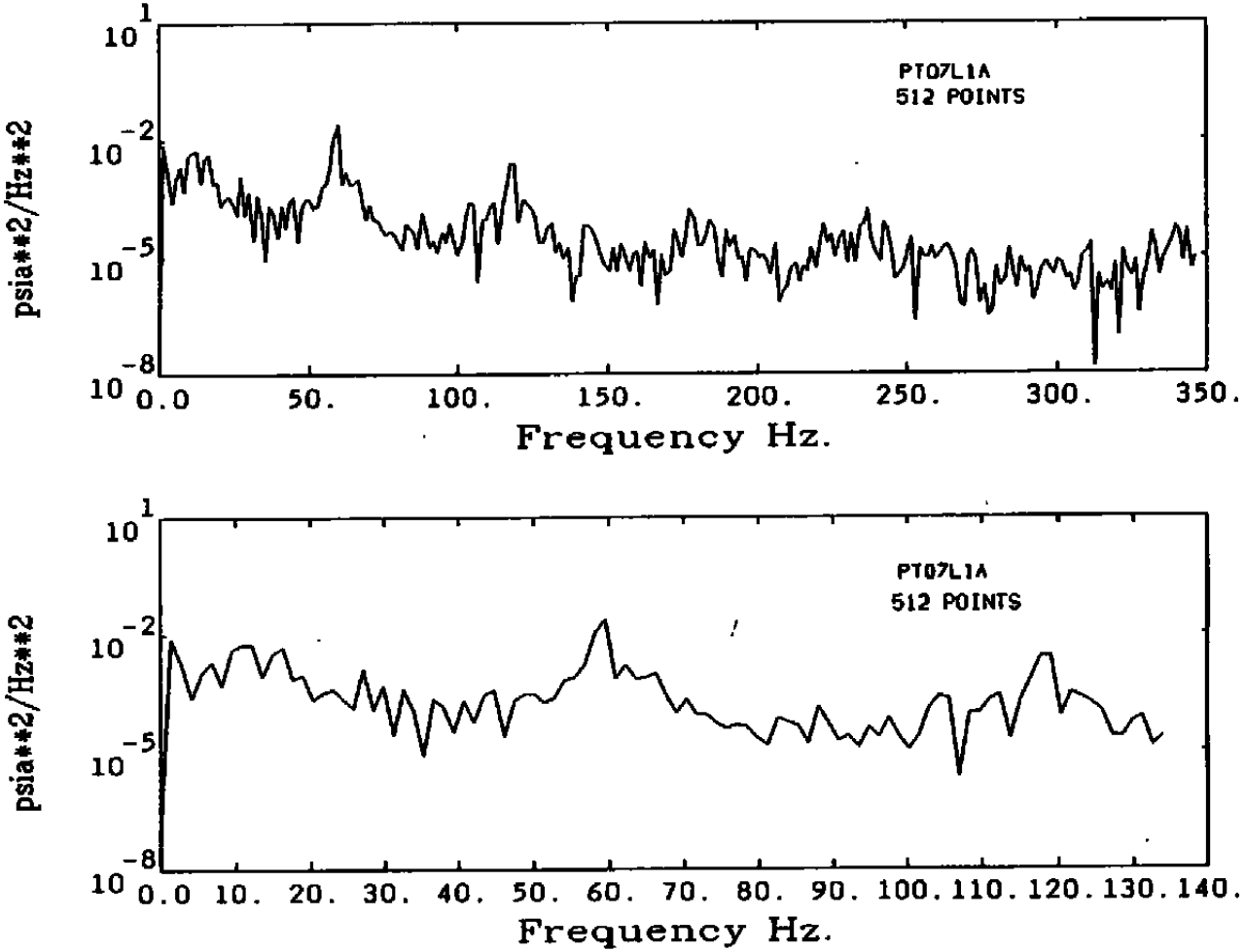

Figure 4.4.4 Power Spectral Densities of Total Pressure at Stage 5

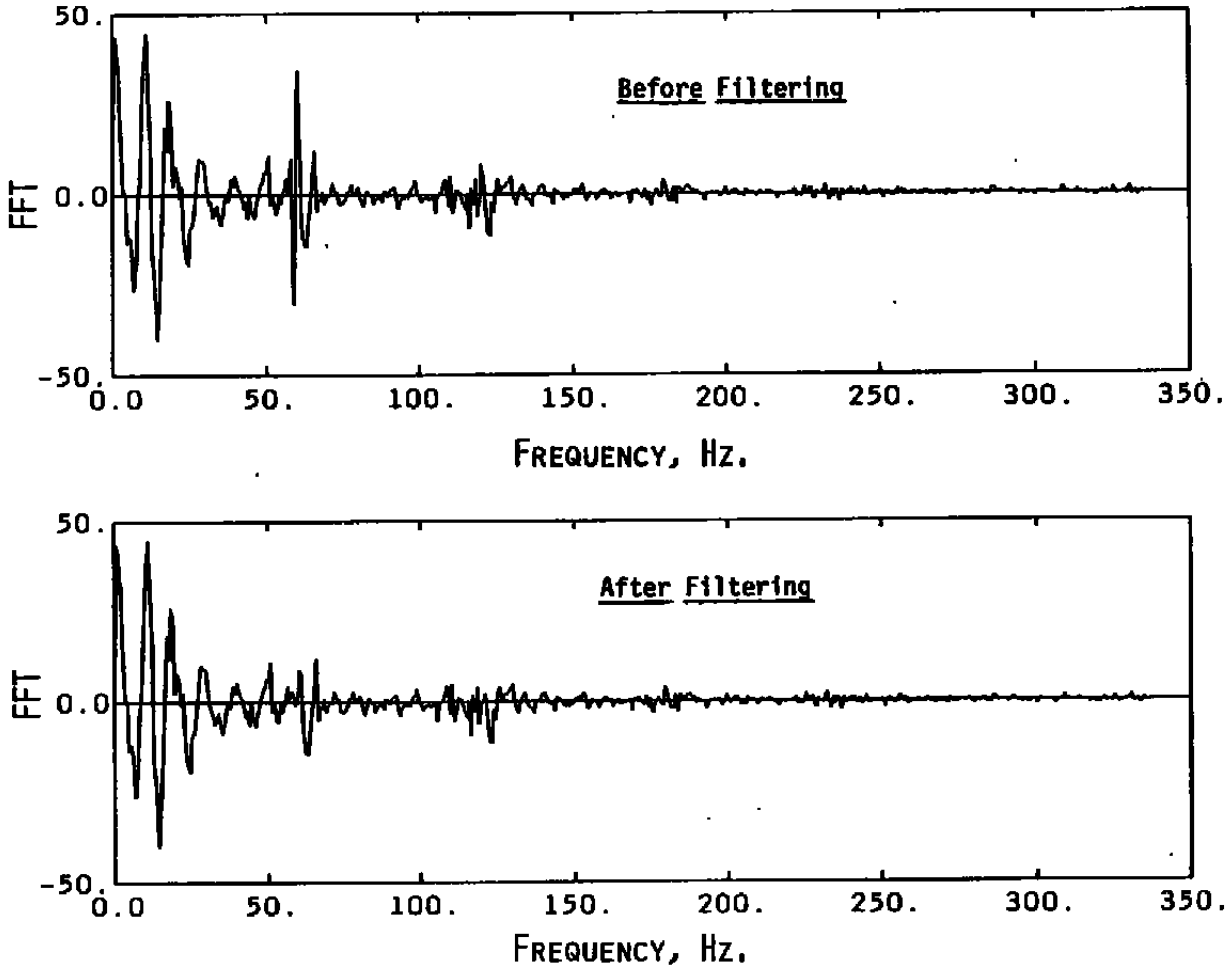

Figure 4.4.5 Fourier Transform of Total Pressure at Stage 5 Before And After Notching

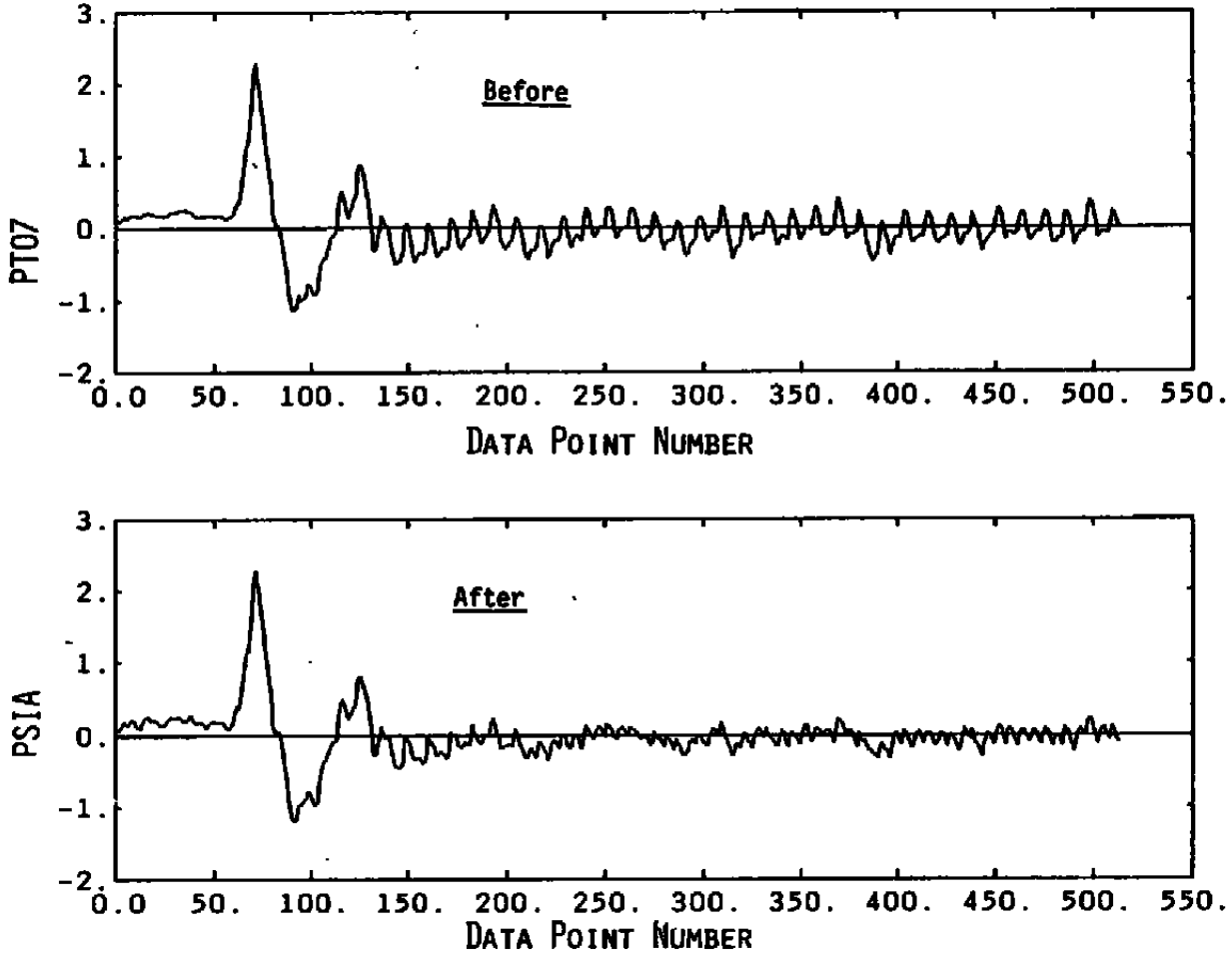

Figure 4.4.6 Total Pressure Signal Before and After Spectral Filtering

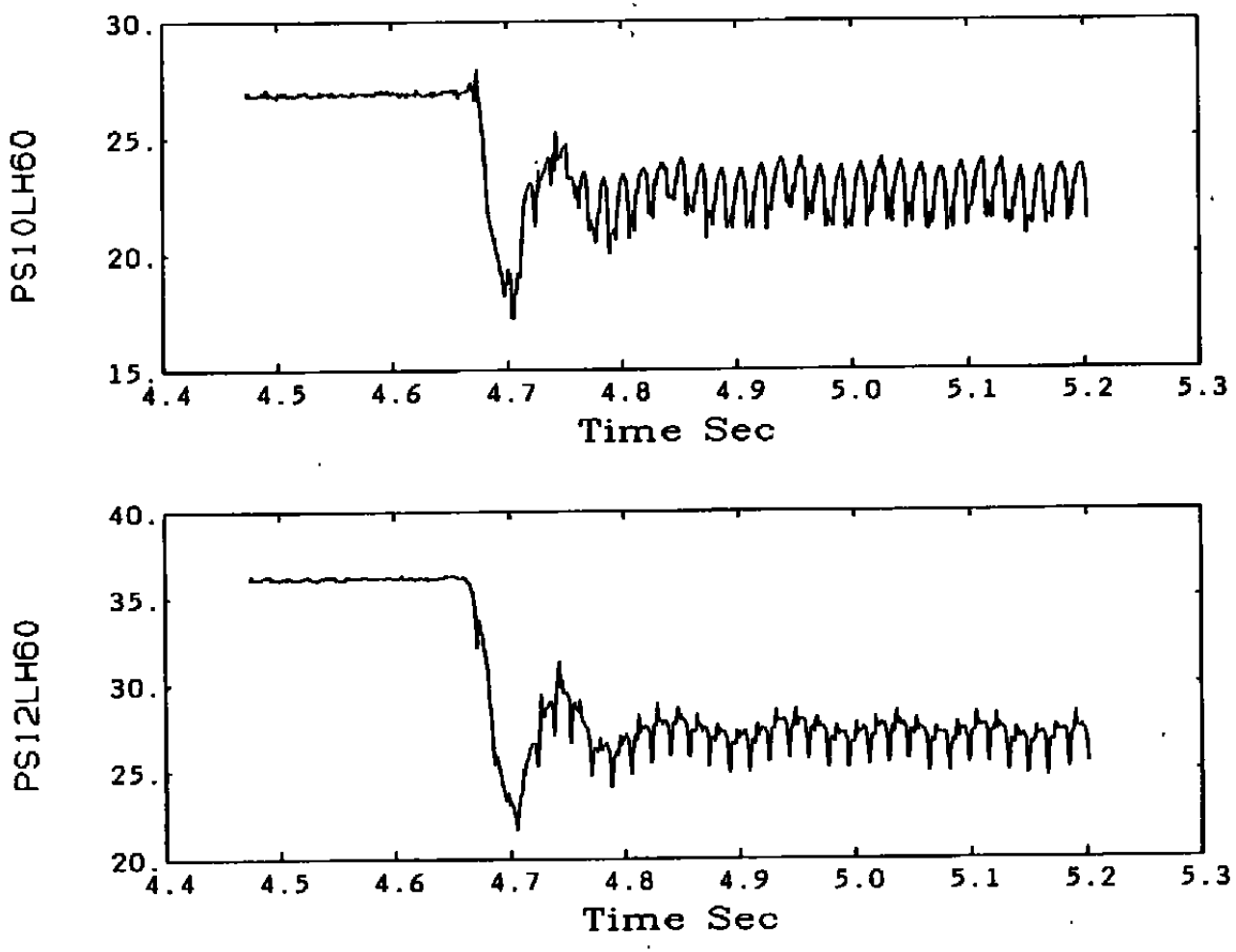

Figure 4.5.1 Stage 8 and 10 Static Pressures from Digital Analog Data at 78.5% Speed

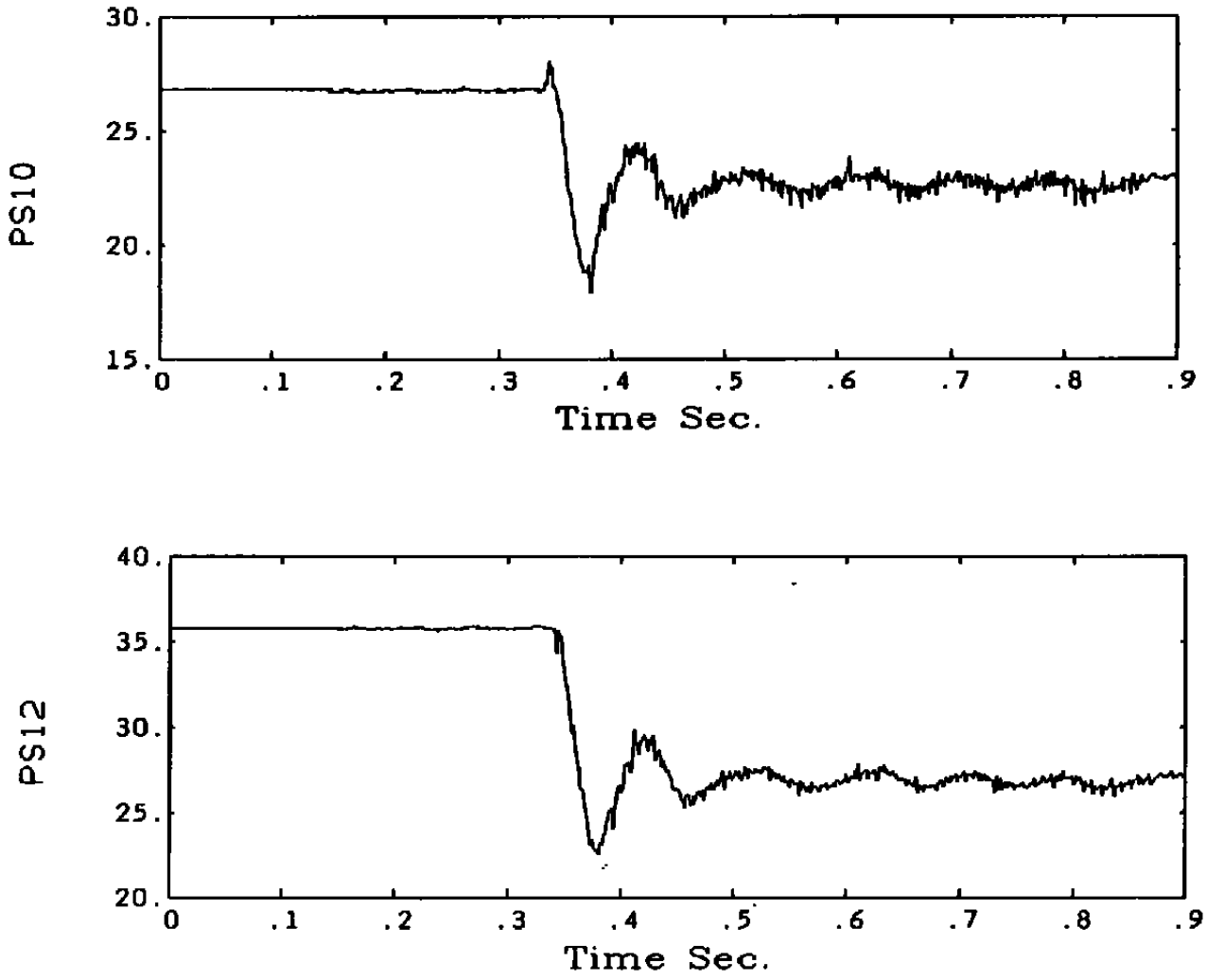

Figure 4.5.2 Resampled, Filtered and Averaged Static Pressure Measurements at Stages 8 and 10

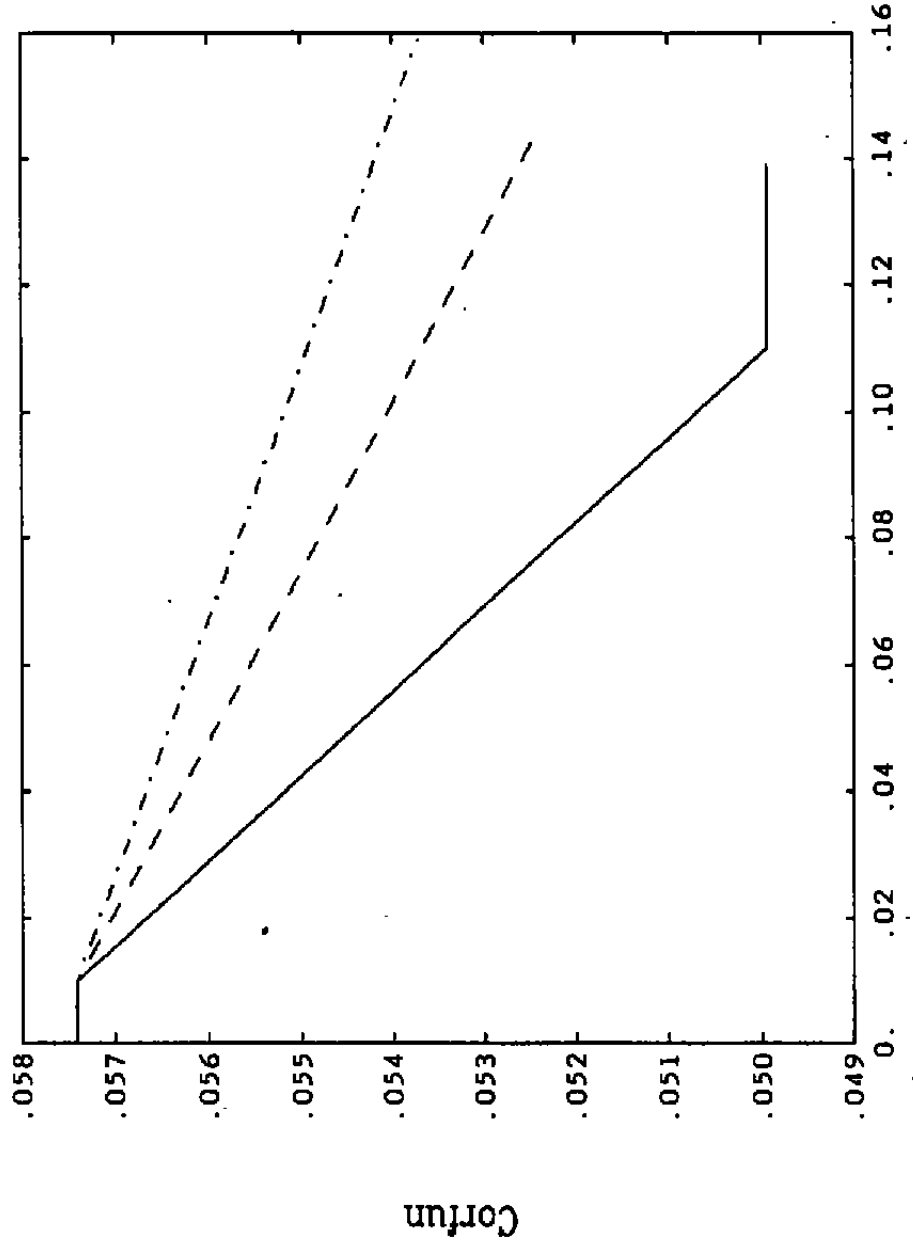

Figure 5.1.1 Three Throttling Function Ramps Used in Evaluation

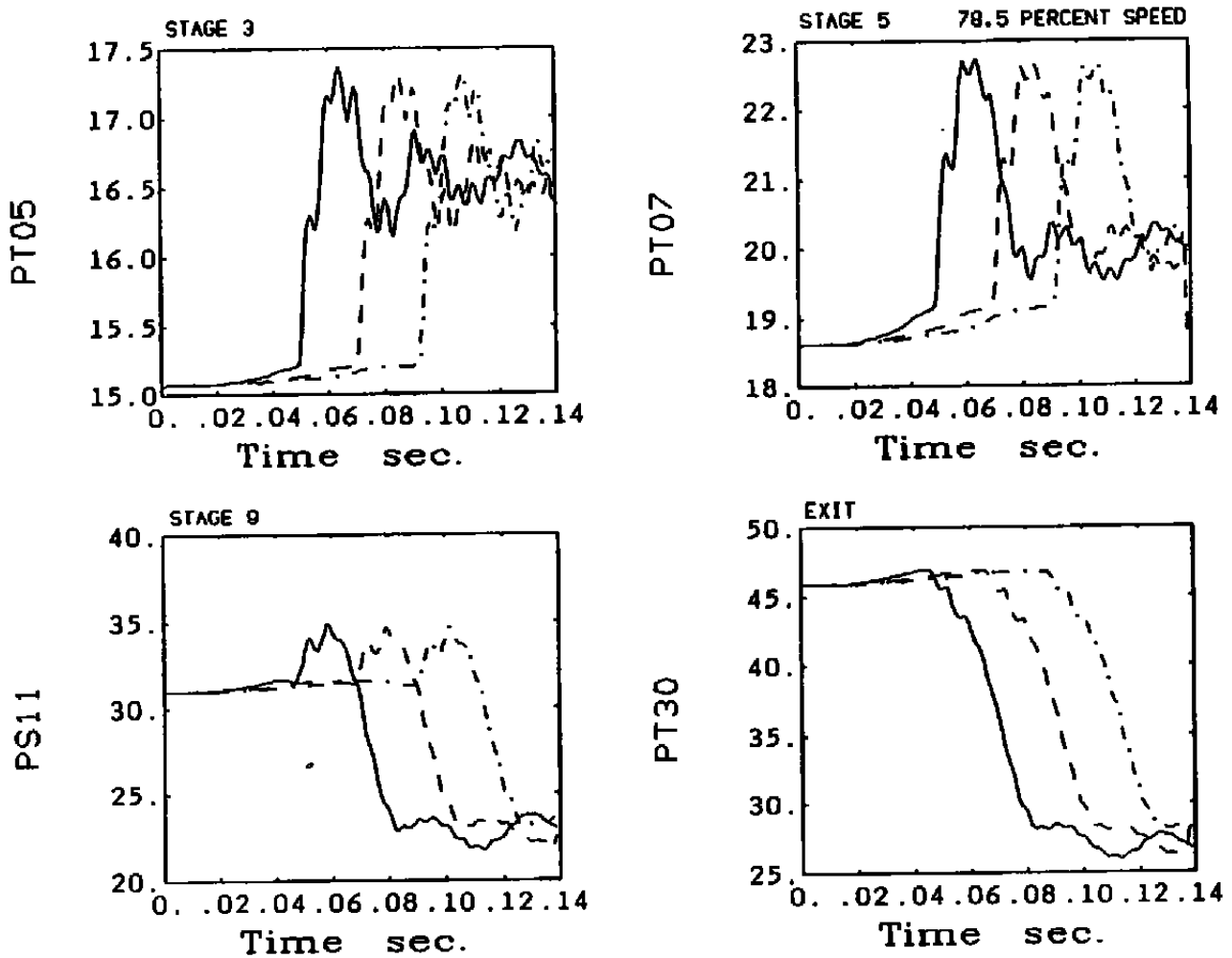

Figure 5.1.2 Transient Outputs Produced by Inputs in Figure 5.1.1

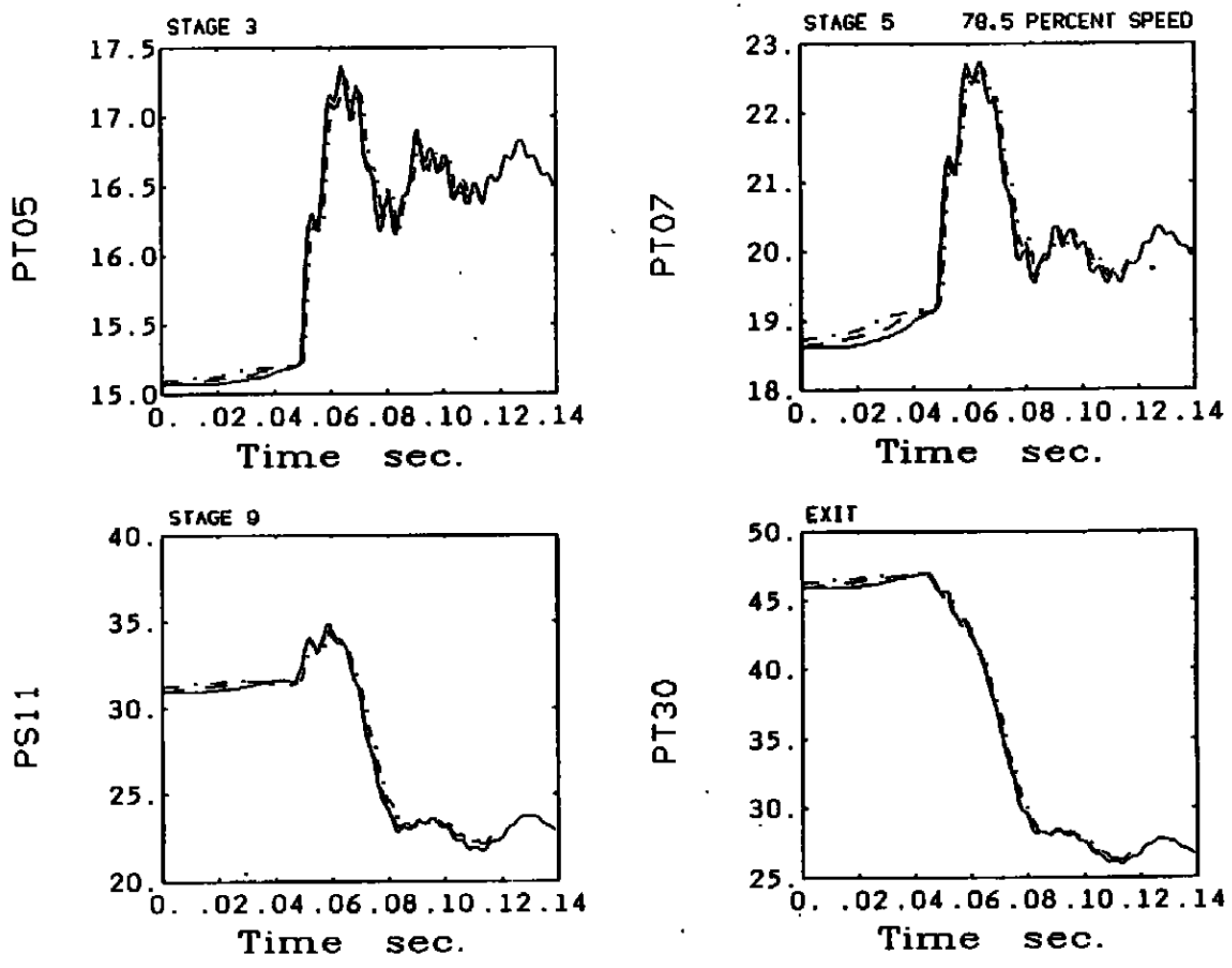

Figure 5.1.3 Throttle Function Ramp Transients Aligned in Time

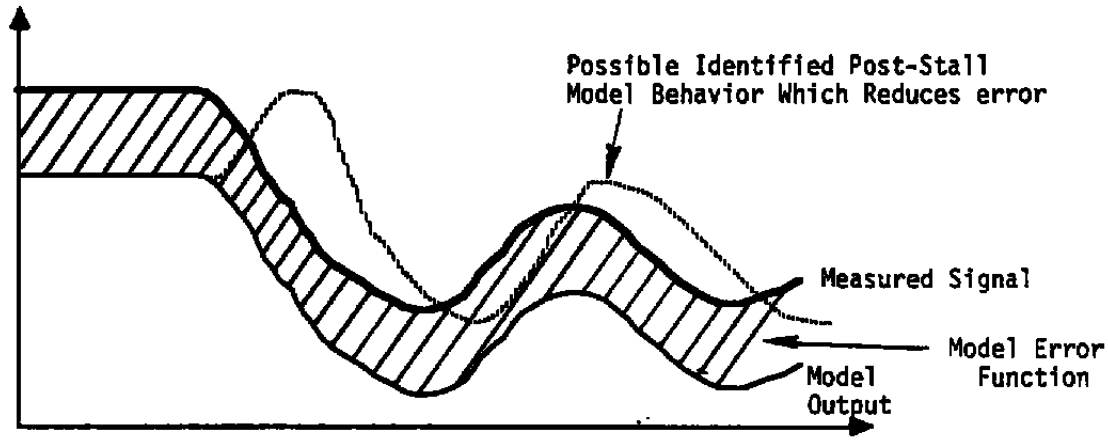

Figure 5.2.1 Prestall Mismatch Will Bias Parameter Estimates

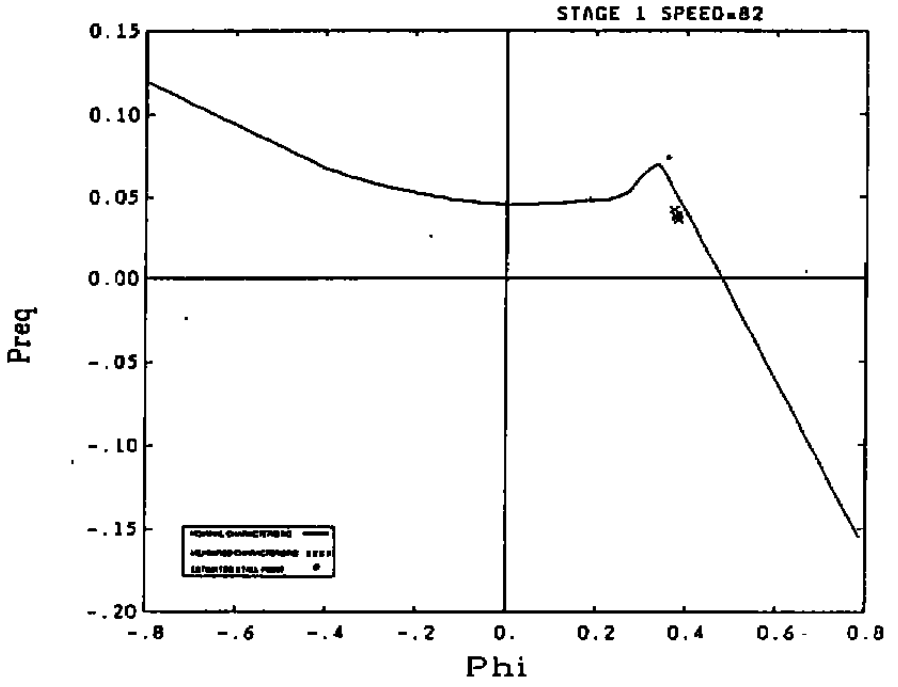

Figure 6.2.1 Estimated Stall Points Compared to Nominal and Measured Characteristics

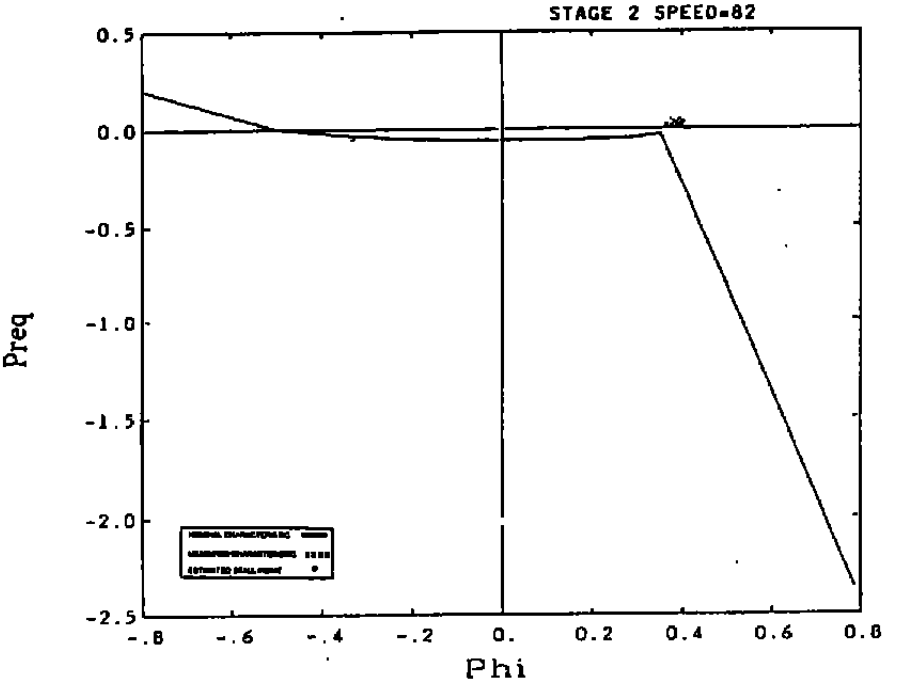

Figure 6.2.1 Estimated Stall Points Compared to Nominal and Measured Characteristics (Cont'd)

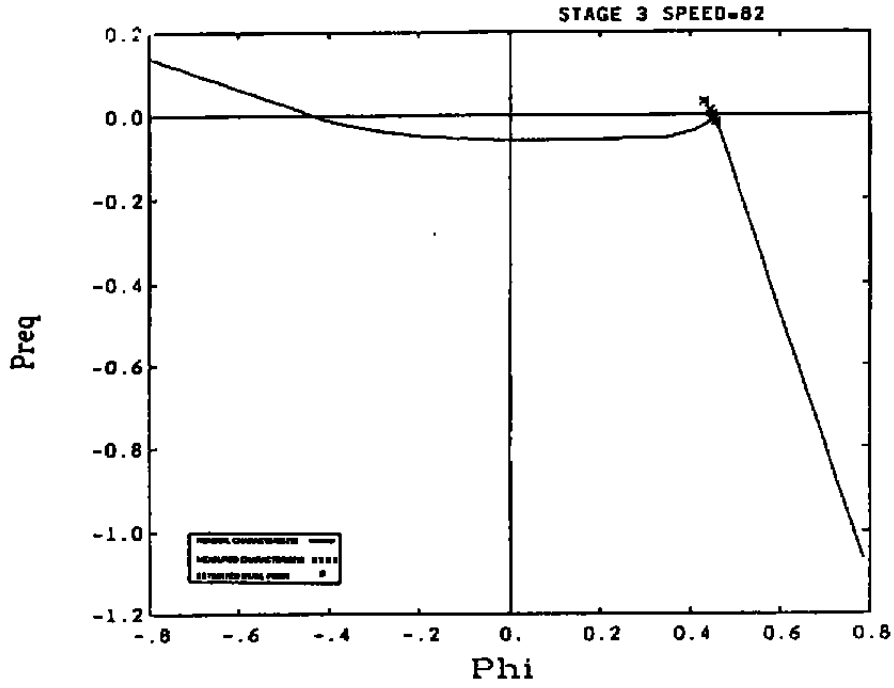

Figure 6.2.1 Estimated Stall Points Compared to Nominal and Measured Characteristics (Cont'd)

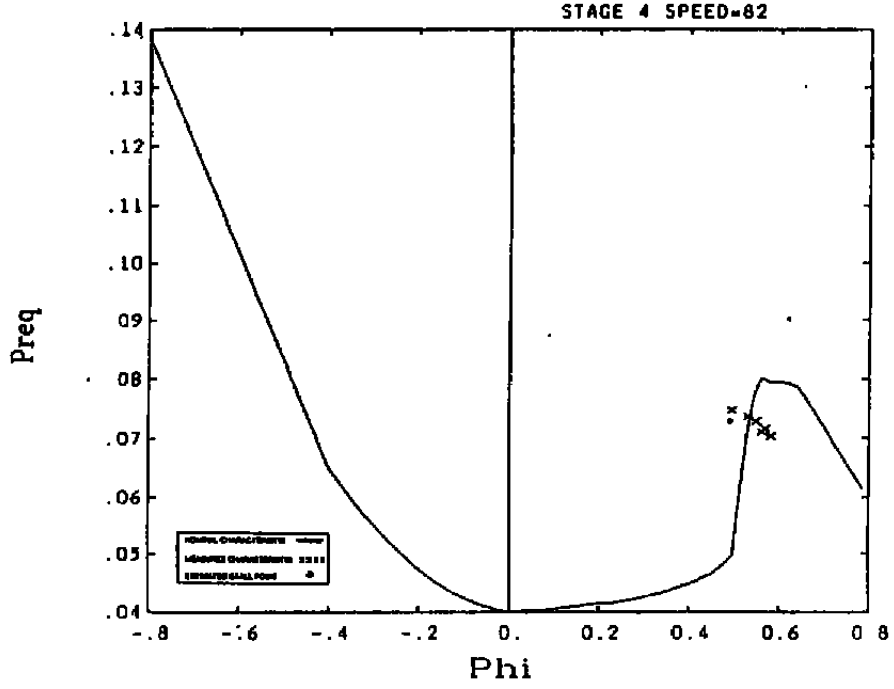

Figure 6.2.1 Estimated Stall Points Compared to Nominal and Measured Characteristics (Cont'd)

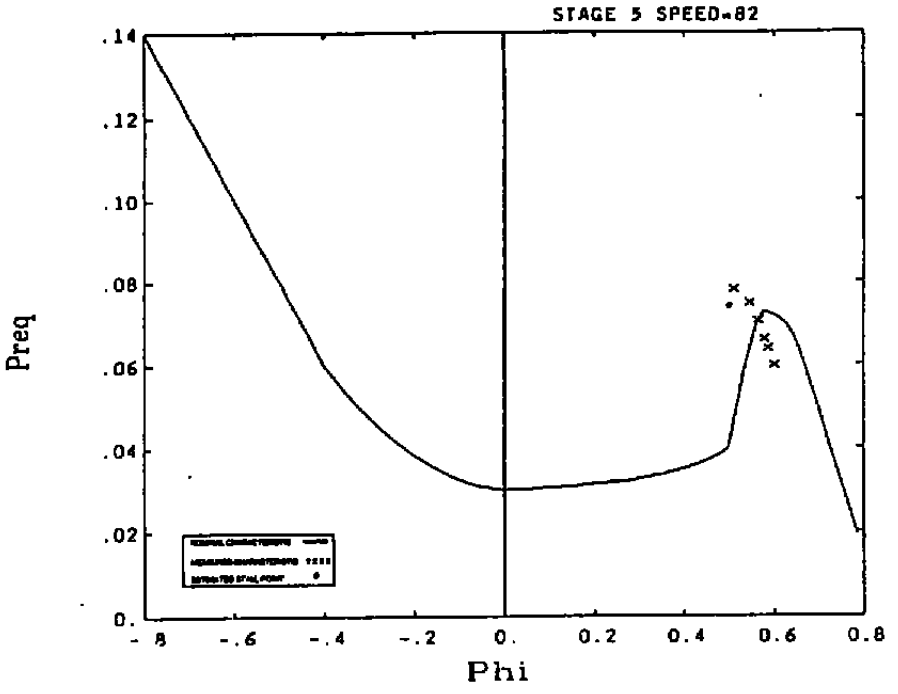

Figure 6.2.1 Estimated Stall Points Compared to Nominal and Measured Characteristics (Cont'd)

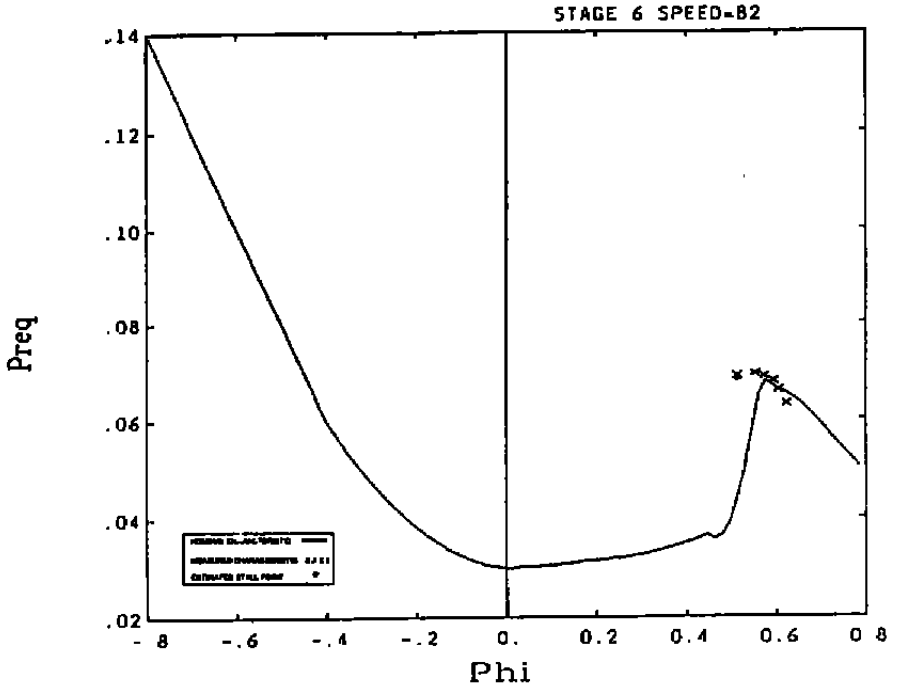

Figure 6.2.1 Estimated Stall Points Compared to Nominal and Measured Characteristics (Cont'd)

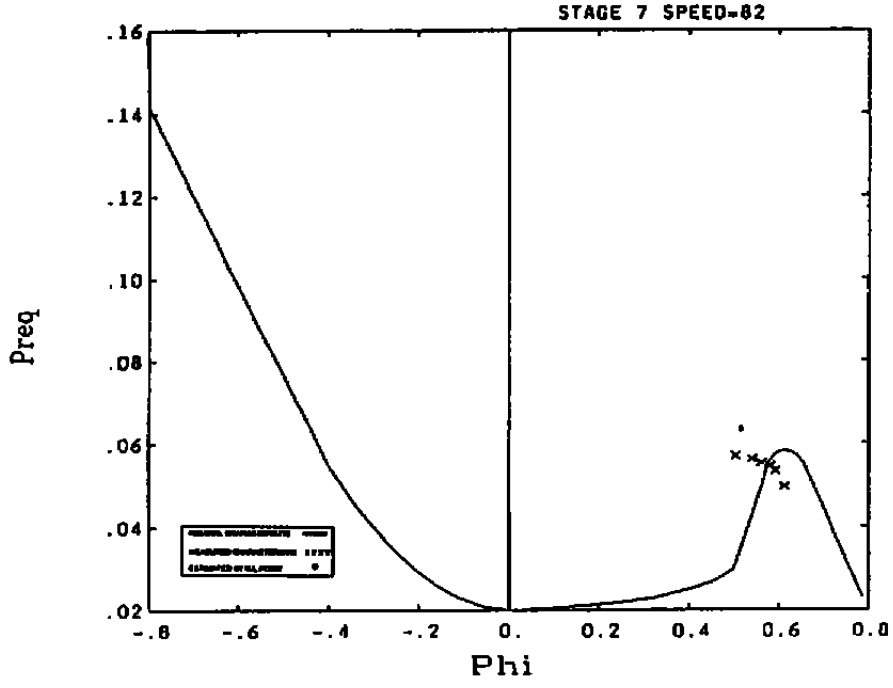

Figure 6.2.1 Estimated Stall Points Compared to Nominal and Measured Characteristics (Cont'd)

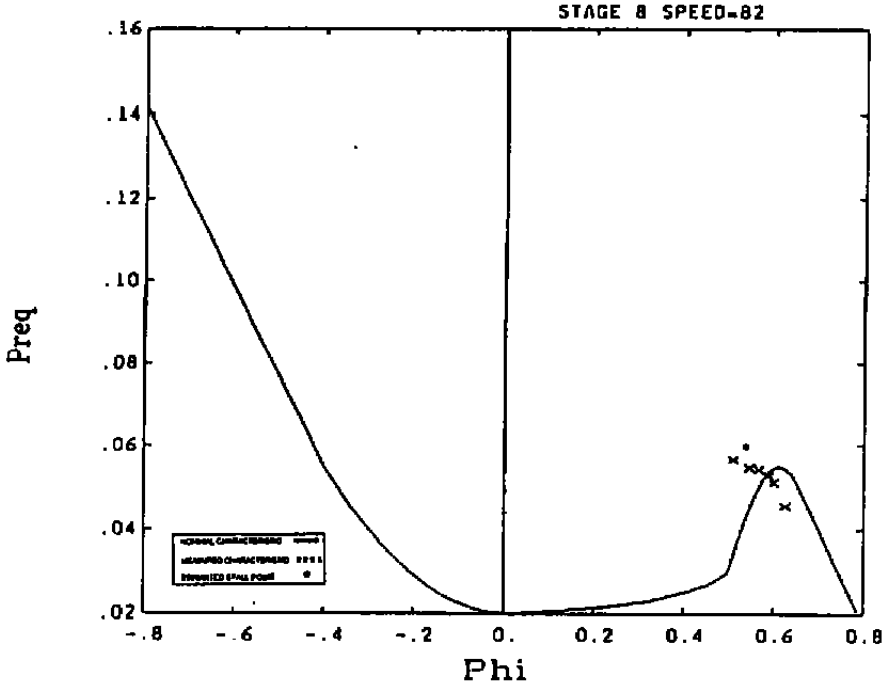

Figure 6.2.1 Estimated Stall Points Compared to Nominal and Measured Characteristics (Cont'd)

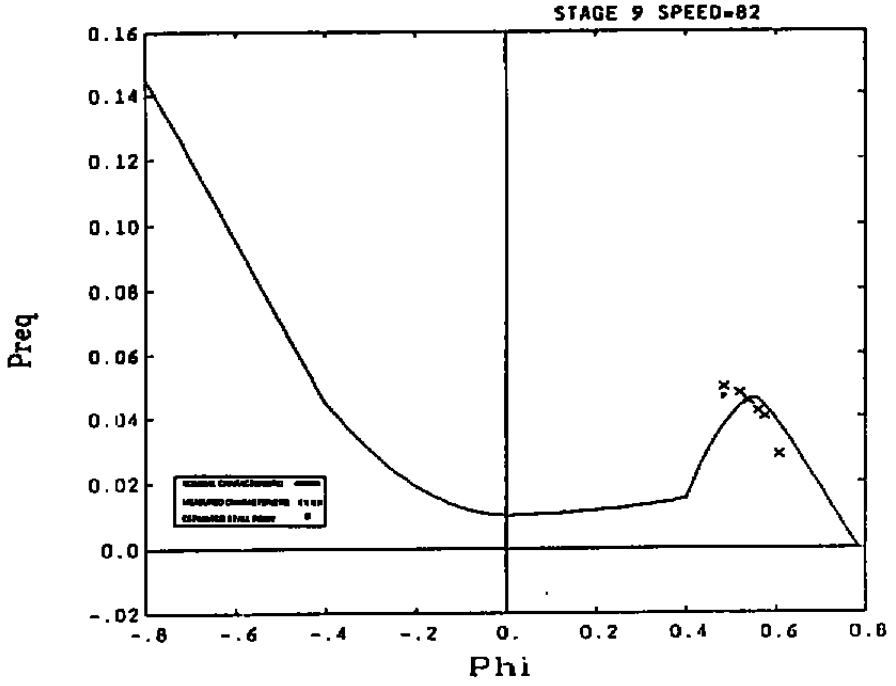

Figure 6.2.1 Estimated Stall Points Compared to Nominal and Measured Characteristics (Cont'd)

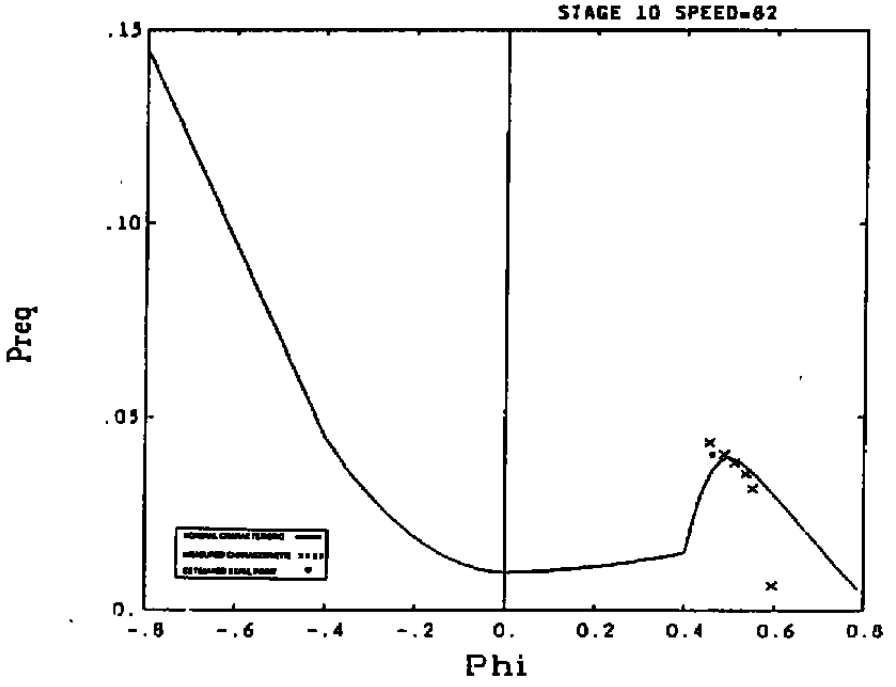

Figure 6.2.1 Estimated Stall Points Compared to Nominal and Measured Characteristics (Cont'd)

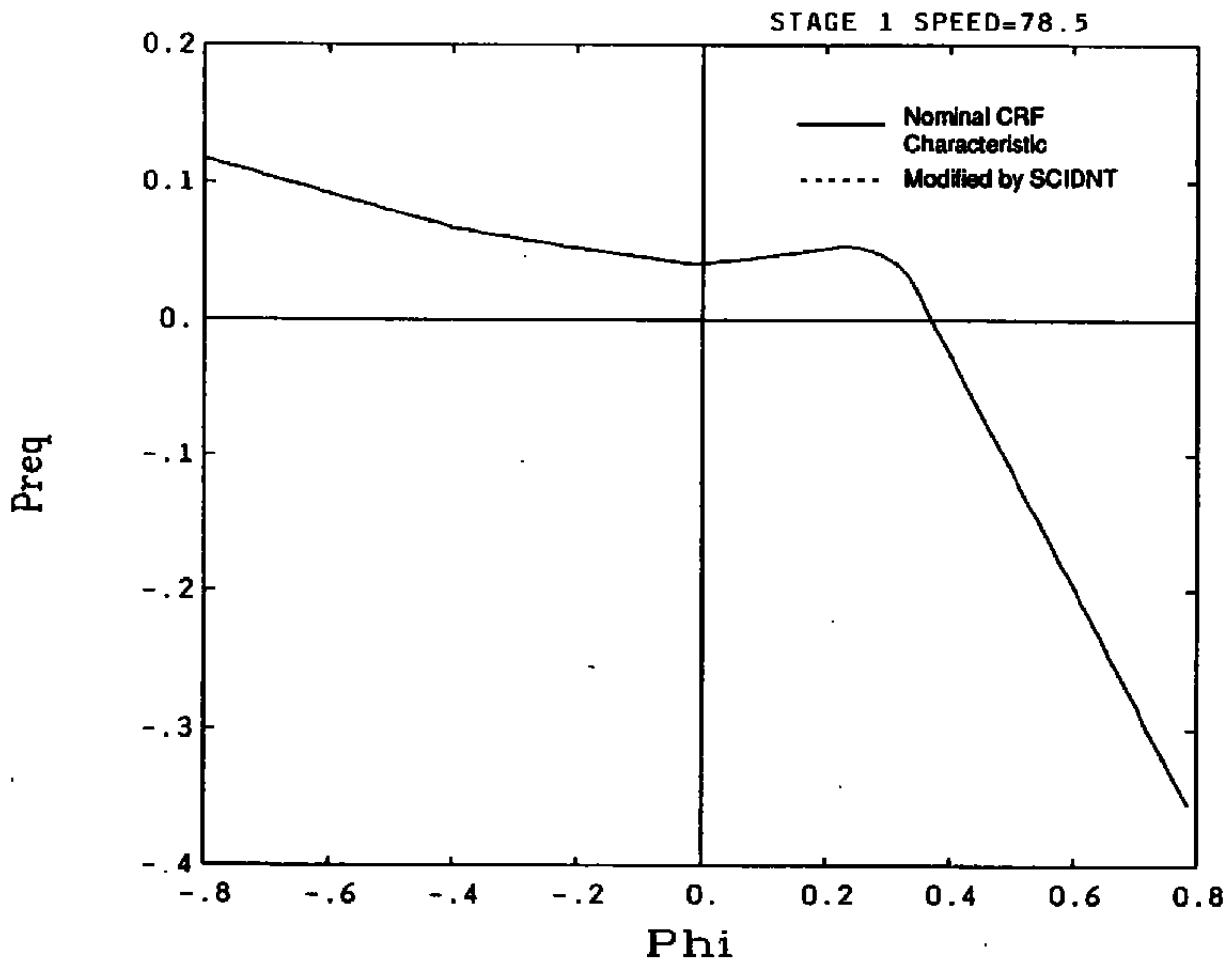

Figure 6.5.1 Estimated Poststall Stage Characteristics

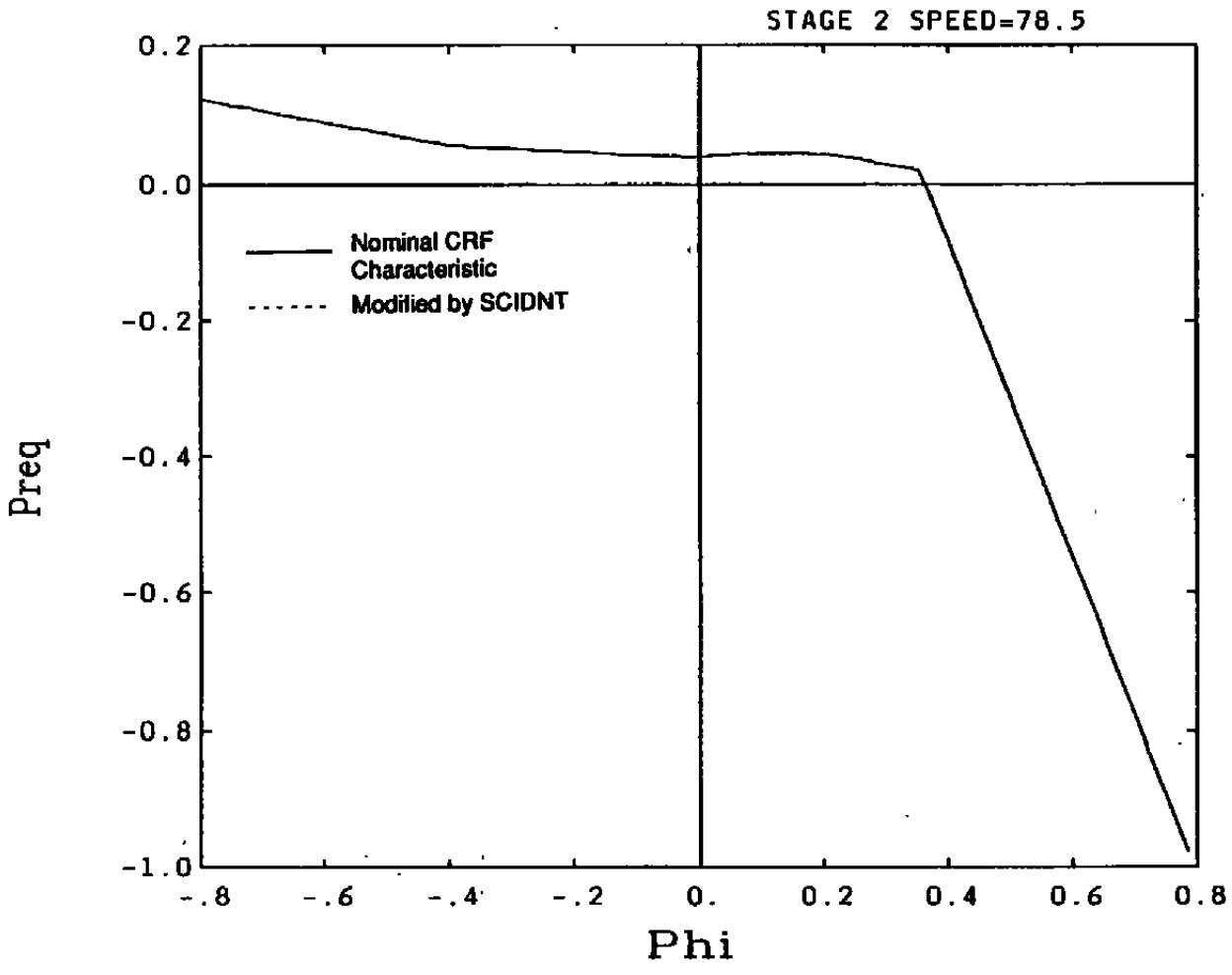

Figure 6.5.1 Estimated Poststall Stage Characteristics (Continued)

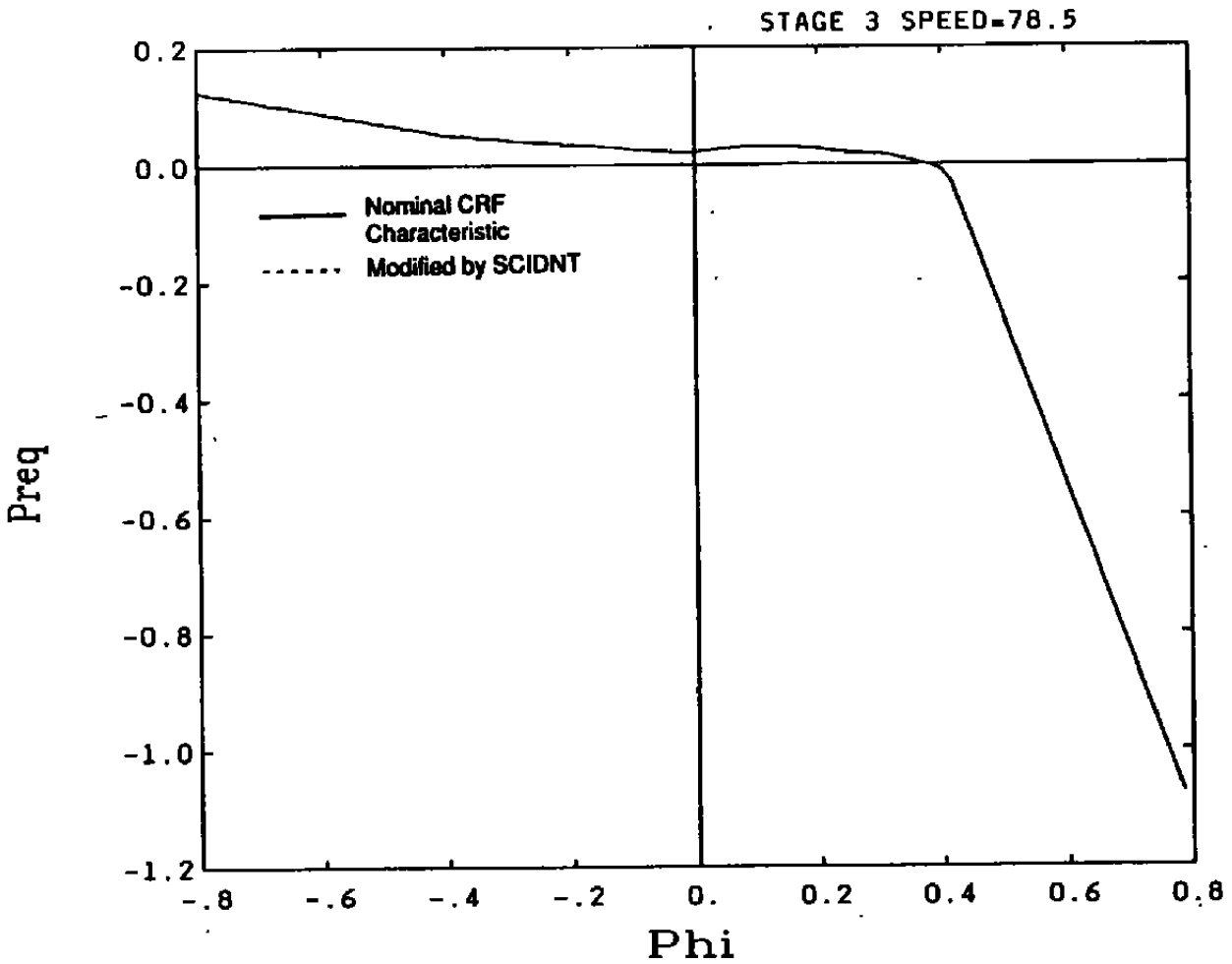

Figure 6.5 1 Estimated Poststall Stage Characteristics (Continued)

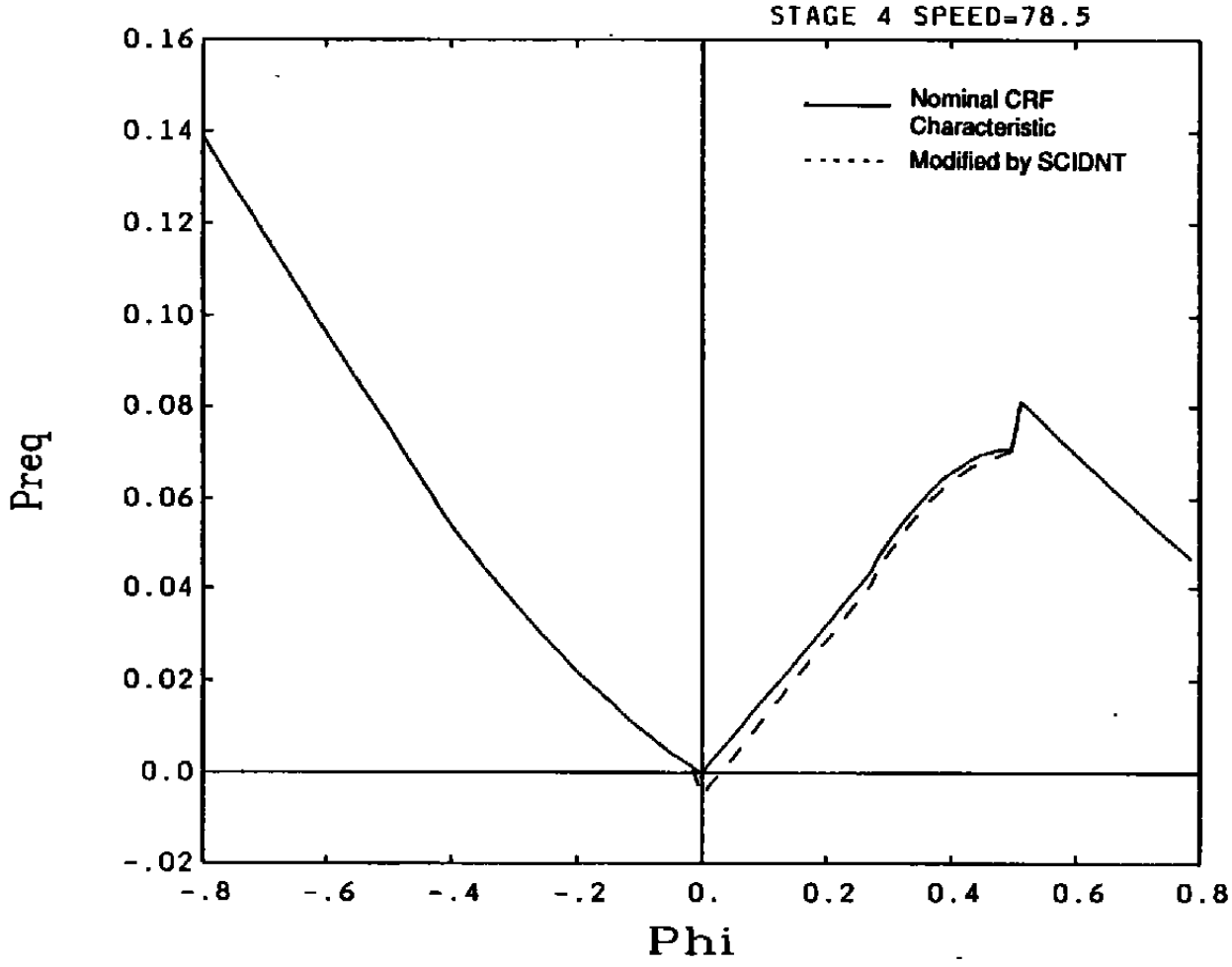

Figure 6.5.1 Estimated Poststall Stage Characteristics (Continued)

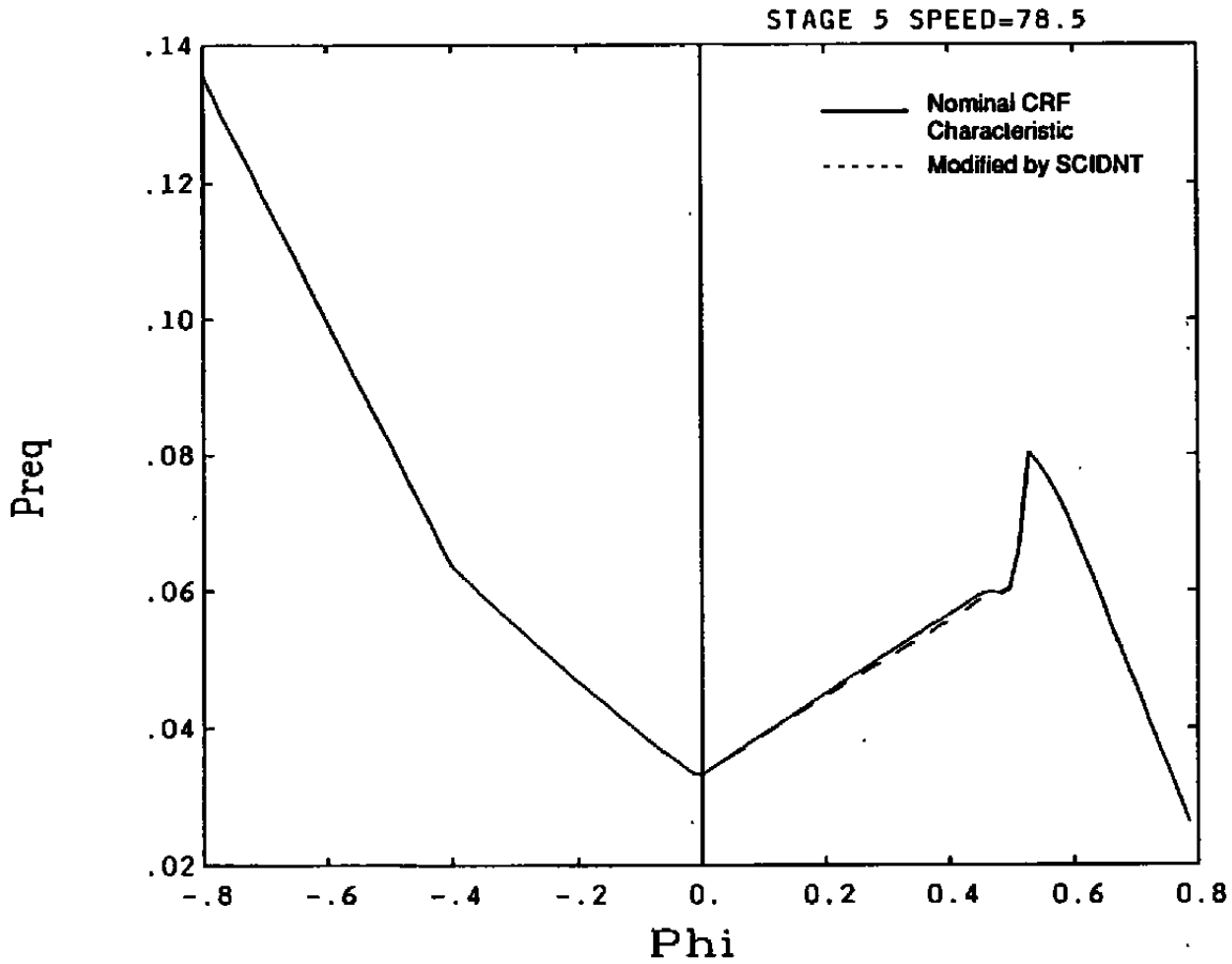

Figure 6.5.1 Estimated Poststall Stage Characteristics (Continued)

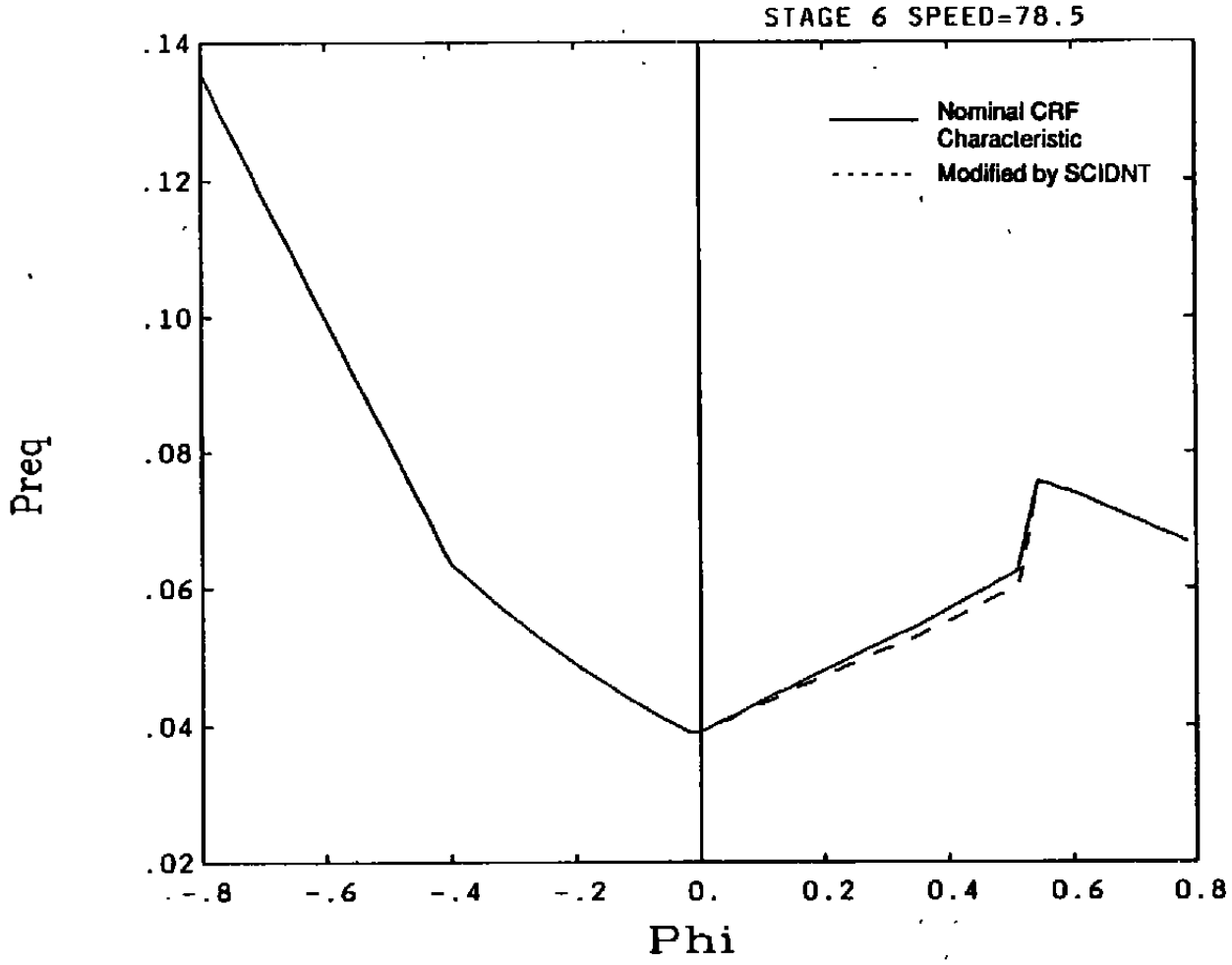

Figure 6.5.1 Estimated Poststall Stage Characteristics (Continued)

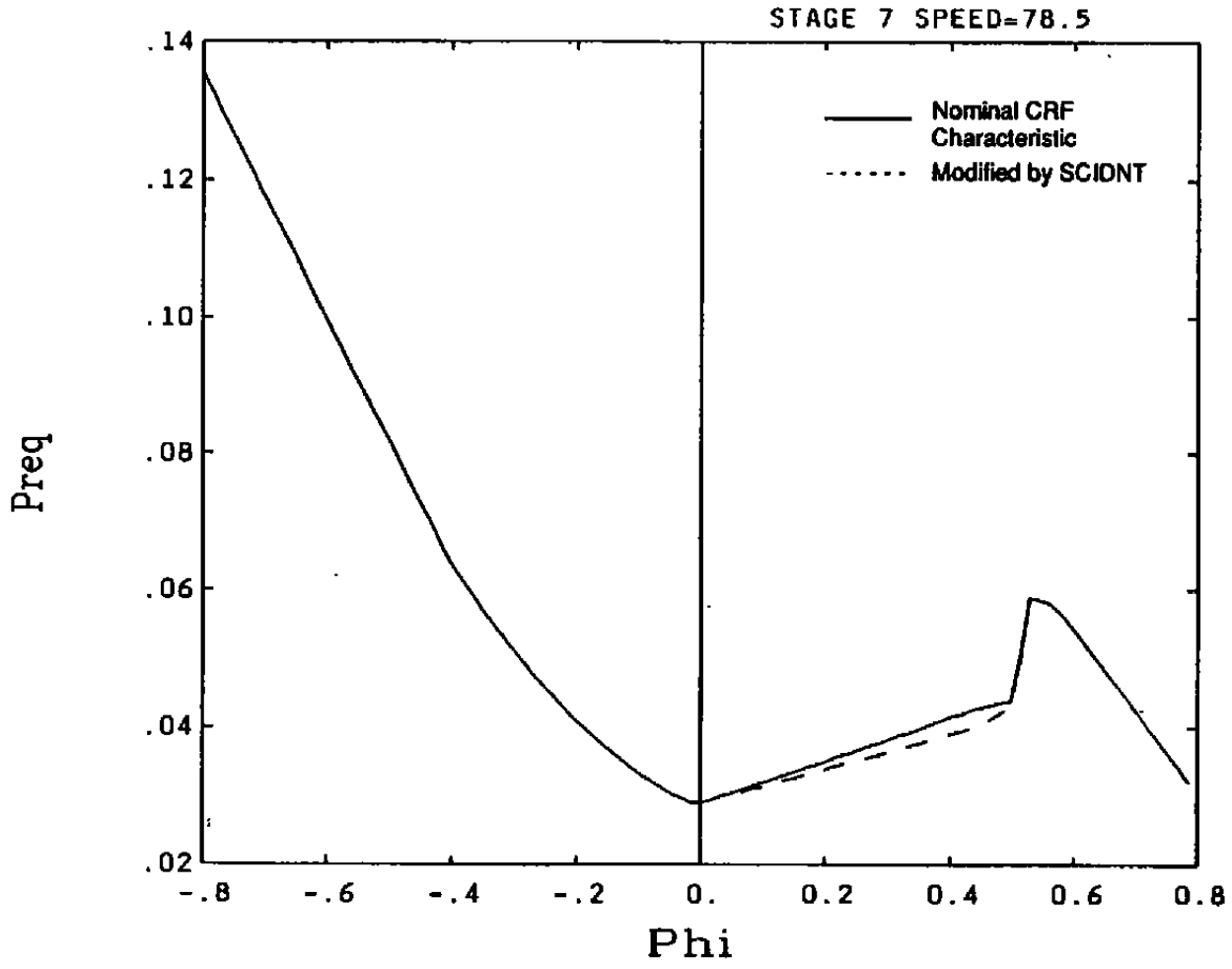

Figure 6.5.1 Estimated Poststall Stage Characteristics (Continued)

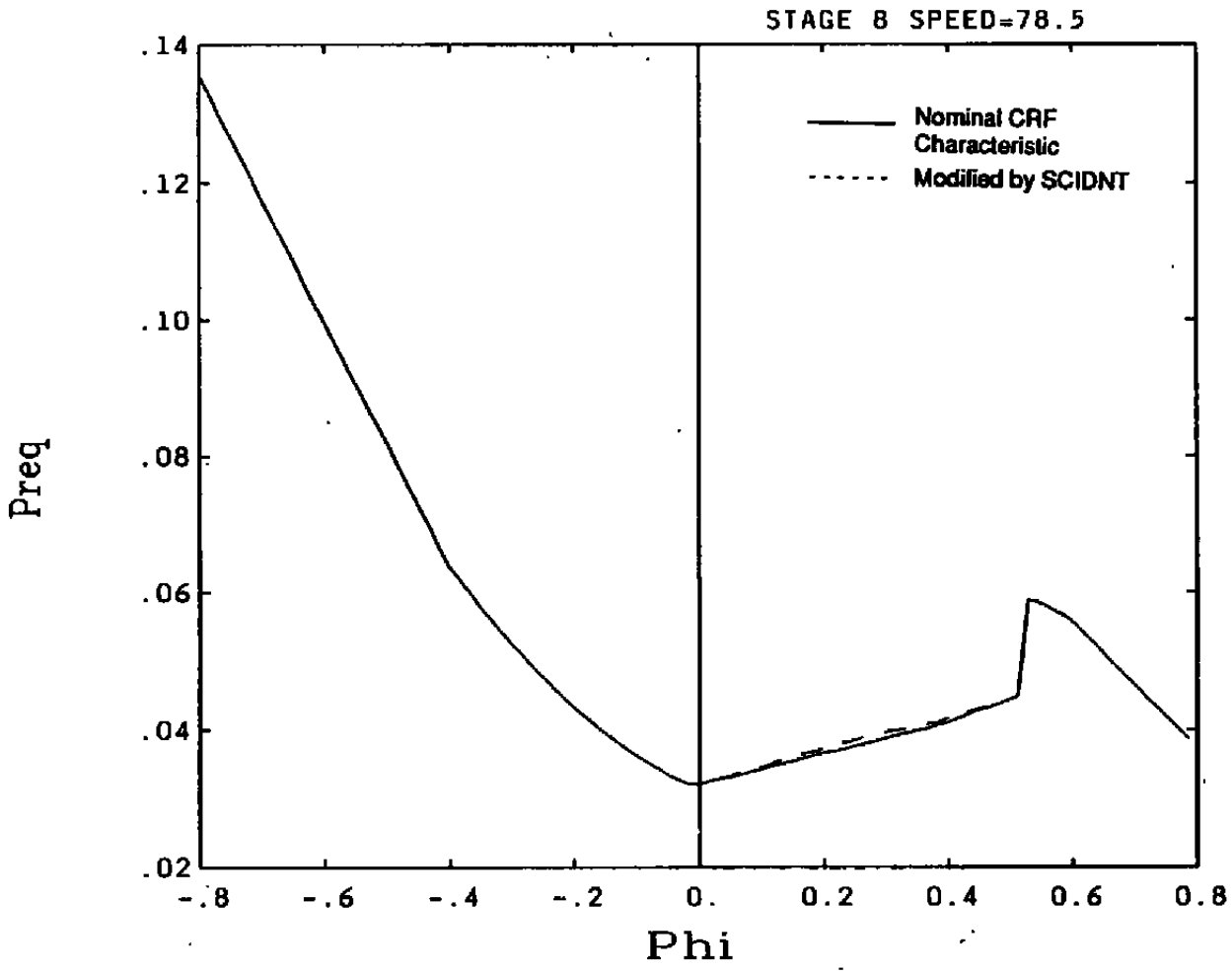

Figure 6.5.1 Estimated Poststall Stage Characteristics (Continued)

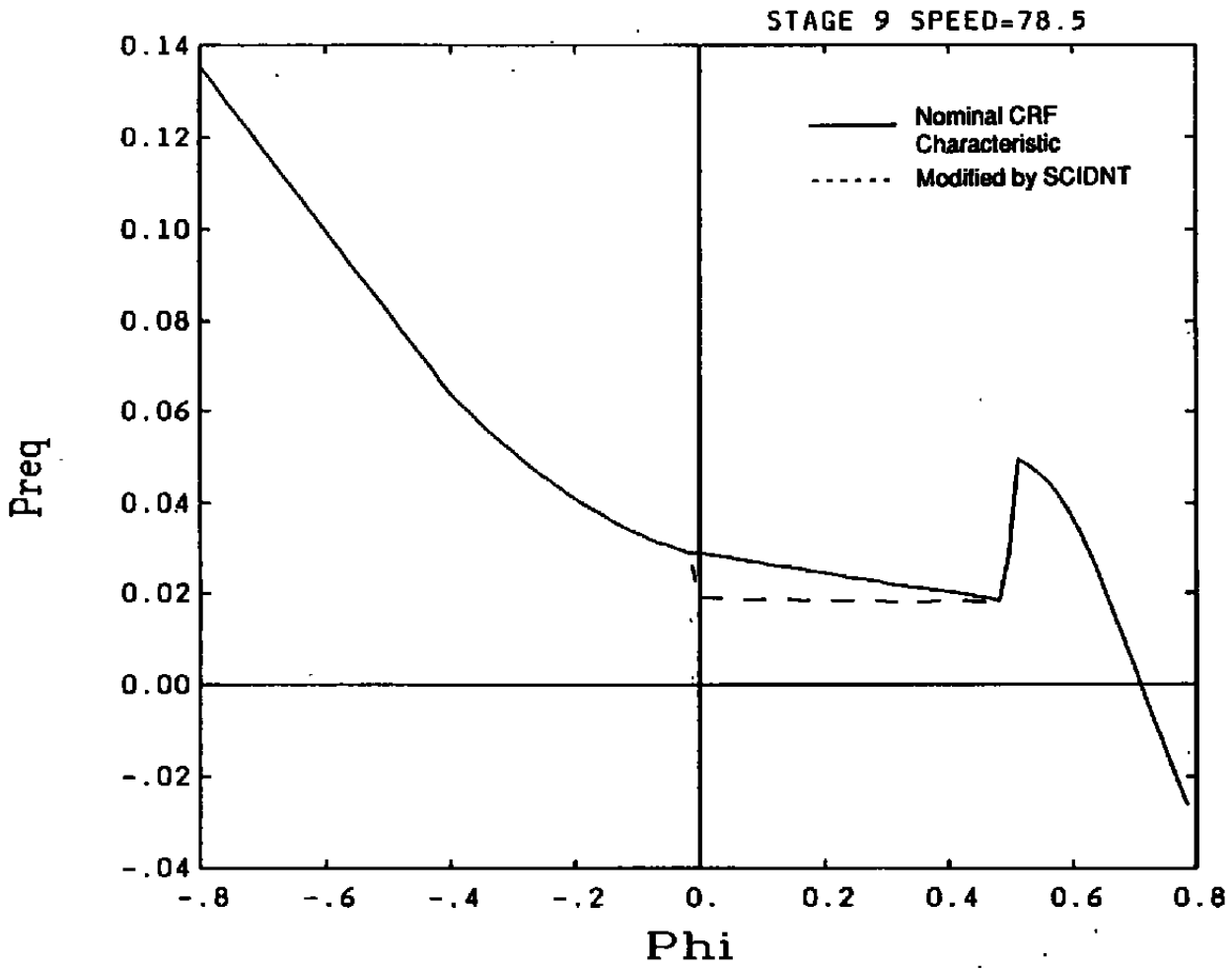

Figure 6.5.1 Estimated Poststall Stage Characteristics (Continued)

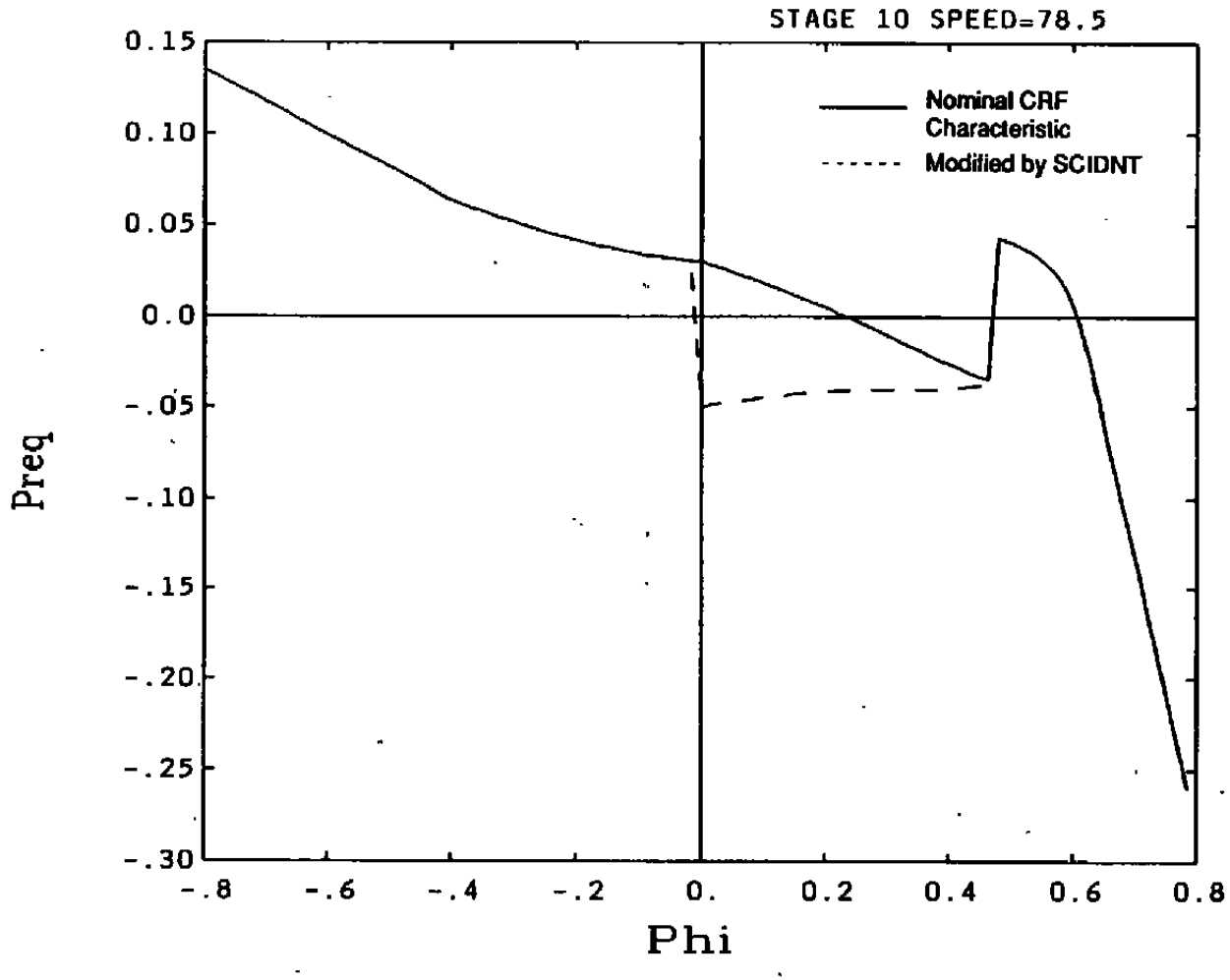

Figure 6.5.1 Estimated Poststall Stage Characteristics (Continued)

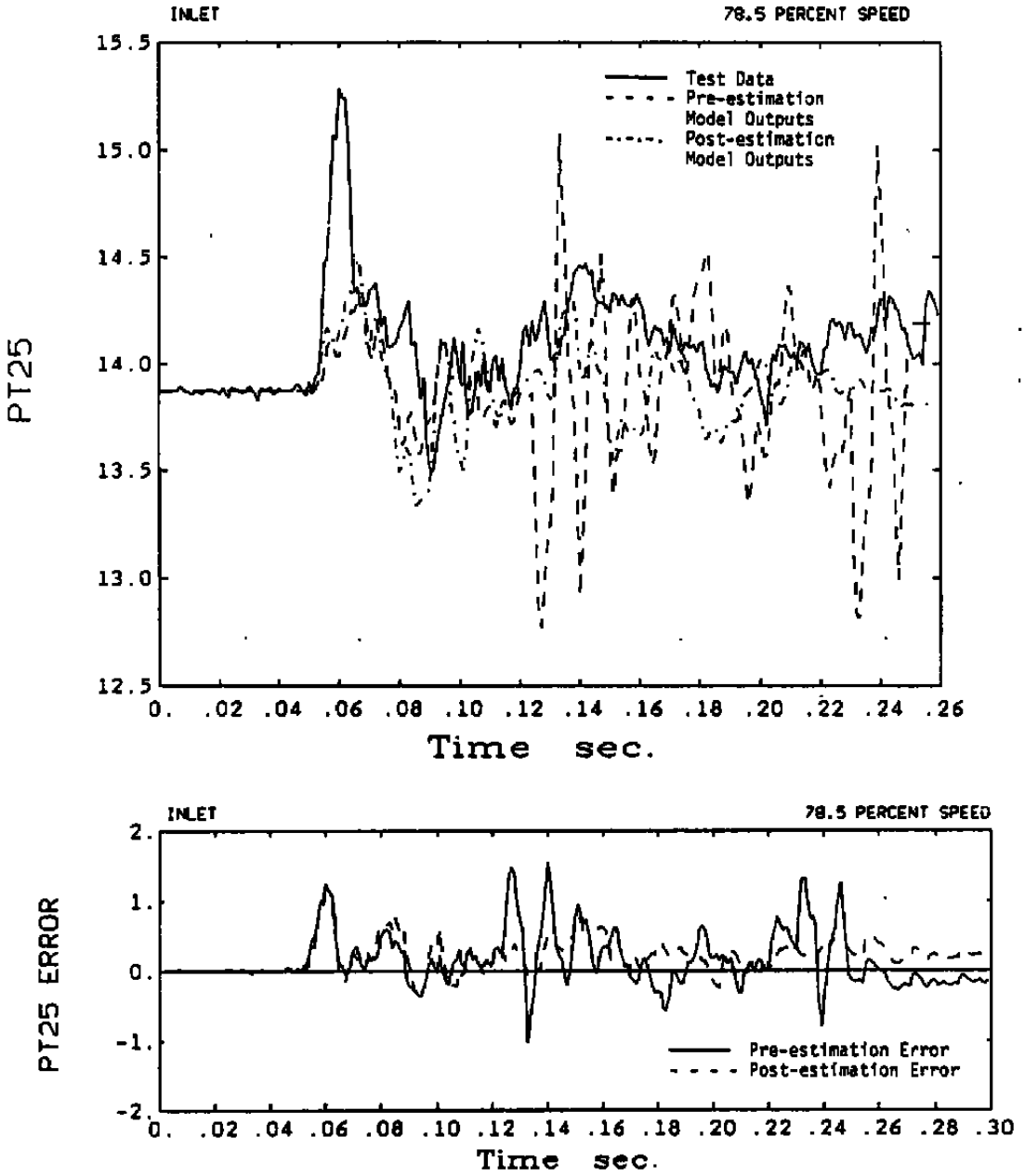

Figure 6.5.2 Comparison of Test Data, Pre-Estimation Model Outputs, and Post-Estimation Model Outputs. Corresponding Pre- and Post-Estimation Model Errors

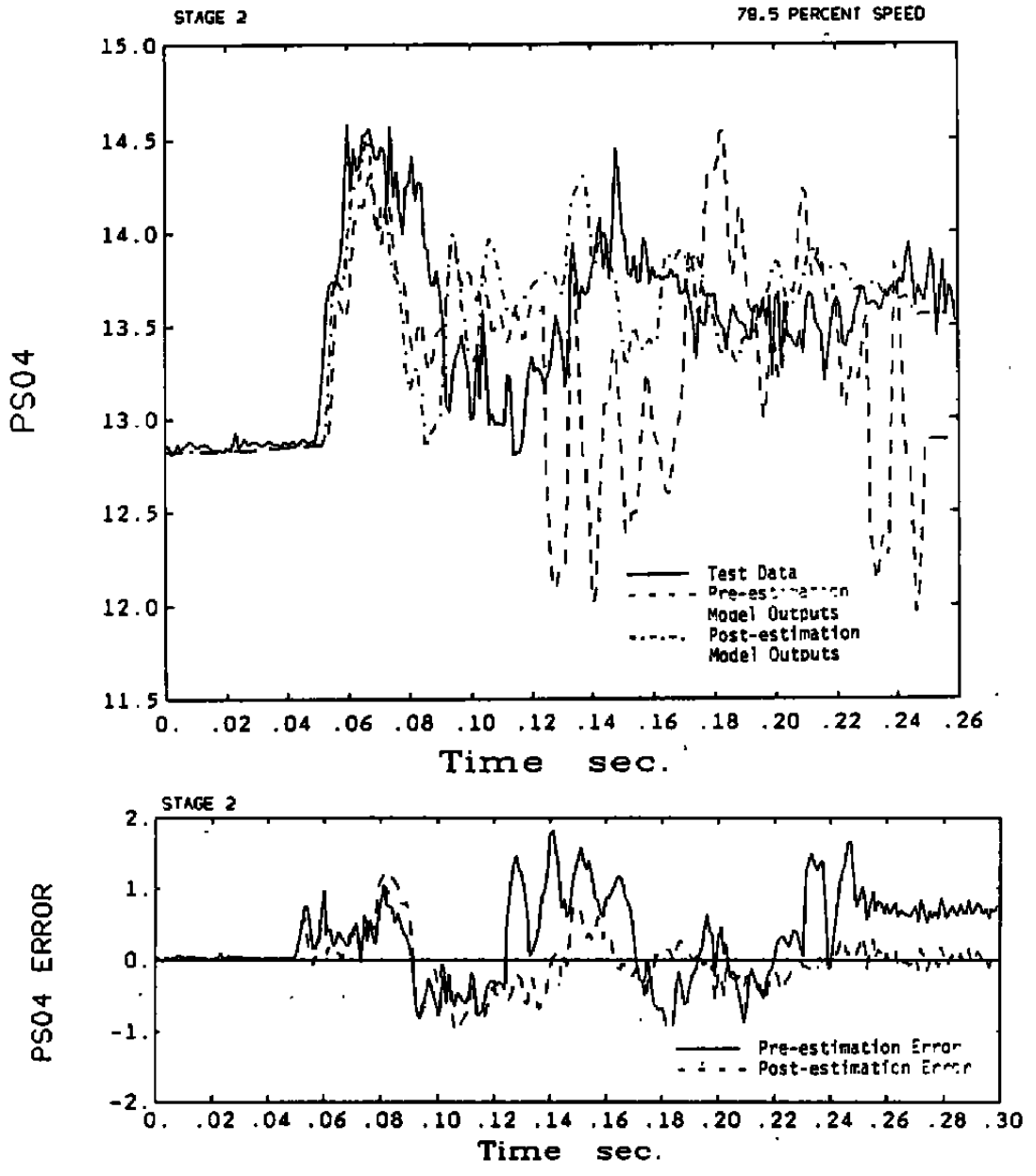

Figure 6.5.2 Comparison of Test Data, Pre-Estimation Model Outputs, and Post-Estimation Model Outputs. Corresponding Pre- and Post-Estimation Model Errors (Cont'd)

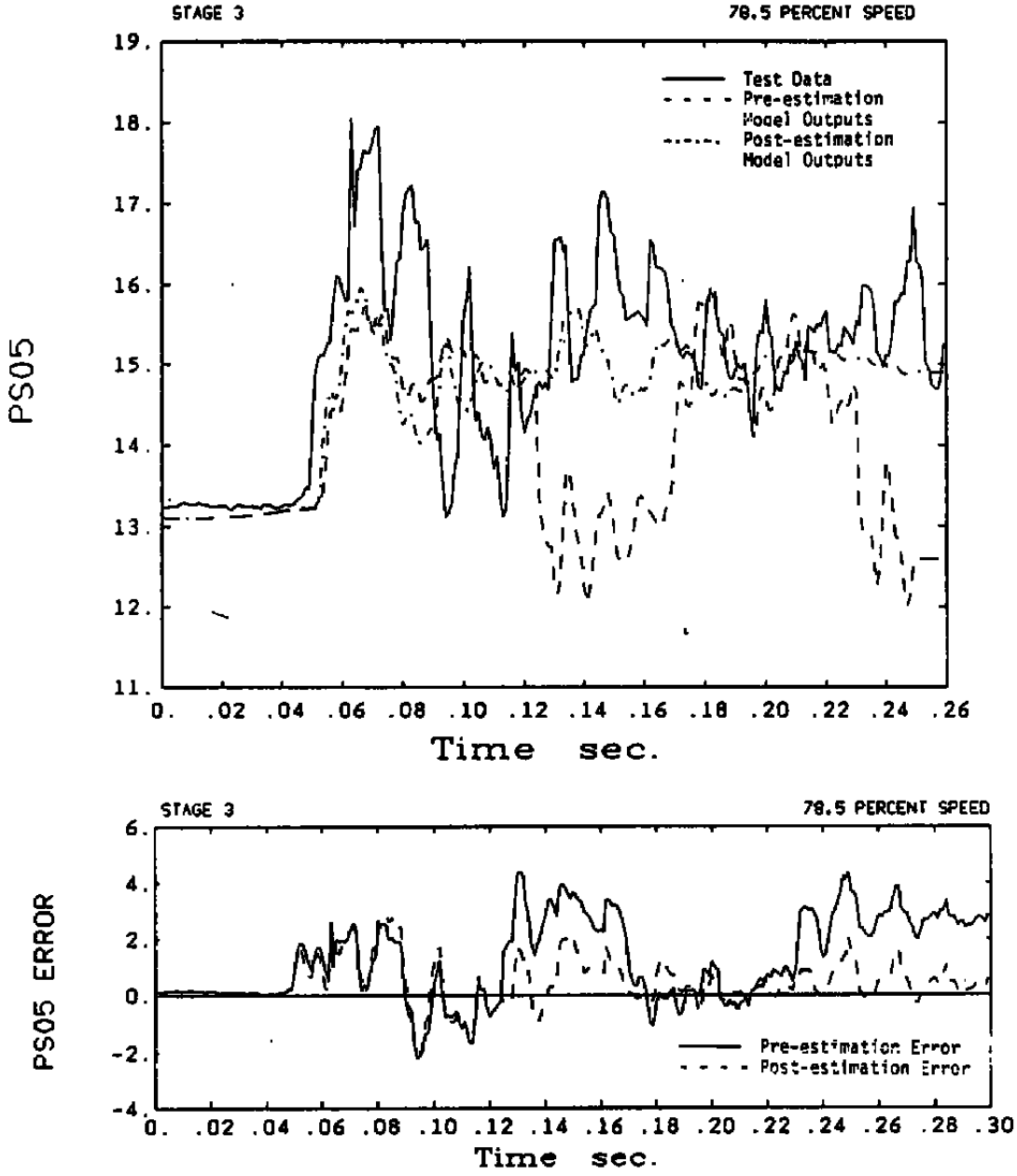

Figure 6.5.2 Comparison of Test Data, Pre-Estimation Model Outputs, and Post-Estimation Model Outputs. Corresponding Pre- and Post-Estimation Model Errors (Cont'd)

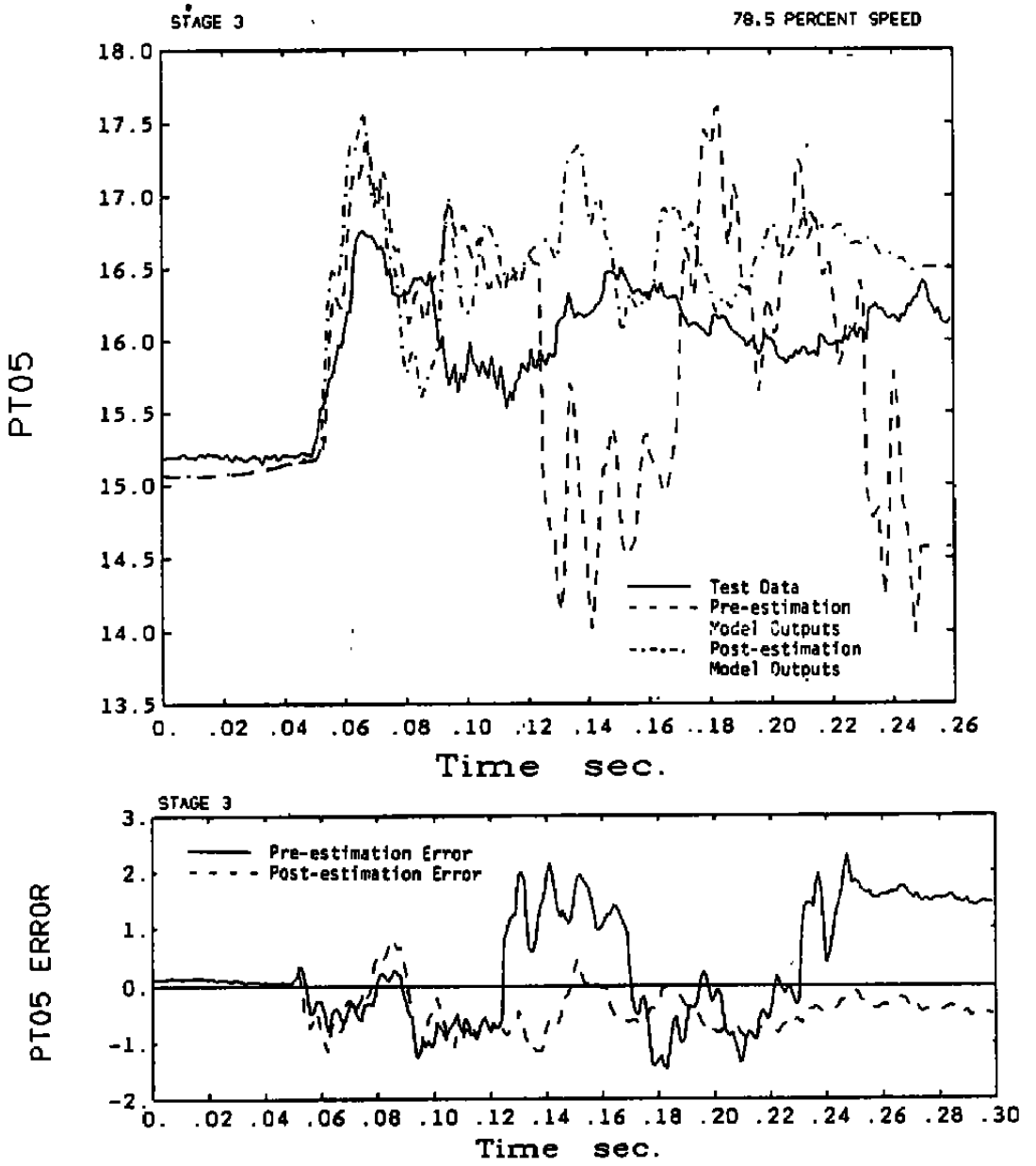

Figure 6.5.2 Comparison of Test Data, Pre-Estimation Model Outputs, and Post-Estimation Model Outputs. Corresponding Pre- and Post-Estimation Model Errors (Cont'd)

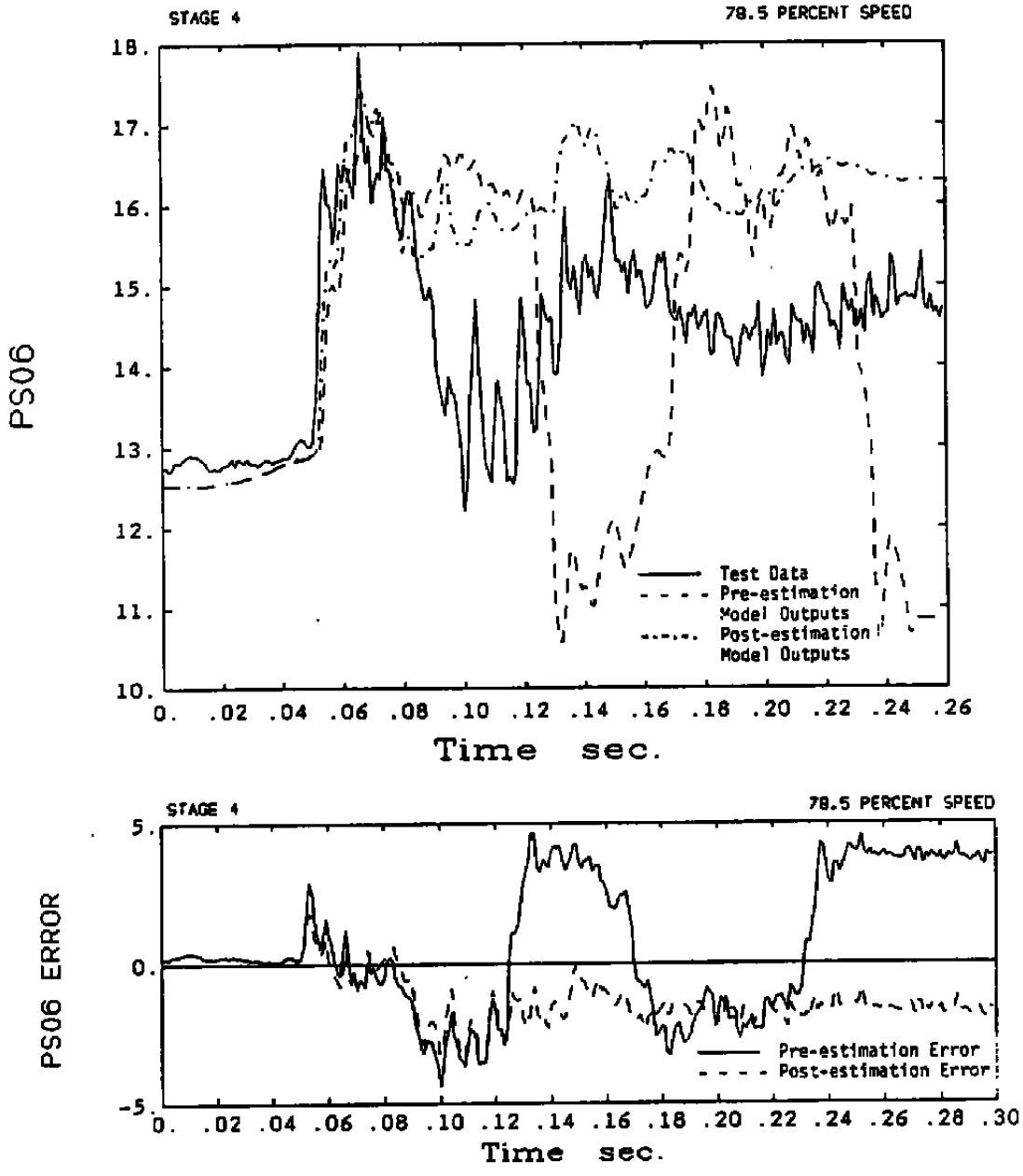

Figure 6.5.2 Comparison of Test Data, Pre-Estimation Model Outputs, and Post-Estimation Model Outputs. Corresponding Pre- and Post-Estimation Model Errors (Cont'd)

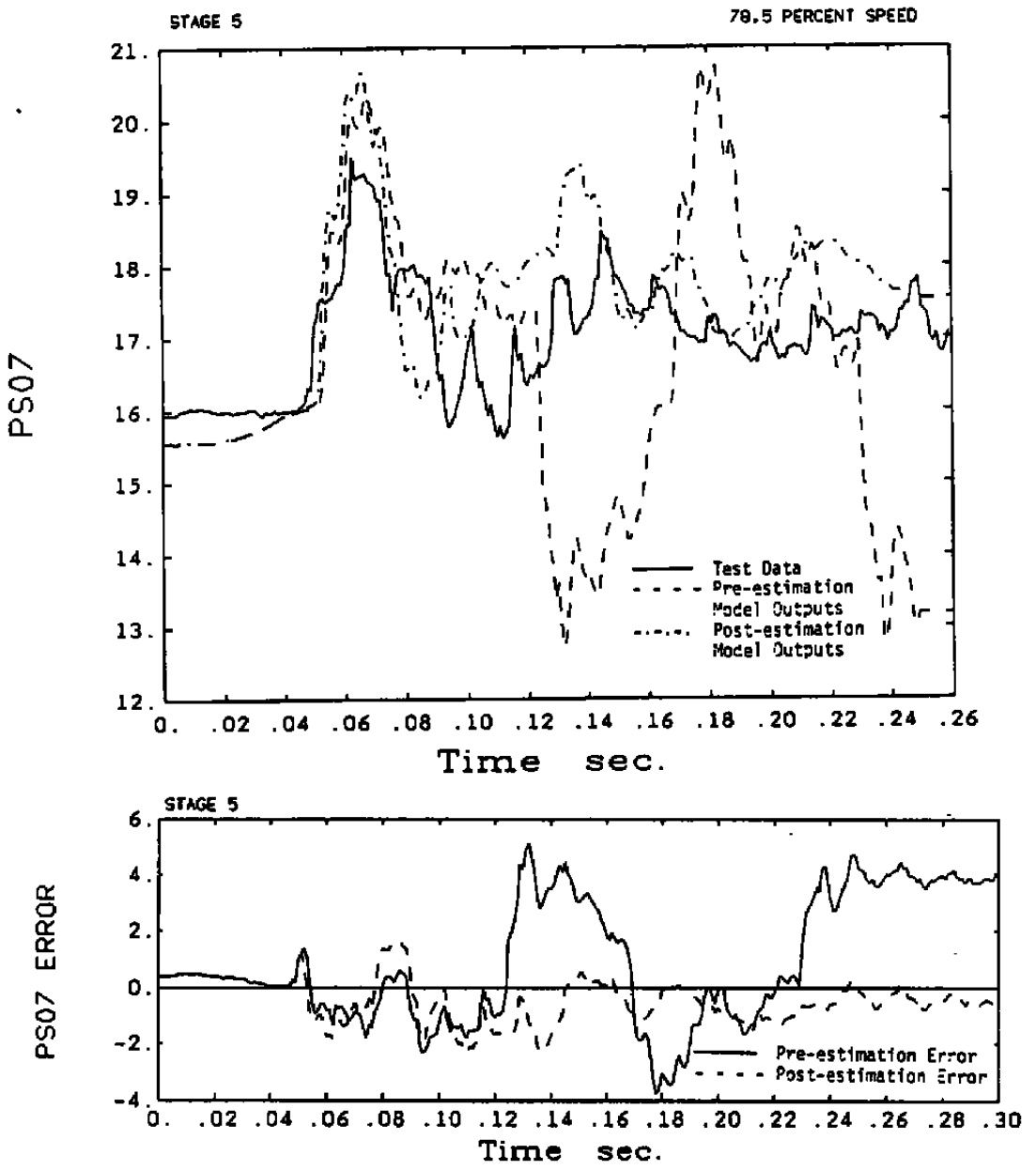

Figure 6.5.2 Comparison of Test Data, Pre-Estimation Model Outputs, and Post-Estimation Model Outputs. Corresponding Pre- and Post-Estimation Model Errors (Cont'd)

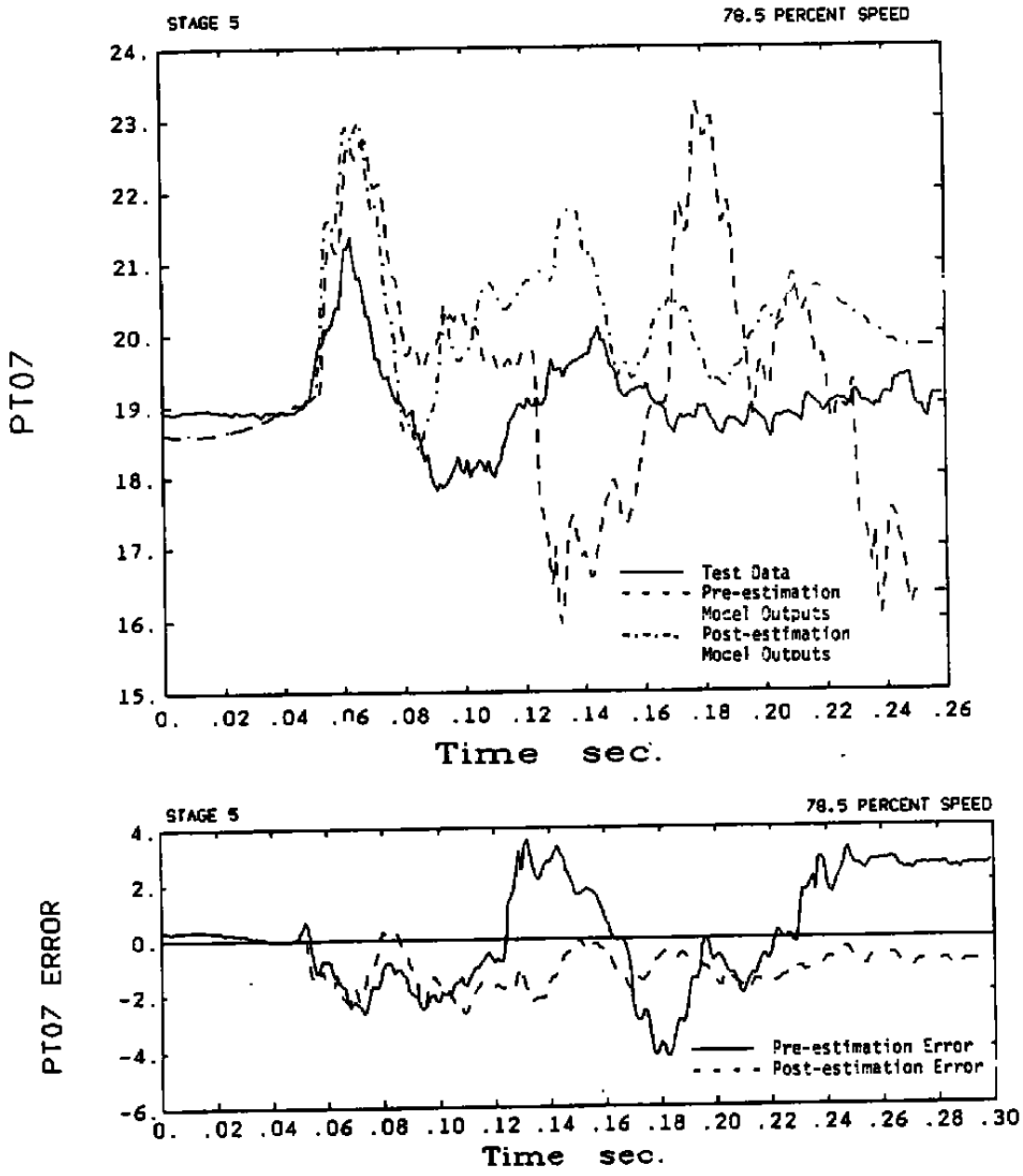

Figure 6.5.2 Comparison of Test Data, Pre-Estimation Model Outputs, and Post-Estimation Model Outputs. Corresponding Pre- and Post-Estimation Model Errors (Cont'd)

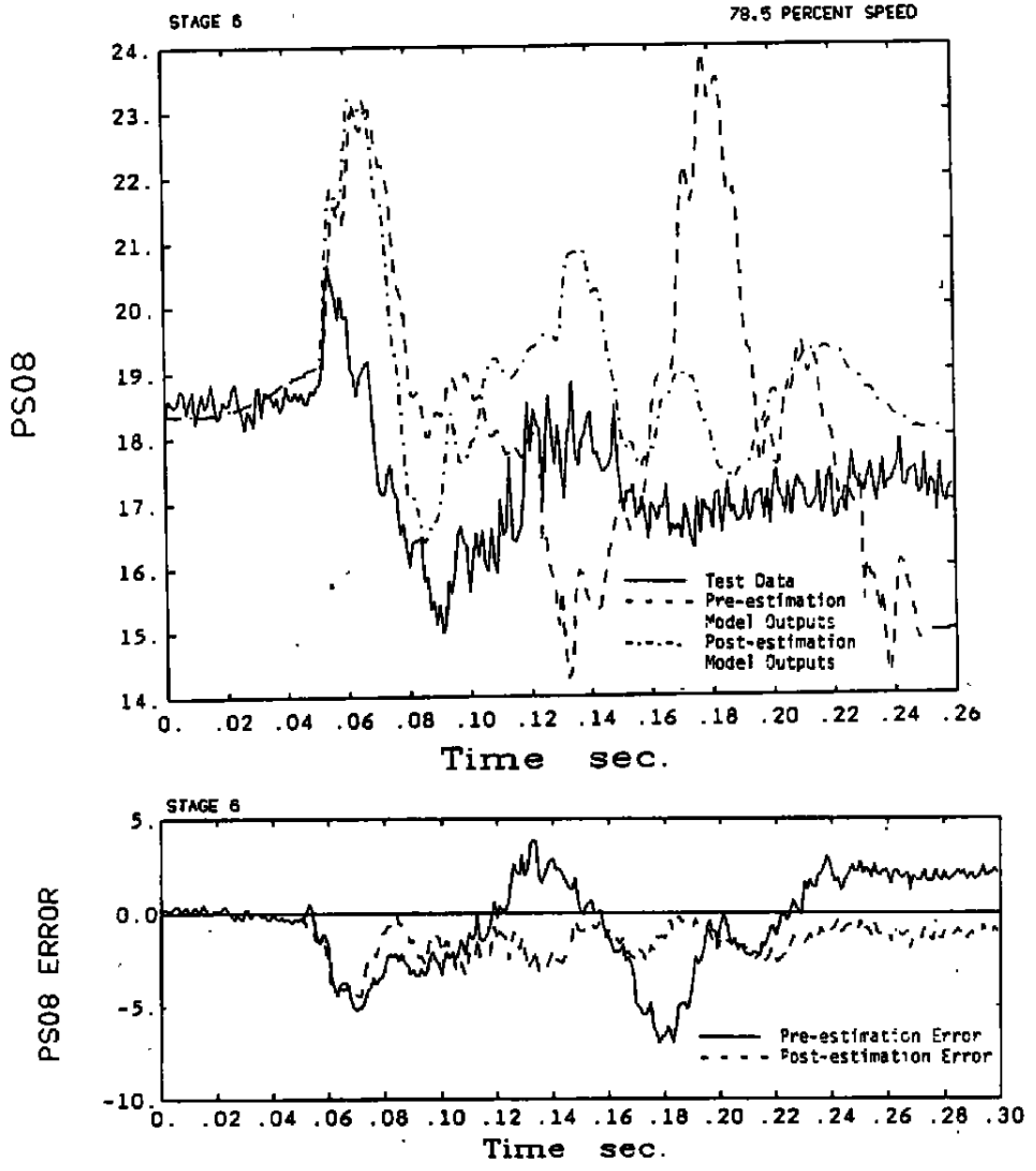

Figure 6.5.2 Comparison of Test Data, Pre-Estimation Model Outputs, and Post-Estimation Model Outputs. Corresponding Pre- and Post-Estimation Model Errors (Cont'd)

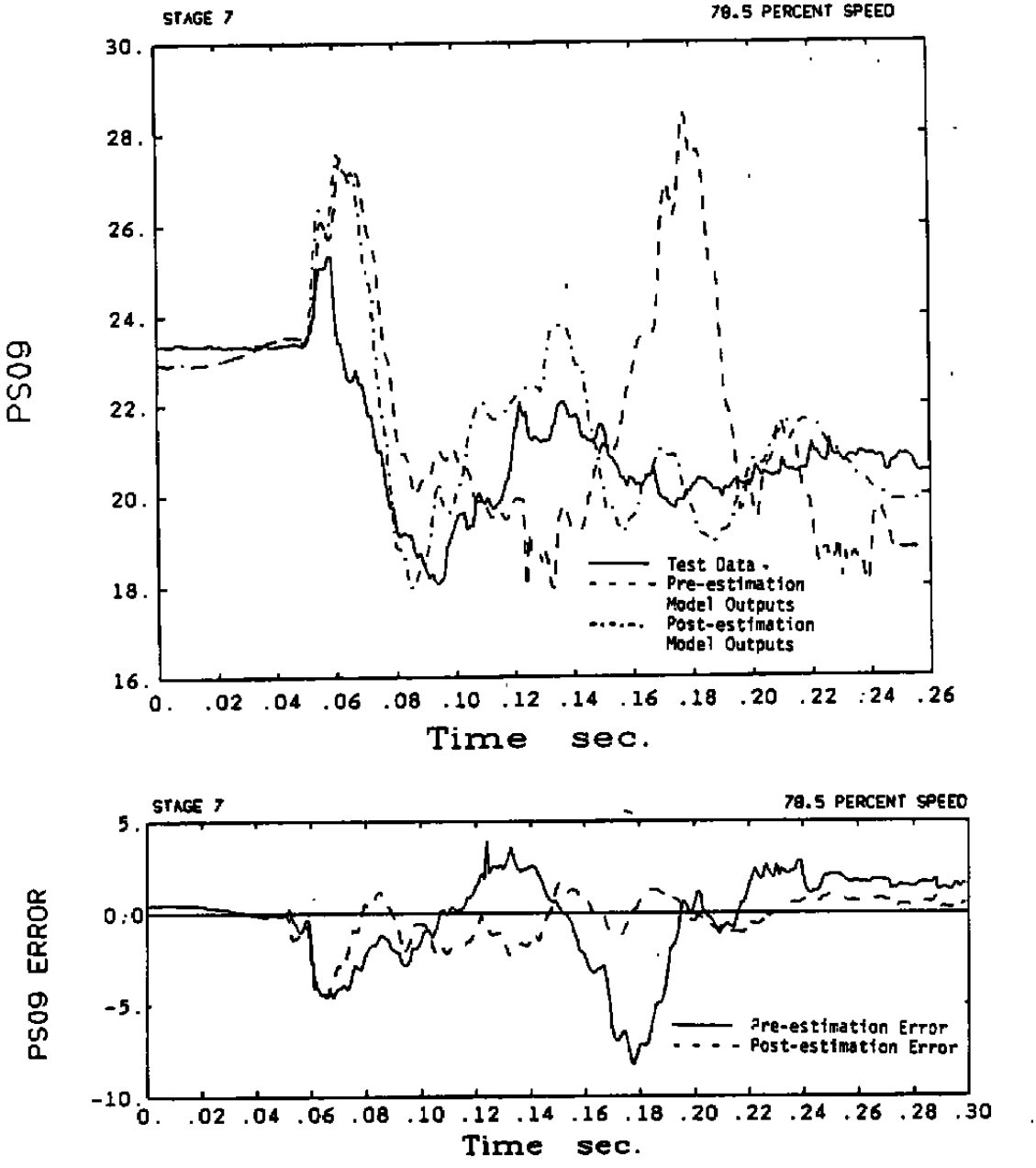

Figure 6.5.2 Comparison of Test Data, Pre-Estimation Model Outputs, and Post-Estimation Model Outputs. Corresponding Pre- and Post-Estimation Model Errors (Cont'd)

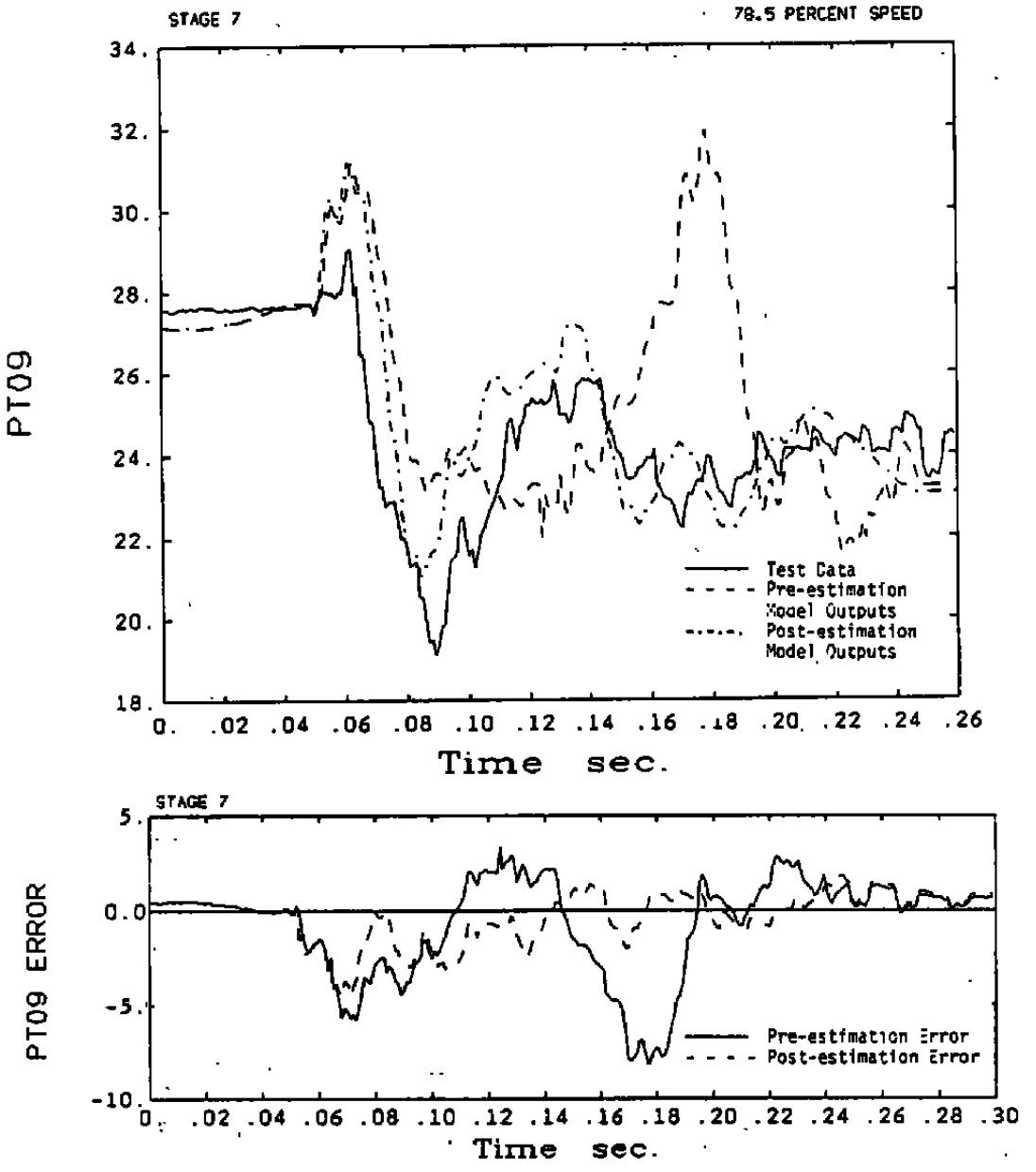

Figure 6.5.2 Comparison of Test Data, Pre-Estimation Model Outputs, and Post-Estimation Model Outputs. Corresponding Pre- and Post-Estimation Model Errors (Cont'd)

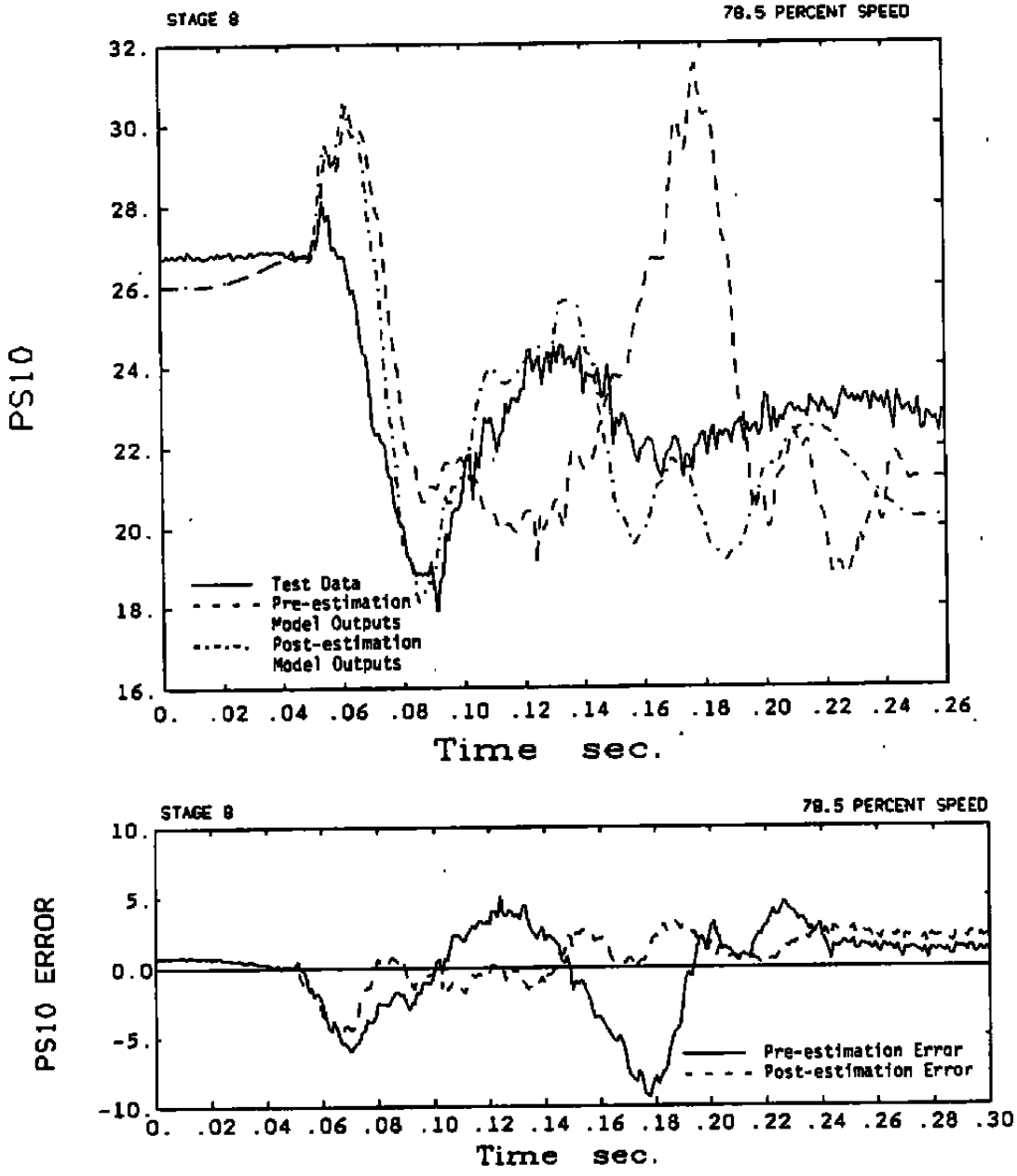

Figure 6.5.2 Comparison of Test Data, Pre-Estimation Model Outputs, and Post-Estimation Model Outputs. Corresponding Pre- and Post-Estimation Model Errors (Cont'd)

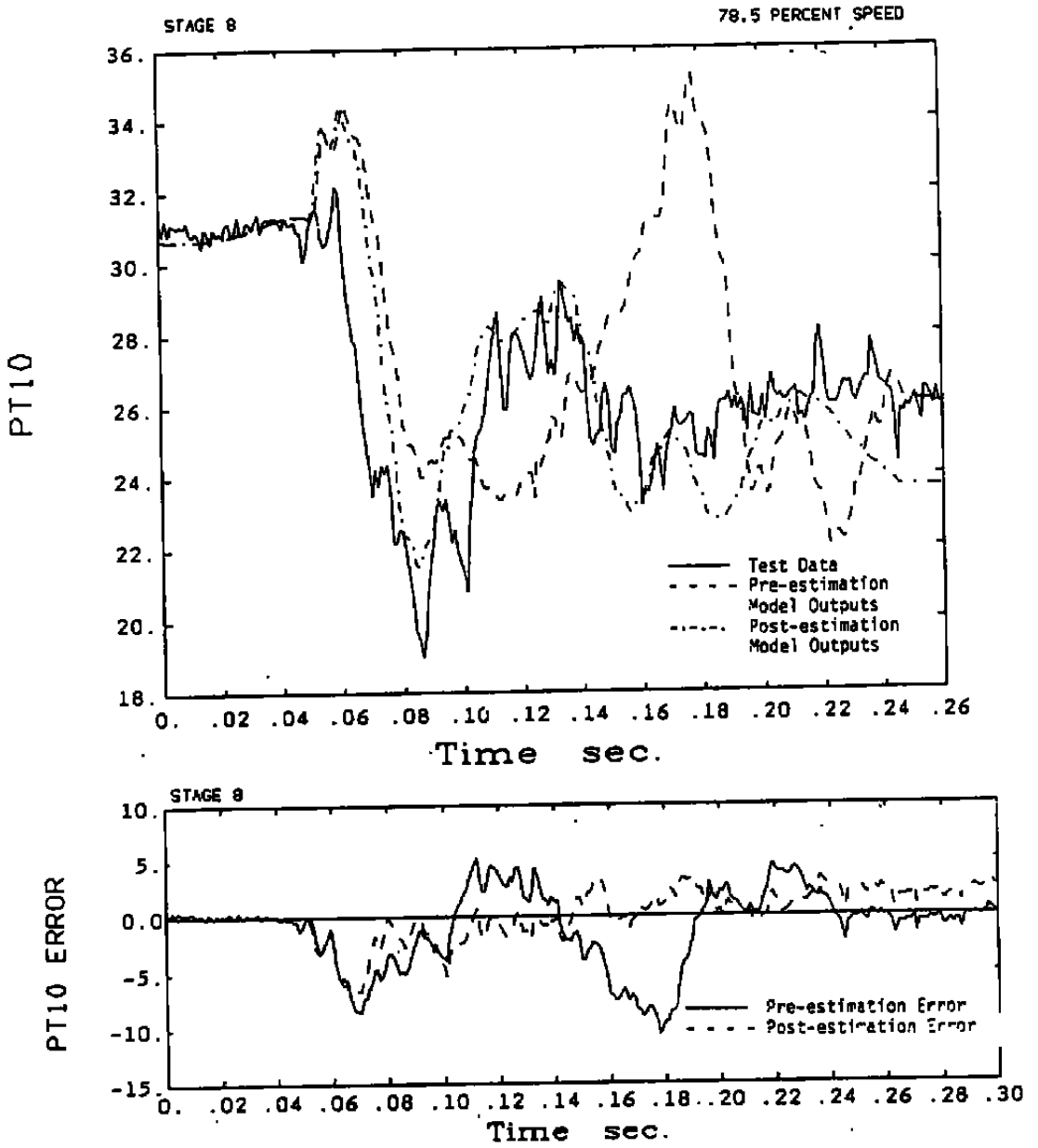

Figure 6.5.2 Comparison of Test Data, Pre-Estimation Model Outputs, and Post-Estimation Model Outputs. Corresponding Pre- and Post-Estimation Model Errors (Cont'd)

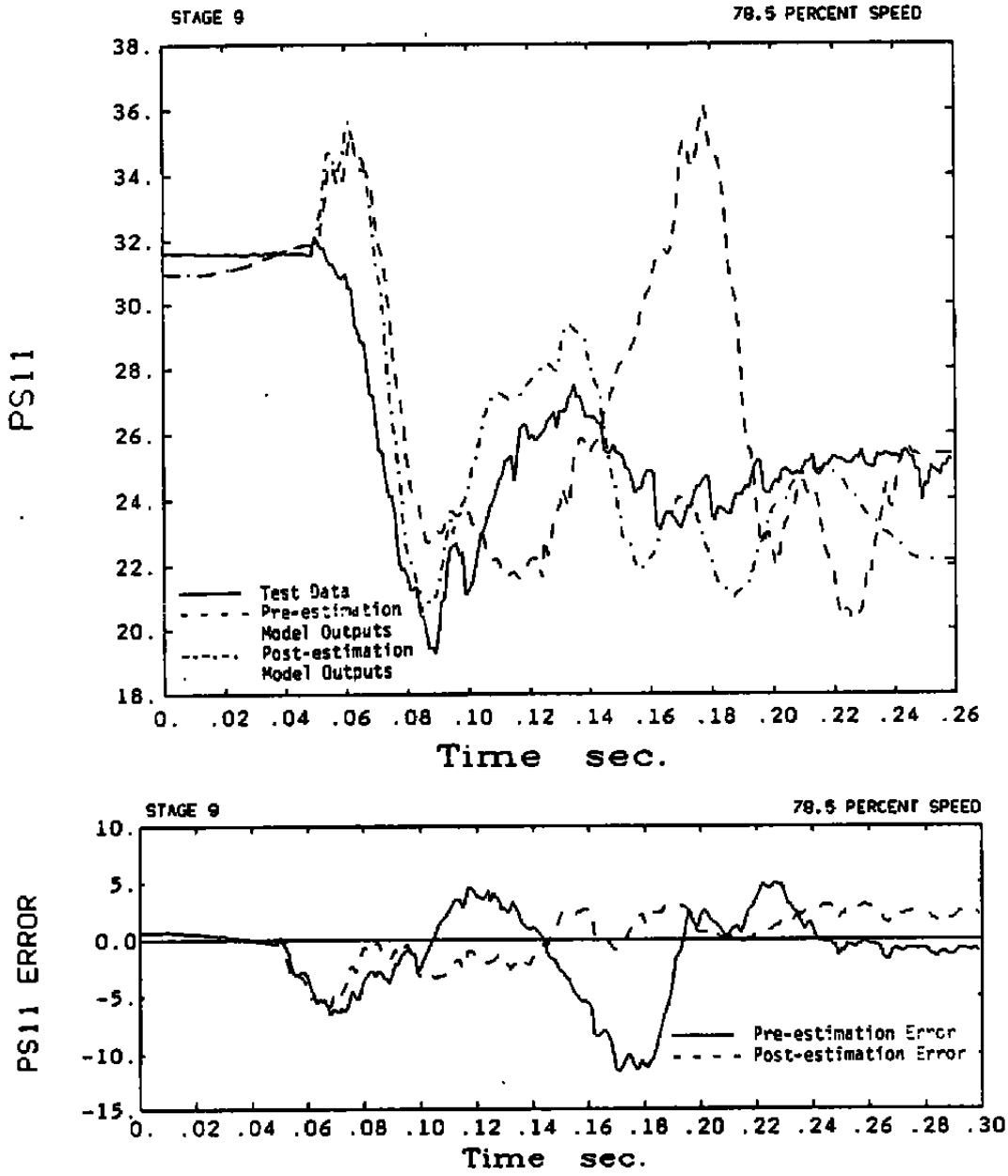

Figure 6.5.2 Comparison of Test Data, Pre-Estimation Model Outputs, and Post-Estimation Model Outputs. Corresponding Pre- and Post-Estimation Model Errors (Cont'd)

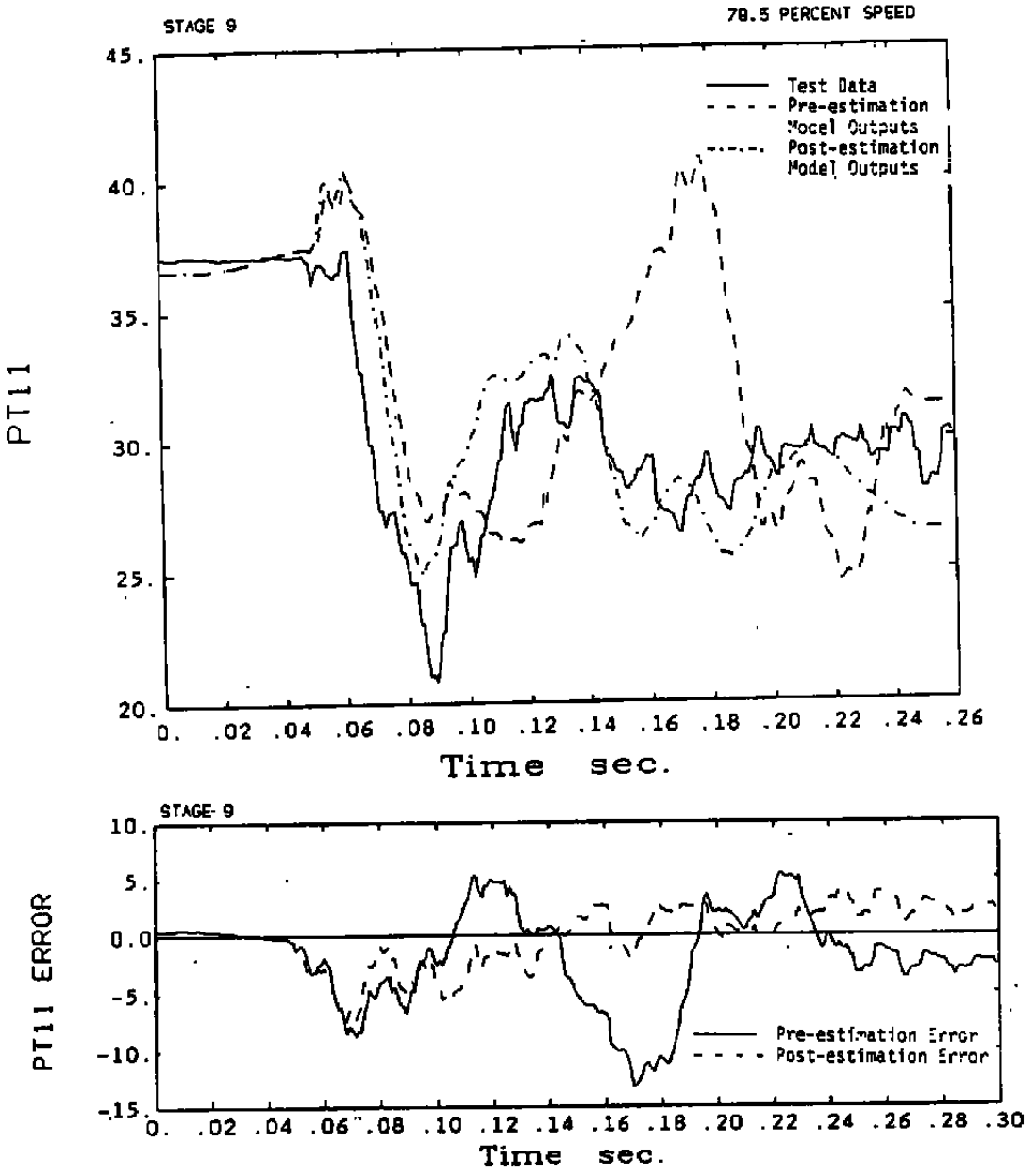

Figure 6.5.2 Comparison of Test Data, Pre-Estimation Model Outputs, and Post-Estimation Model Outputs. Corresponding Pre- and Post-Estimation Model Errors (Cont'd)

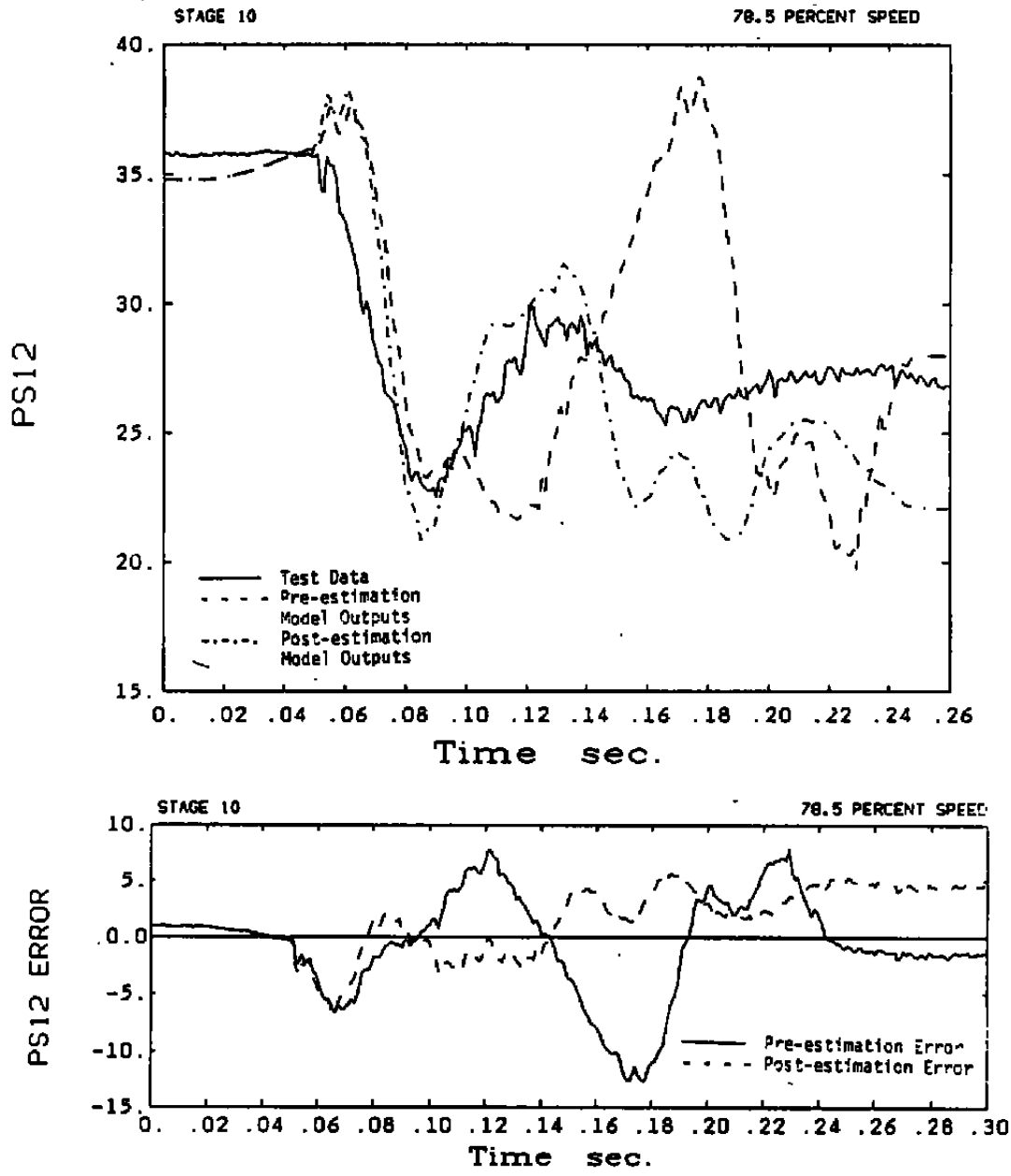

Figure 6.5.2 Comparison of Test Data, Pre-Estimation Model Outputs, and Post-Estimation Model Outputs. Corresponding Pre- and Post-Estimation Model Errors (Cont'd)

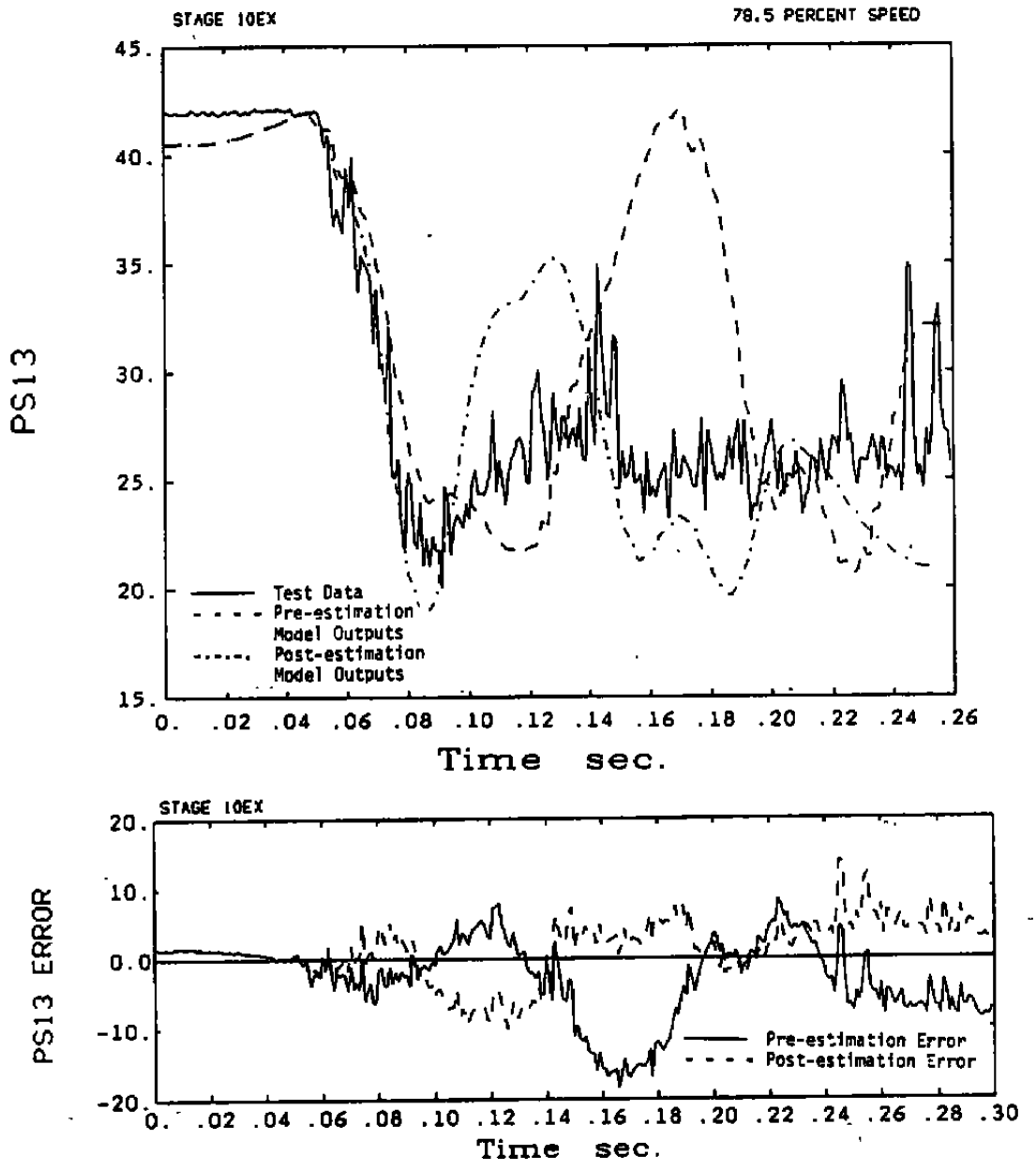

Figure 6.5.2 Comparison of Test Data, Pre-Estimation Model Outputs, and Post-Estimation Model Outputs. Corresponding Pre- and Post-Estimation Model Errors (Cont'd)

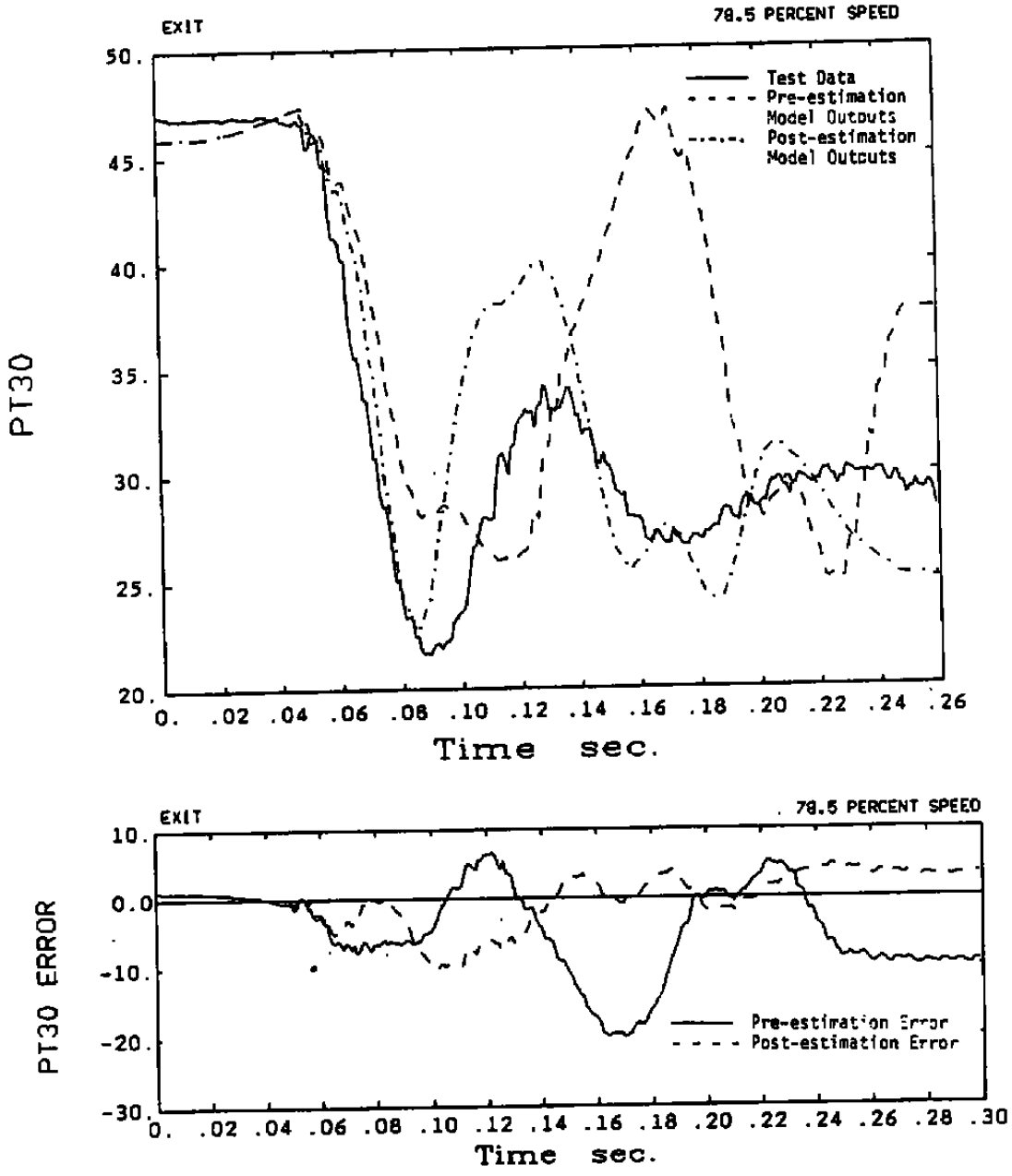

Figure 6.5.2 Comparison of Test Data, Pre-Estimation Model Outputs, and Post-Estimation Model Outputs. Corresponding Pre- and Post-Estimation Model Errors (Cont'd)